

## **The role of the miR-26 family in neurogenesis**

## **Die Rolle der miR-26 Familie in der Neurogenese**

Doctoral thesis for a doctoral degree  
at the Graduate School of Life Sciences,  
Julius-Maximilians-Universität Würzburg,  
Section Biomedicine

submitted by

**Thomas Ziegenhals**

from

**Rodewisch, Germany**

Würzburg 2017



**Submitted on:**.....

**Members of the *Promotionskomitee*:**

**Chairperson:** Prof. Dr. Alexander Buchberger

**Primary Supervisor:** Prof. Dr. Utz Fischer

**Supervisor (Second):** Prof. Dr. Albrecht Müller

**Supervisor (Third):** Dr. Stefan Juranek

**Date of Public Defence:** .....

**Date of Receipt of Certificates:** .....



**Table of Contents**

1	Summary .....	9
2	Zusammenfassung.....	11
3	Introduction.....	13
3.1	Neurogenesis .....	13
3.1.1	Gene regulation during neurogenesis.....	14
3.1.2	Transcriptional Gene regulation via REST .....	15
3.2	Post transcriptional gene regulation via non coding RNAs .....	17
3.2.1	miR targeting and mode of function.....	21
3.3	The role of miR in neurogenesis .....	22
3.4	miR 26 family .....	23
3.5	Aim of thesis.....	24
4	Results .....	27
4.1	Investigation of miR-26 biogenesis regulation .....	27
4.2	pre-miR-26 nuclear export is indistinguishable from export of other miRs upon micro-injection into <i>Xenopus laevis</i> oocytes.....	30
4.3	pre-miR 26b is not processed in early zebrafish embryos: indication for an inhibitor of miR-26 maturation .....	31
4.4	Identification of miR-26 regulatory proteins.....	33
4.4.1	Identification of miR hairpin binding proteins using the indirect binding approach.....	34
4.4.2	Investigation of pre-miR-26 processing regulation by the potential candidates .....	38
4.4.3	Identification of miR hairpin binding proteins using S1 aptamer approach .....	44
4.5	Analyzing the role of the miR-26 family in an murine <i>in vitro</i> neuronal differentiation system .....	48
4.5.1	Knock out of the miR-26 family members in murine ESCs.....	50
4.5.2	The KO of miR-26 does not effect the differentiation to NPC but final neural differentiation .....	50
4.6	Transcriptome analysis of miR-26 KO cell lines.....	53
4.7	REST regulated miR show target sites in mRNAs of REST complex members .....	55
4.8	The majority of REST-miRs are down regulated in miR KO cell lines .....	58

## Table of contents

---

4.9	miR-26 initiates the activation of the REST-miRs .....	60
5	Discussion .....	63
5.1	Role of miR-26 is conserved in vertebrates .....	63
5.2	pre-miR-26b shows normal nucleo-cytoplasmic transport .....	64
5.3	pre-miR-26 shows stage specific processing in zebrafish development.....	65
5.4	Identification of pre-miR-26 binding proteins.....	66
5.4.1	ZnF346 .....	66
5.4.2	FXR1, FXR2 and FMRP .....	67
5.4.3	Eral1 .....	68
5.4.4	Alternative approaches for detection of pre-miR factors.....	69
5.5	miR-26 KO cells show loss of neural identity .....	70
5.6	miR-26 KO affects the REST – REST-miR feedback loop.....	71
5.7	REST-miR function aside REST regulation .....	73
5.8	The Role of miR-26 in neurogenesis.....	73
6	Material & Methods .....	75
6.1	Materials.....	75
6.1.1	Nucleotide and Protein Ladders .....	75
6.1.2	Buffers and Solution .....	75
6.1.3	Bacterial culture Media .....	78
6.1.4	Bacterial Cells.....	79
6.1.5	Zebrafisch Cell lines .....	79
6.1.6	Antibodies .....	79
6.1.7	Plasmid Vectors.....	79
6.1.8	DNA nucleotides .....	81
6.1.9	Morpholino Oligos.....	86
6.2	Methods .....	86
6.2.1	Molecular methods .....	86
6.2.2	Biochemical Methods.....	90
6.2.3	Zebrafisch Methods .....	92
6.2.4	Cell lysate preparation .....	92
6.2.5	Immunobiological methods.....	93
6.2.6	RNA methods .....	94
6.2.7	Bioinformatics' Methods.....	105
6.2.8	Cell Culture Work.....	105

7	Appendix .....	107
8	References .....	113
9	Table of figures.....	123
10	Publication.....	124
11	Acknowledgment.....	125
12	Curriculum vitae .....	127
13	Affidavit.....	130





## 1 Summary

For the differentiation of embryonic stem cells (ESCs) to neuronal cells (NCs) a complex and coordinated gene regulation program is needed. One important control element for neuronal differentiation is the *repressor element 1 silencing transcription factor* (REST) complex, which represses neuronal gene expression in non-neuronal cells. Crucial effector proteins of the REST complex are small phosphatases such as the CTDSPs (C-terminal domain small phosphatases) that regulate polymerase II activity by dephosphorylating the C-terminal domain of the polymerase, thereby repressing target genes. The stepwise inactivation of REST, including the CTDSPs, leads to the induction of a neuron-specific gene program, which ultimately induces the formation of neurons. The spatio-temporal control of REST and its effector components is therefore a crucial step for neurogenesis.

In zebrafish it was shown that the REST-associated CTDSP2 is negatively regulated by the micro RNA (miR) -26b. Interestingly, the miR-26b is encoded in an intron of the primary transcript of CTDSP2. This gives the fundament of an intrinsic regulatory negative feedback loop, which is essential for the proceeding of neurogenesis. This feedback loop is active during neurogenesis, but inactive in non-neuronal cells. The reason for this is that the maturation of the precursor miR (pre-miR) to the mature miR-26 is arrested in non neuronal cells, but not in neurons. As only mature miRs are actively repressing genes, the regulation of miR-26 processing is an essential step in neurogenesis.

In this study, the molecular basis of miR-26 processing regulation in the context of neurogenesis was addressed. The mature miR is processed from two larger precursors: First the primary transcript is cleaved by the enzyme DROSHA in the nucleus to form the pre-miR. The pre-miR is exported from the nucleus and processed further through the enzyme DICER to yield the mature miR. The mature miR can regulate gene expression in association with the RNA-induced silencing complex (RISC).

Multiple different scenarios in which miR processing was regulated were proposed and experimentally tested. Microinjection studies using *Xenopus laevis* oocytes showed that slowdown or blockage of the nucleo-cytoplasmic transport are not the reason for delayed pre-miR-26 processing. Moreover, *in vitro* and *in vivo* miR-

processing assays showed that maturation is most likely regulated through a *in trans* acting factor, which blocks processing in non neuronal cells.

Through RNA affinity chromatographic assays using zebrafish and murine lysates I was able to isolate and identify proteins that interact specifically with pre-miR-26 and could by this influence its biogenesis. Potential candidates are FMRP/FXR1/2, ZNF346 and Eral1, whose functional characterisation in the context of miR-biogenesis could now be addressed.

The second part of my thesis was executed in close collaboration with the laboratory of Prof. Albrecht Müller. The principal question was addressed how miR-26 influences neuronal gene expression and which genes are primarily affected. This research question could be addressed by using a cell culture model system, which mimics *ex vivo* the differentiation of ESCs to NCs via neuronal progenitor.

For the functional analysis of miR-26 knock out cell lines were generated by the CRISPR/Cas9 technology. miR-26 deficient ESC keep their pluripotent state and are able to develop NPC, but show major impairment in differentiating to NCs. Through RNA deep sequencing the miR-26 induced transcriptome differences could be analysed.

On the level of mRNAs it could be shown, that the expression of neuronal gene is downregulated in miR-26 deficient NCs. Interestingly, the deletion of miR-26 leads to selectively decreased levels of miRs, which on one hand regulate the REST complex and on the other hand are under transcriptional control by REST itself. This data and the discovery that induction of miR-26 leads to enrichment of other REST regulating miRs indicates that miR-26 initiates neurogenesis through stepwise inactivation of the REST complex.

## 2 Zusammenfassung

Für die Differenzierung von embryonalen Stammzellen (ESCs) zu Neuronen (NCs) bedarf es eines komplexen Genregulationsprogramms, welches sowohl zeitlich als auch räumlich reguliert werden muss. Ein wichtiger Faktor während der neuronalen Differenzierung ist der sogenannte „*repressor element 1 silencing transcription factor*“ (REST)-Komplex, welcher die Expression neuronaler Gene in nicht neuronalen Zellen unterdrückt. Wichtige Effektorproteine im REST-Komplex sind kleine Phosphatasen (sog. CTDSPs), welche durch die Dephosphorylierung der C-terminalen Domäne der RNA-Polymerase II deren Aktivität an Zielgenen reprimiert. Die schrittweise Inaktivierung von REST, einschließlich der CTDSPs, führt hingegen zur Einleitung des neuronalen Genprogramms und damit zur Entwicklung von neuronalen Zellen. Die zeitliche Regulierung des REST-Komplexes und seiner assoziierten Effektor-Komponenten ist daher auf molekularer Ebene das entscheidende Ereignis in der Neurogenese.

Studien in Zebrafisch haben gezeigt, dass die REST-assoziierte Phosphatase CTDSP2 von der micro-RNA (miR) -26b negativ reguliert wird, was zu einer reduzierten REST Aktivität führt. Interessanterweise liegt diese miR in einem Intron von CTDSP2, also dem Gen, welches sie selbst reprimiert. Diese Konstellation stellt die Basis für eine intrinsische negative Rückkopplungsschleife dar und ist essentiell für das Voranschreiten der Neurogenese. Diese Schleife ist aktiv während der Neurogenese, jedoch inaktiv in neuronalen Stammzellen. Der Grund hierfür ist, dass die Reifung der miR-26b auf der Stufe der Prozessierung des miR-Vorläufers (pre-miR) zur reifen miR in Stammzellen, nicht aber in Neuronen, angehalten ist. Da nur reife miR funktionell aktiv sein können, ist die Regulation der miR-26 Reifung ein essentieller Schritt im Rahmen der Neurogenese.

In dieser Dissertation sollte der Frage nach der molekularen Basis der regulierten Prozessierung der miR-26 im Rahmen der Neurogenese nachgegangen werden. Die Prozessierung von miR erfolgt über zwei Intermediate: Zunächst wird aus dem primären Transkript im Zellkern die pre-miR durch das Enzym DROSHA gebildet. Diese wird dann aus dem Kern exportiert und durch das Enzym DICER zur reifen miR weiterverarbeitet, die im Kontext des „*RNA-Induced Silencing Complex*“ (RISC) die post-transkriptionale Genexpression reguliert.

Mirkoinjektionsstudien an *Xenopus laevis* Oocyten zeigten, dass eine Verlangsamung bzw. Blockade des nukleo-zytoplasmatischen Transports nicht Ursache für die verzögerte Prozessierung der pre-miR-26 sein kann. Stattdessen haben *in vitro* und *in vivo* Prozessierungsexperimente gezeigt, dass die Reifung der miR-26 sehr wahrscheinlich durch einen *in trans* agierenden Faktor gesteuert wird, der die Prozessierung in nicht-neuronalen Zellen blockiert.

Durch RNA affinitätschromatographische Versuche gelang es, Proteine aus Maus- und Zebrafischlysaten zu isolieren und diese zu identifizieren, die spezifisch mit der pre-miR-26b interagieren und deren Biogenese beeinflussen könnten. Vielversprechende Kandidaten sind die Proteine FMRP/FXR1/2, ZNF346 und Eral1, deren funktionelle Charakterisierung im Kontext der miR-Biogenese nun möglich ist.

In einer Kooperation mit der Arbeitsgruppe von Prof. Albrecht Müller wurde im zweiten Teil der Arbeit der prinzipiellen Frage nachgegangen, wie die miR-26 die neuronale Genexpression steuert und welche Gene hiervon primär betroffen sind. Diese Untersuchungen wurden durch die Etablierung eines Zellkultur-Protokolls ermöglicht, welches *ex vivo* die Differenzierung von ESC über neuronal Vorläufer Zellen (NPC) zu NCs erlaubte und so eine systematische Analyse dieses Prozess erlaubte.

Für die Funktionsanalyse von miR-26 wurden über die CRISPR/Cas9 Technologie Zelllinien hergestellt, welche keine miR-26 mehr im Genom haben. miR-26 defiziente ESCs behalten ihren pluripotenten Status und ließen sich zu NPCs entwickeln. Die Weiterentwicklung von NPCs zu NCs war hingegen massiv eingeschränkt. Durch RNA Hochdurchsatzsequenzierung gelang es die miR-26 induzierten Genexpressionsunterschiede genau zu identifizieren.

Auf der Ebene der mRNA konnte gezeigt werden, dass die Expression von neuronalen Genen in miR-26 defizienten NCs herunterreguliert ist und dass unter diesen Bedingungen offensichtlich kein anderer Differenzierungsweg eingeschlagen werden konnte. Interessanterweise führte die Deletion von miR-26 zu einer selektiven Verminderung von miRs, die einerseits den REST Komplex regulieren, andererseits aber auch unter dessen transkriptionaler Kontrolle stehen. Diese Daten und die Entdeckung, dass die Induktion von miR-26 zur Anreicherung anderer REST regulierender miRs führt, lässt vermuten, dass miR-26 die Neurogenese durch die schrittweise Inaktivierung des REST Komplexe initiiert.

## 3 Introduction

### 3.1 Neurogenesis

The different cell types of a developing vertebrate that give rise to specialized tissues and organs all originate from a single fertilized zygote. The zygote is a totipotent cell, which has the ability to produce all cell types of an organism. This totipotent cell initially gives rise to pluripotent stem cells, which can further differentiate into any of the three germ layers: ectoderm, endoderm and mesoderm. Out of these germ layers progenitor cells form, which are restricted to a defined lineage (or tissue) for further differentiation. As the differentiation proceeds, the more determined the cell fate becomes.

The most complex organ in vertebrates is the nervous system and its formation is crucial for vertebrate survival and behaviour. To develop the nervous system in the course of embryogenesis, a neuronal plate and a neuronal tube are initially formed. These single layered structures are composed of neuroepithelial cells, which derive from the ectoderm. Differentiating cells convert the neuroepithelium into more complex structures, which eventually forms the central nervous system (CNS). The CNS forms connections to the peripheral nervous system (PNS) to create the fully functional nervous system.

The nervous system is made from two special cell types, neurons, which rapidly transduce information (electrical or chemical) and glia cells (neuron supporting cells). Neurons are formed in a process termed neurogenesis. They derive from multipotent neuronal stem cells (NSC; more general neuronal progenitor cells) during embryonic development and throughout the life. During neurogenesis not only neurons but also oligodendrocytes and astrocytes can be formed out of the NSCs lineage. Neurons are fully differentiated and cannot divide any longer.

The neuron forming cell division scheme starts with symmetric cell division of neuroepithelial cells (NE), where two daughter cells emerge with identical cell fate (NE  $\rightarrow$  2x NE). A further asymmetric cell division yields one daughter cell, which is identical to the mother cell and one neuronal progenitor cell (NPC) (NE  $\rightarrow$  NE +NPC). These non-stem cell neural progenitor cells are typically radial glial cells (RG). In higher vertebrates there are additional fate restricted intermediate progenitors (also termed basal progenitors), which allow brains to build an even higher complexity in neuronal network formation. Typically non-neural progenitors

divide symmetrically to form two terminally differentiated (post mitotic) neurons (N; NPC → 2x N)(Figure 1A)<sup>1,2</sup>.

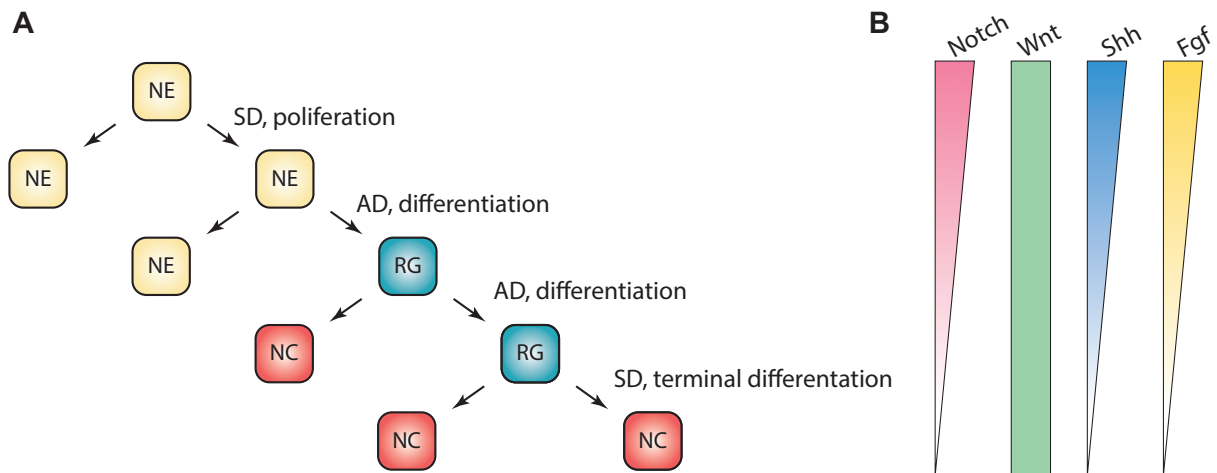


**Figure 1 Cellular differentiation during neurogenesis**

**A** Lineage tree showing the neurogenesis starting from neuroepithelial cells (NE), over radial glial cells (RG) to neuronal cells (NC). Also shown are the different types of divisions, symmetrically (SD) and asymmetrically (AD). **B** Signalling pathway activity over neurogenesis of notch, Wnt, sonic hedgehog (Shh) and folical growth factor (fgf).<sup>1,2</sup>

### 3.1.1 Gene regulation during neurogenesis

Neurogenesis depends on extrinsic signals that trigger four pathways important for neurogenesis: the Notch-, Wnt/ $\beta$ -Catenin- (Wnt), Sonic hedgehog- (Shh) and follice growth factor- (fgf) pathways. Membrane bound receptors respond to these signals and trigger cascades, which eventually activate specific transcription events relevant for neurogenesis<sup>2</sup>.

Notch acts through lateral inhibition, which means that the notch sending cell inhibits differentiation of neighbouring cells. Pro-neural genes are restrained and the cells are kept in proliferation. During asymmetric division of NPCs, the daughter cells with lower levels of Notch will differentiate into neurons, whereas the other daughter cells stays at the NPC level. Wnt signalling during early neurogenesis promotes the symmetric divisions of NPCs, however later in neurogenesis Wnt promotes the differentiation into neurons. Fgf and Shh are important to keep the cells at the proliferation self renewing state of NPCs and down regulation of these signalling pathways leads to further differentiation (Figure 1). These signalling pathways undergo crosstalk and regulate each other. They are also all gradient forming morphogens, which are essential for correct embryogenesis and correct patterning of the CNS.

During neurogenesis, many genes are tightly regulated in a spatio-temporal manner. Genes that are required for neuronal cell formation are repressed during early development and activated only in the process of neurogenesis. Many of these regulatory events are implemented at the transcriptional level, for example the major activating regulator of neurogenesis Pax6. It induces among others the transcription of notch signalling components as well as the pro-neural transcription factors NeuroD1 and Neurog2.<sup>3</sup> A key regulator that acts on the level of transcriptional repression is the Wnt controlled<sup>4</sup> repressor element 1 silencing transcription factor (REST, also known as neuron-restrictive silencing factor, NRSF).

### **3.1.2 Transcriptional Gene regulation via REST**

For fate specific cell differentiation, it is important that the differentiation promoting genes are transcribed. However, during early differentiation, it is necessary that these genes are actively repressed, to keep the cells from differentiation commitment.

One of these repressing factors is the REST complex composed of the name giving REST protein as well as several additional cofactors. Its main function is the suppression of neuronal genes in non-neuronal tissues and cells. The REST complex exerts its activity on genes, which are under regulation of the repressor element 1 (RE1), also known as neuron specific silencer element, NRSE). The RE1 site is a *cis*-acting DNA silencing element, 21-23 base pairs in length and found in promoters of many neuronal genes. The REST protein can directly bind to the RE1 and acts as hub for the formation of multi-protein REST complex. At the promoter, this complex allows transcription regulation via several synergistic mechanisms. Long term transcription repression occurs via epigenetic silencing by remodelling and modification of chromatin<sup>5</sup>. Short-term regulation can be directly achieved by modifying RNA-polymerase II (Pol II) activity on adjacent RE1 regulated transcription sites<sup>6</sup>(Figure 2).

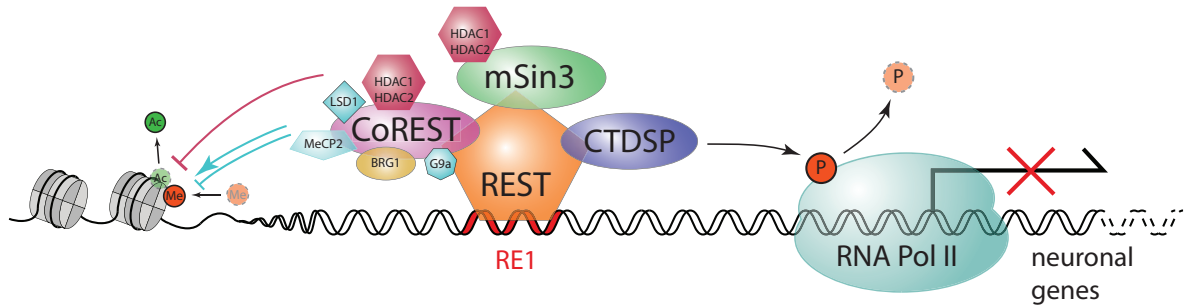


**Figure 2 The REST-complex in action**

The REST complex acting on RE1-controlled genes. Actions to the left show long term gene repression through epigenetic histone modification and chromatin remodeling. On the right, short term regulation through Pol II inactivation by dephosphorylation is shown.<sup>5,6</sup>

The epigenetic REST regulation is mainly accomplished by the recruitment of two repressing modules, the mSin3- and the CoREST-complex. The CoREST complex consists of two class I histone deacetylases (HDAC1 and HDAC2)<sup>7</sup>, the chromatin remodelling enzyme BRG1<sup>8</sup>, the histone H3K4 demethylase LSD1<sup>9</sup> and a methyl-CPG-binding-protein (MeCP2)<sup>7,10</sup>. The mSin3 complex recruits, like coREST, the acetylases HDAC1/2 and the retinoblastoma-associated proteins RbAp48 and -46 (also known as RBBP4 and RBBP7)<sup>11</sup>. These REST associated factors modify in the vicinity of their binding sites via reversible acetylation and methylation of histones (Figure 2)<sup>5</sup>.

Apart from chromatin remodelling REST can also directly impact on the core transcription apparatus by targeting Pol II. The C'-terminal domain (CTD) of the largest subunit of Pol II consists of multiple tandem hepta-repeats (YS<sup>2</sup>PTS<sup>5</sup>PS<sup>7</sup>), which form a docking platform for proteins regulating transcription. By changing the pattern of modification (phosphorylation, isomerisation) of these repeats, Pol is guided through the different stages of transcription (initiation, elongation, termination and RNA processing)<sup>12</sup>. For efficient initiation of transcription S<sup>5</sup> becomes phosphorylated. The REST-associated CTDSPs (C-terminal domain small phosphatases) counteract this event by dephosphorylating S<sup>5</sup>. As a consequence, transcription is inhibited<sup>6,12,13</sup> (Figure 2).

REST is the crucial factor that keeps neuronal gene expression under control in non-neuronal cells. To induce differentiation of NPGs into neurons therefore requires the gradual inactivation of REST and the activation of a neuronal gene expression program.<sup>6</sup> The process of REST inactivation is regulated at several levels including



the targeted degradation of subunits thereof. However, recent studies indicated that small regulatory RNAs likewise play a crucial role in this process.

### 3.2 Post transcriptional gene regulation via non coding RNAs

Noncoding RNAs have recently been recognized as key regulators in biological systems. Micro-RNAs (miRs) are the most prominent members of this family and have been implicated in widespread post-transcriptional regulation of protein-coding genes in modern eukaryotes<sup>14</sup>. miRs are typically 21 nucleotides in length and identify their targets via sequence complementary. Upon binding, they serve as a binding platform for effector proteins that either cause translational silencing or degradation.

In humans there are more than 400 confidently identified miRs<sup>15</sup> and each of those can regulate many target genes<sup>16</sup>. It is likely that more than half of all coding genes are in fact miR controlled, underpinning the importance of this class of post-transcriptional regulators. miR are genome-encoded and are found in introns or exons of genes or as independent transcription-units. Intron- and exon-encoded miRs are often under transcriptional control of their host genes. However, some intronic miRs do not show concordance with their host gene expression, suggesting that they are under independent transcriptional control as well<sup>17</sup>. A lot of miRs are in close proximity of other miRs and are transcribed as a single polycistronic unit, forming so-called miR clusters<sup>18</sup> (Figure 3).

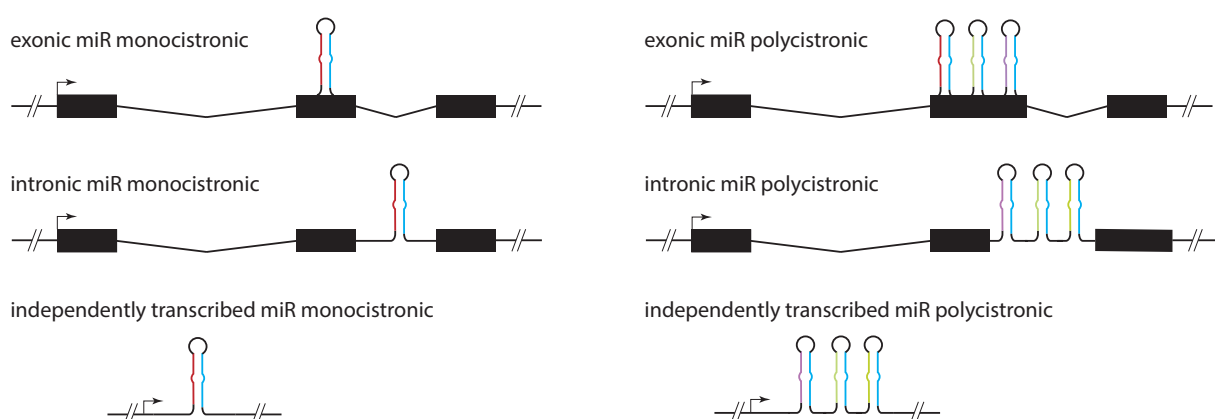


**Figure 3 Genomic organisation of miR genes**

miRs can be encoded in exons or introns in coding or non-coding genes. They also can be transcribed independently. In all cases they can appear alone (monocistronic) or in a cluster of several miRs (Polycistronic).

miRs stepwise undergo extensive processing before they are functionally matured (Figure 4). The primary transcript (pri-miR) is transcribed in many cases by Pol II and

acquires a m<sup>7</sup>G (7-methylguanosine) cap and a poly(A) tail<sup>19,20</sup>. However, a few human<sup>21</sup>- and virus<sup>22,23</sup>-derived miRs are transcribed by Pol III. The typical pri-miR is ~1 kb in length and contains an apical loop, a stem of 33-35 bp, and single stranded RNA (ssRNA) segments on both the 3'- and 5'- ends (Figure 4).

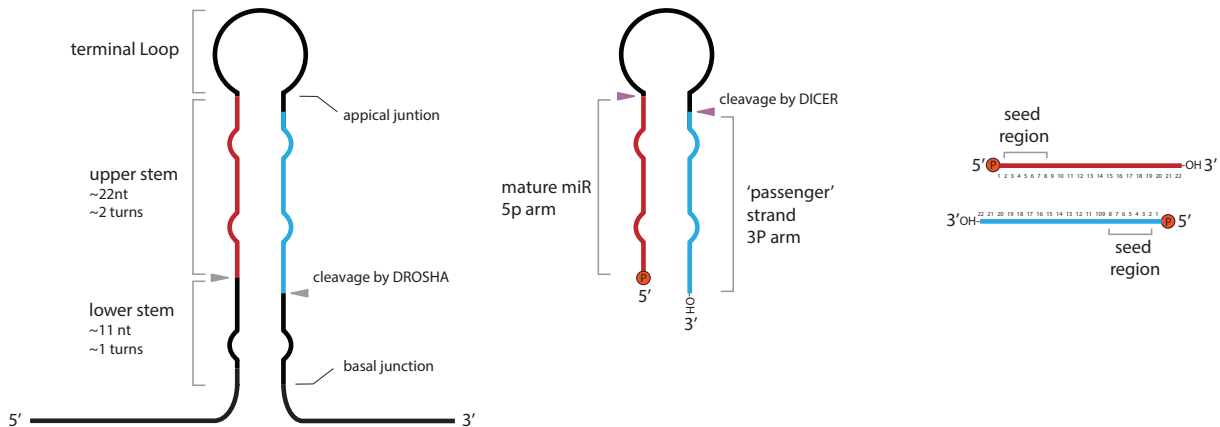


**Figure 4 miR processing**

**pri-miR** molecule (left) with, starting from the basal side, lower stem, upper stem and terminal stem. Drosha cutting site is between lower stem and upper stem (arrows) with 2 nt 3' overhang, around 11 nt away from basal junction. **pre-miR** (middle) forms hairpin structure. DICER cleavage occurs between terminal loop and upper stem (arrowheads) around 22 nt away from terminal ends. **Mature miR** duplex (right) indicated are both seed regions. One strand will become the mature miR active in RISC silencing, The other strand will be degraded. Here the 5p miR (red) is the exemplary mature miR and the 3p miR (blue) as the passenger miR.

The first miR-processing step is mediated inside the nucleus by the microprocessor complex. It cleaves the pri-miR to release a short hairpin termed precursor miR (pre-miR)<sup>24</sup>. The microprocessor consisting of one DROSHA protein and two DGCR8 (DiGeorge Syndrome critical Region 8) proteins<sup>25</sup> (Figure 5) recognises the stem loop structure of the pri-miR. DROSHA contacts the basal region where the stem bifurcates in single stranded RNA and the two DGCR8 proteins interact with the apical part of the precursor<sup>25,26</sup>. DROSHA is a class II RNase III enzyme and cleaves the pri-miR<sup>27</sup> at the 3' and 5' sides of the stem, thereby producing a characteristic 2 nucleotide 3' overhang<sup>27</sup>. The cleavage site is ~11 base pairs or one helical turn away from the junction where the stem separates into single stranded RNA, showing DROSHAs feature as a molecular ruler<sup>26,28</sup> (Figure 4). DGCR8 assists stable and site-specific miR binding of DROSHA thereby ensuring accuracy and efficiency of processing<sup>25,29</sup>. In case the pri-miR is located in an intron, the processing takes place co-transcriptionally prior to the splicing reaction<sup>30</sup>.

A DROSHA-independent processing pathway has also been described that utilizes the splicing machinery for pre-miR production. These miR genes are called mirtrons.

The 5' and 3'-end of the mirtrons display features similar to the 5' and 3'-splice junction of the adjacent exons. The formed pre-miR-lariat is debranched and refolds into a short hairpin (Figure 5)<sup>31,32</sup>. Some mirtrons have an extended 3' end. This prolonged 3' arm is trimmed by the exosome, yielding the correct precursor structure<sup>33</sup>.

Following pri-miR processing the resulting hairpin is exported into the cytoplasm, where the final steps of maturation takes place. The export is performed by exportin 5 (EXP-5), which binds in the presence of Ran-GTP to the pri-miR (Figure 5). EXP-5 recognizes only pre-miR having the characteristic 2 nucleotide 3' overhang generated by DROSHA cleavage, which ensures that only the properly processed intermediate is transported<sup>34</sup>. After translocation to the cytoplasm, Ran-bound GTP is hydrolysed, which leads to the release of the pre-miR and the dissociation of the complex<sup>35-37</sup>.

The 3' overhang is not only important for the export but is also necessary for further processing in the cytoplasm. DICER, another RNase III family member processes the pre-miR by cleaving both arms near the loop (Figure 4/5) DICER binds preferentially to the 3' overhang of the pre-miR generated by Drosha, and the cleavage takes place ~22 nt from the 3' termini (3' counting rule)<sup>38,39</sup>. If the pre-miR termini (especially the 5' end) is thermodynamically less stable (forming a fork-like end) DICER will cleave ~22 nt away from the 5' terminus (5' counting rule)<sup>40-42</sup>. The catalytic centre of DICER is similar to DROSHAs and generates 2 nucleotide 3' overhangs (Figure 4).<sup>39</sup> The generated small double stranded RNA duplex consists of the mature miR on one strand and a star (passenger) miR on the other strand. In most cases either only the 3' strand or 5' strand (termed 3p- or the 5p- arms) functions as miR (Figure 4),<sup>43-45</sup> but in rare cases both arms or even loop-derived sequences are used<sup>46,47</sup>.

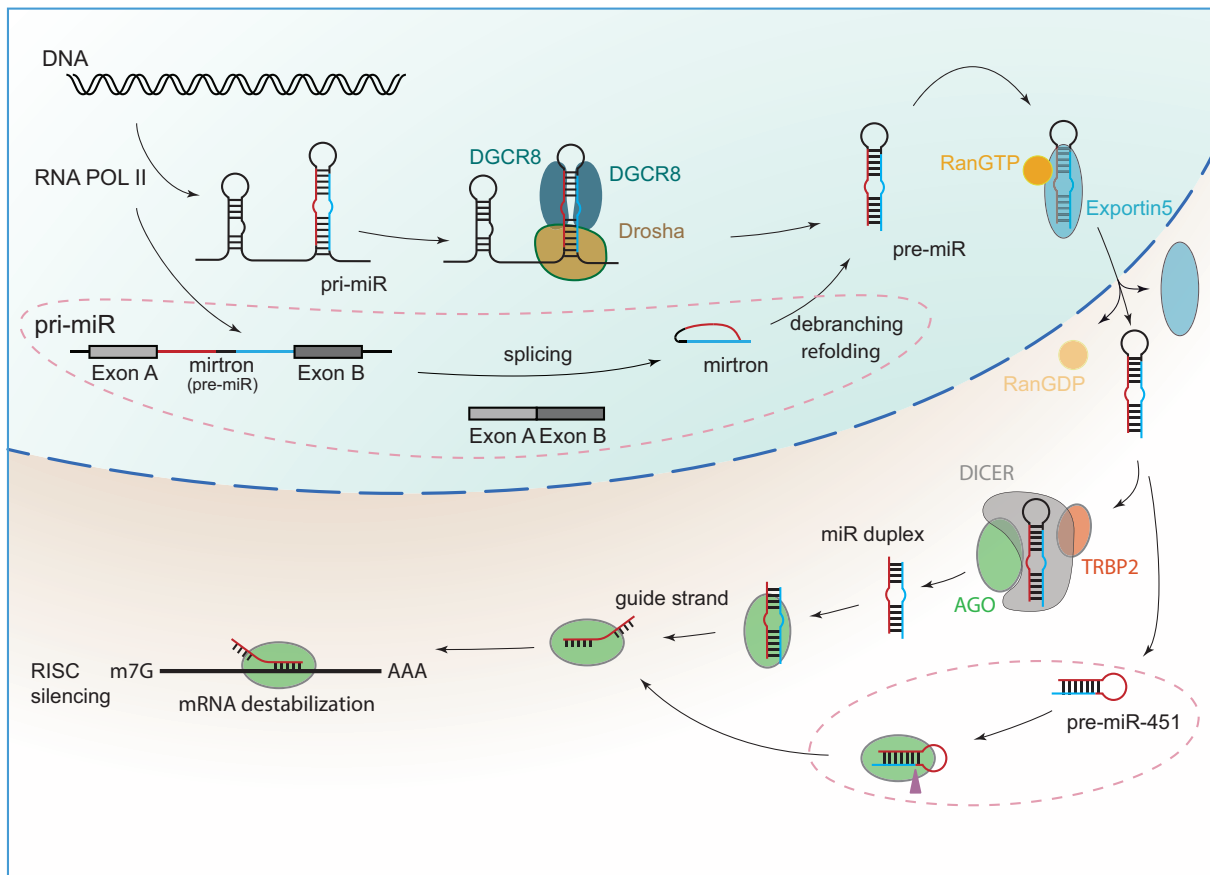


**Figure 5 Vertebrate miR Biogenesis**

In vertebrates, the primary miR transcript (pri-miR) is stepwise processed by nucleases of the ribonuclease III family, to form mature miR. The first processing step is done by Drosha in interplay with DGCR8 inside the nucleus, which leaves a ~65-nt long stem loop precursor with a two-nucleotide overhang at the 3'-end. This hairpin structure is then exported out of the nucleus via the Exportin5/Ran complex and further cleaved by Dicer. One strand of the resulting duplex is loaded into Argonaute (AGO) and forms the RNA-induced silencing complex (RISC), which leads to destabilization of target mRNA. During canonical miR biogenesis regulation can occur at various stages. A Drosha independent processing is indicated, where pre-miR arise as splicing by-products. Dicer independent processing is shown for the miR-451, which is processed by active AGO2. Non-canonical processing steps are encircled red. Mature miR indicated as red, passenger strand indicated as blue.

So far there are two RNA binding proteins (RBPs) that can interact with DICER, TRBP and PACT<sup>48,49</sup>. Both cofactors do not seem to be essential for DICER processing, as recombinant DICER shows similar processing activity compared to the DICER-RBP complexes<sup>49</sup>. However, TRBP is able to tune the length of mature miR generated by DICER<sup>50</sup>.

Once the miR is properly processed, it can interact with proteins to form its effector complex, the RNA induced silencing complex (RISC). Crucial effector proteins of RISC are members of the highly conserved Argonaute family (AGO)<sup>51-53</sup>, which bind the miR whereas the passenger strand is degraded (Figure 5). Generally, the side of the duplex which possess the thermodynamically less stable terminus at the 5' end of

the duplex is selected as miR and is loaded onto AGO<sup>54,55 56</sup>. Upon loading the miR serves as a sequence specific guide towards the RISC target.

### 3.2.1 miR targeting and mode of function

The RISC silencing complex leads to post transcriptional repression of target mRNAs. It is a multi protein complex that uses a single stranded RNA (here miR) as a template to recognise complementary mRNA. The main effector proteins of the complex are members of the AGO family.

Essential for targeting and miR specificity are the nucleotides 2 – 8 of the mature miR strand. This so called ‘seed region’ guides the miR to base pair complementary sites in the 3'-UTR of mRNA targets<sup>57,58</sup> (Figure 4). miR-loaded AGO efficiently scans mRNAs for target sites in the transcriptome. For initiation of AGO target recognition interactions of only 3 nucleotides (nt 2-5) are sufficient. This sub-seed pairing is then superseded by the even more stable seed pairing (nt 2-8)<sup>59-61</sup>. AGO facilitates base pairing by bending the nucleotide backbone of the seed region and displaying the nucleotides in a more open structure<sup>62</sup>.

RISC bound to mRNA can negatively alter gene expression in two ways: via translational repression or target degradation. miR mediated translational repression is mainly achieved through inhibition of cap-dependent translation initiation<sup>63,64,65</sup>. How this is achieved on a molecular level is still a matter of intense research<sup>56</sup>.

The miR mediated mRNA degradation can occur directly by AGO II cleavage or, more commonly, by recruiting deadenylation complexes. mRNA degradation through the slicer activity of Ago II depends critically on the high degree of complementarity of miR to its target sequence<sup>66,67</sup> (Figure 6). A bioinformatics investigation of miRs and their targets in vertebrates revealed, however, the degree of complementarity on average is rather low and confined to the seed region. This partial complementarity still allows specific RISC binding to its target but does prevent direct Ago cleavage. (Figure 6).

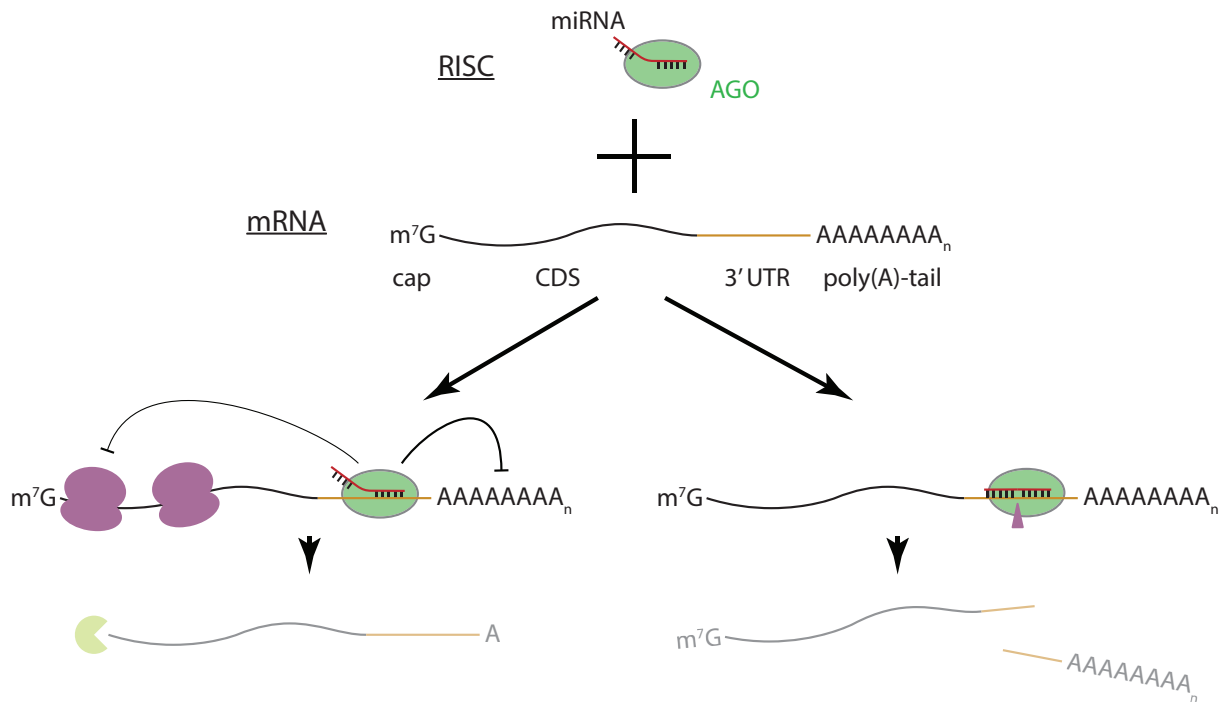


**Figure 6 functionality of the RNA induced silencing complex**

Depending on the miR target complementarity the RISC can act on its targets in two ways. Seed (6mer to 8mer) pairing leads to deadenylation decapping and subsequent degradation of mRNA. Additionally it can block the initiation of translation of the mRNA. Higher match miR target mRNA pairing lead to AGO II mediated cleavage in the 3' UTR which highly destabilizes the mRNA.

At the core of this regulation is the recruitment of GW182 to RISC by AGO. In vertebrates the GW182 family comprises three paralogues, named trinucleotide repeat-containing 6 protein A (TNRC6A), TNRC6B and TNRC6C<sup>56,68,69</sup>.

Once recruited to RISC bound to mRNA, GW182 can bind to two major mRNA deadenylation complexes, PAN2-PAN3 and CCR4-NOT-CAF1. The deadenylation of target mRNAs is followed by decapping (via DCP2) and subsequent 5' to 3' decay (via XRN1).<sup>70,71</sup> Additionally, GW182 inhibits the closed loop formation on translating mRNA by interacting with the poly-A binding protein PAPBC<sup>70,72</sup>.

miRs are also involved in a unique way of reversible post transcriptional gene silencing. Upon binding to their mRNA targets, some miR can mediate their specific sequestration in subcellular cytosolic domains termed processing bodies (P-bodies). mRNAs targeted to these sites are prevented from translation and can either be re-activated in response to appropriate signals or degraded.<sup>73,74</sup>

### 3.3 The role of miR in neurogenesis

As outlined in chapter 3.1 neurogenesis is facilitated in vertebrates through the initiation of a specific gene expression program. A crucial factor in this event is the REST complex, which acts at the transcriptional level to prevent the expression of

neuronal genes in non-differentiated cells. To initiate neurogenesis, REST is gradually inactivated to allow the neuronal gene expression program to start<sup>75</sup>.

Apart from these transcriptional mechanisms more recent data support the idea that miRs likewise play a critical role in neurogenesis. In fact miR have been shown to be important at almost every step in neurogenesis including neuronal lineage commitment (let-7, miR-7, miR-9, miR 124), to promote neuronal differentiation (miR-23, miR-200, miR-279) and inhibit cell proliferation (miR-9, miR-124, miR-125).<sup>76</sup>

A specific set of miRs influence neurogenesis by directly targeting components of the REST complex (REST-miR). The miRs 9 and 9\* (3p- and 5p-arm of miR-9) have been shown repress REST and coREST and thus interfere with all functions for the repressor complex. miR-124 and miR-132, in contrast selectively repress the Pol II regulator CTDSFs<sup>46,77,78</sup> and the chromatin modifier MeCP2<sup>77,79</sup>, respectively.

The level of these miRs typically increases during neuronal differentiation and brain development<sup>77,80</sup> and, as a consequence, the activity of the REST-complex declines<sup>6,77</sup>. Interestingly, even though these miRs regulate REST, their encoding genes are under control of RE1 elements and thus controlled by REST. A critical question is hence how this negative feedback loop is interrupted to set in train neurogenesis. Recent studies performed in zebrafish raised the possibility that the miR-26 family may serve this function.<sup>81</sup>

### 3.4 miR 26 family

The miR-26 family encompasses miR-26a and miR-26b and has been shown to regulate a large variety of cellular processes including proliferation, cell cycle process and apoptosis<sup>82-86</sup>, neurite outgrowth<sup>87</sup>, axon regeneration<sup>83</sup> and long-term potentiation maintenance<sup>88</sup>. This miR family has also implicated in major human diseases such as Alzheimer and cancer.<sup>89,90,91</sup>

In adult vertebrates, miR-26 is ubiquitously expressed with particular high expression levels in neuronal tissue<sup>92-95</sup> (Figure 29). In zebrafish however, mature miR-26 cannot be detected until the onset of neurogenesis<sup>81,95-97</sup>. Also in retinoic acid (RA)- induced differentiation of murine P19 teratocarcinoma cells the pre-miR is robustly expressed over differentiation, but the mature miR shows only minute amounts in early differentiation and higher amounts in later stages. Interestingly, this is due to the fact that the processing of all miR-26 family members is arrested at the precursor level, i.e. at the level of DICER processing. Upon induction of neurogenesis, however, processing of miR-26 is initiated via an unknown mechanism. Inactivation of miR-26

in zebrafish results in impaired formation of secondary neuron but has no effect on NPCs neurogenesis linking miR-26 to terminal differentiation of neurogenesis<sup>81</sup>.

An interesting feature of all miR-26 family members is that they are encoded in introns of genes encoding for various isoforms of the REST-associated effector protein CTDSP. Furthermore, all mRNAs encoding CTDSPs contain in their 3' UTR multiple binding sites for miR-26, thus providing the basis for an ultra-short negative feedback loop. This feedback loop is inactive in non neuronal tissue and NPC but gets activated as soon as the pre-miR get processed and forms the mature miR-26 during final neuronal differentiation steps (Figure 7)<sup>81</sup>.

These results indicate that the miR-26 family plays a major role for the terminal neuronal differentiation, and that this impact comes from its host feedback interactions and its subsequent REST-complex regulation.

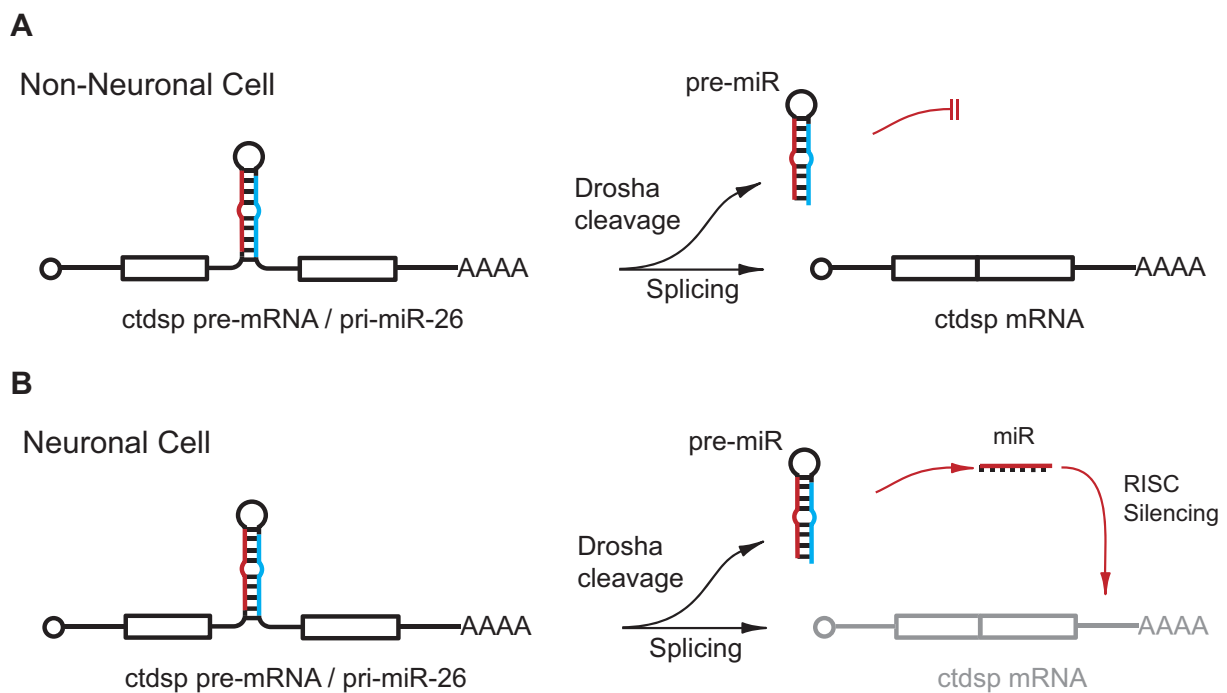


**Figure 7 miR-26 and CTDSP regulatory feedback loop**

**A** in non-neuronal cells or NPCs, CTDSP is transcribed with the intronically encoded miR-26. While the mRNA gets spliced the pre-miR-26 is not processed further. **B** in neuronal cells the pre-miR gets processed further and gives rise to the mature miR which that can negatively regulate CTDSP mRNA.

### 3.5 Aim of thesis

As outlined above, the investigation of miR-26b in zebrafish revealed a critical role of this miRNA in neurogenesis. The picture that emerged is that miR-26b (and probably other members of this family) are expressed as part of the CTDSP pre-mRNA and deposited in the early embryo as inactive pre-miR. Upon induction of neurogenesis,



processing is activated and mature miR-26 sets in train of events that allow the neuronal gene expression program to start.

Based on these findings, two major questions arise, which will be addressed in this thesis. In the **first part** of my thesis, I will focus on the question how the processing of miR-26 is regulated and how the spatio-temporal expression of miR-26 required for neurogenesis is established.

Several scenarios appear possible and will be addressed experimentally.

**a) miR-26 processing is prevented by retention of the pre-miR in the nucleus.**

Pre-miR are formed in the nucleus and only can be processed up on export in the cytoplasm. The accumulation of pre-miR-26 in NCS may hence be a consequence of the specific nuclear retention of pre-miR26. I will test this possibility by microinjection studies in *Xenopus laevis* oocytes, which allows the direct analysis of export nuclear injected radio-labeled miR-26.

**b) miR-26 DICER processing is inhibited by a trans-acting factor.** Alternatively, inhibition of DICER processing interferes with miR26 maturation. This might be achieved by preventing DICER binding or the modification/alteration of the miR-precursor. Such mechanism has been reported for the regulation of the miR let-7. The factor lin-28 blocks DROSHA as well as DICER processing<sup>98,99 100,101</sup>. Lin28 can also alter let-7 levels by recruiting the enzyme TUT4, which polyuridylylates miR and causes its degradation<sup>102,103,104</sup>.

I will use a combination of enzymatic assays as well as biochemical approaches to identify potential trans-acting factors interfering/enabling miR-26 processing. Extracts derived from murine ESC or zebrafish embryos defective in miR-26 processing will be used to affinity-purify pre-miR-26 binding factors by proteomics approaches. Candidates will then be tested for binding specificity, expression during development or differentiation and regulatory effect on miR-26 abundance.

In the **second part** of my thesis, I will focus on the question whether miR-26 functions as an upstream regulator of REST repression and thus acts as a master switch in the neuronal gene expression program.

To address this question a cell culture based neural differentiation protocol will be established that allows the differentiation of NSC to mature neurons. These studies will be performed together with the group of Prof. Albrecht Müller, (Zentrum für Molekulare Medizin, University of Würzburg). Using this cell culture system we will

use CRISPR/CAS knockout technology to investigate at the systems biology level the role of the miR-26 members in neurogenesis. We will evaluate global RNA-Seq datasets (non-coding and coding). This will help our understanding of the genetic programs that are regulated by the miR-26 family. Based on the miR-26 KO-induced gene expression changes we will validate targets and we will perform pharmacological rescue approaches in neural differentiating KO cultures.

## 4 Results

### 4.1 Investigation of miR-26 biogenesis regulation

Earlier studies by several labs have provided clear evidence for a role of the miR-26 family in neurogenesis<sup>81,94,105</sup>. These data indicated that members of this family are present as precursors in zebrafish even at very early developmental stages when the nervous system has not been developed. However, conversion of the precursors to the mature form of miR-26 is initiated when NPCs are formed at 24 hours post fertilization (hpf)<sup>81</sup>. This scenario strongly suggests that regulation of miR-26 maturation is a key event in an initial phase of neurogenesis and it is likely to occur in the phase between DROSHA cleavage and AGO loading (Figure 8 brackets). In the first set of experiments, I addressed the question how the conversion of pre-miR26 to mature miR26 is regulated. I considered several scenarios:

- 1) **Regulation of miR-26 maturation at the level of nucleo-cytoplasmic transport.** As DICER processing is restricted predominantly to the cytoplasm, a regulated nuclear export of the pre-miR would allow the spatio-temporal expression of mature miR-26 (Figure 8-1).
- 2) **Direct regulation of pre-miR-26 processing.** DICER, as the processing enzyme might be inactive or regulated at early developmental stages. Processing might be inhibited by one or several factors in *trans* that bind specifically to miR-26 family members. This suppression would be released upon entry into the differentiation process (Figure 8-2). Likewise, it is possible that miR-26 requires specific processing factors enabling their maturation in a spatio-temporal fashion.
- 3) **Regulation by limited Argonaute protein.** If the concentration of AGO, the factor that accepts the mature miR, is a limiting factor, miRs could not be incorporated into RISC and presumably would be degraded (Figure 8-3).

In the following paragraphs I will analyze these regulation possibilities.

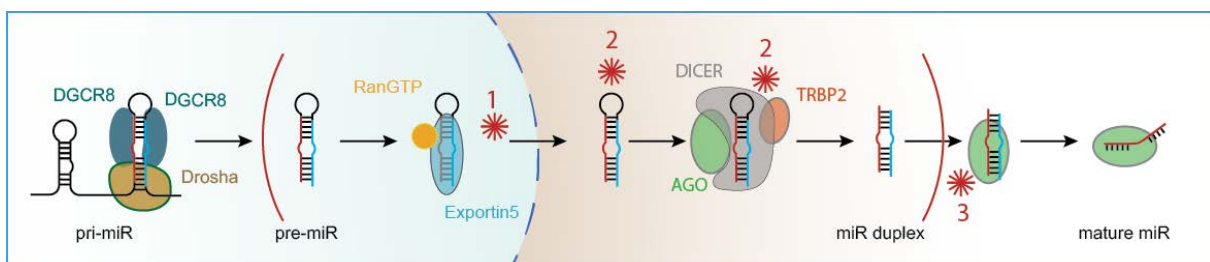


**Figure 8 Possible processing regulation scenarios**

A schematic of the canonical miR processing pathway in animals. Indicated are the possible points of regulation. **1** pre-miR export **2** DICER processing of the pre-miR **3** Limited AGO concentration

To enable these analyses, I first investigated the degree of conservation of the pre-miR-26 in vertebrates. A high degree of conservation does imply that also associated, regulatory mechanisms are conserved. This would give me the opportunity to utilize different experimental model systems such as zebrafish or *Xenopus laevis* to study the different scenarios summarized above.

To this end the sequences of the miRs of human, mouse, Zebrafisch and *Xenopus* were aligned using sequences from Ensembl (<http://www.ensembl.org/index.html>; release 90). These alignments revealed a high degree of conservation for the miR-26 family in all vertebrates (Figure 9A)<sup>106</sup>. The difference between miR-26a and miR-26b is the nucleotide at the 21<sup>st</sup> position, where 26b has a C instead of a U. Mammalian miR-26b has a U in position nine whereas the zebrafish miR-26b has a C. *Xenopus laevis* has only one miR-26, which is equivalent to miR-26a. All variations in the miR sequences occur not in the seed region (nucleotides 2 to 7), which is most important for target mRNA binding<sup>107</sup>.

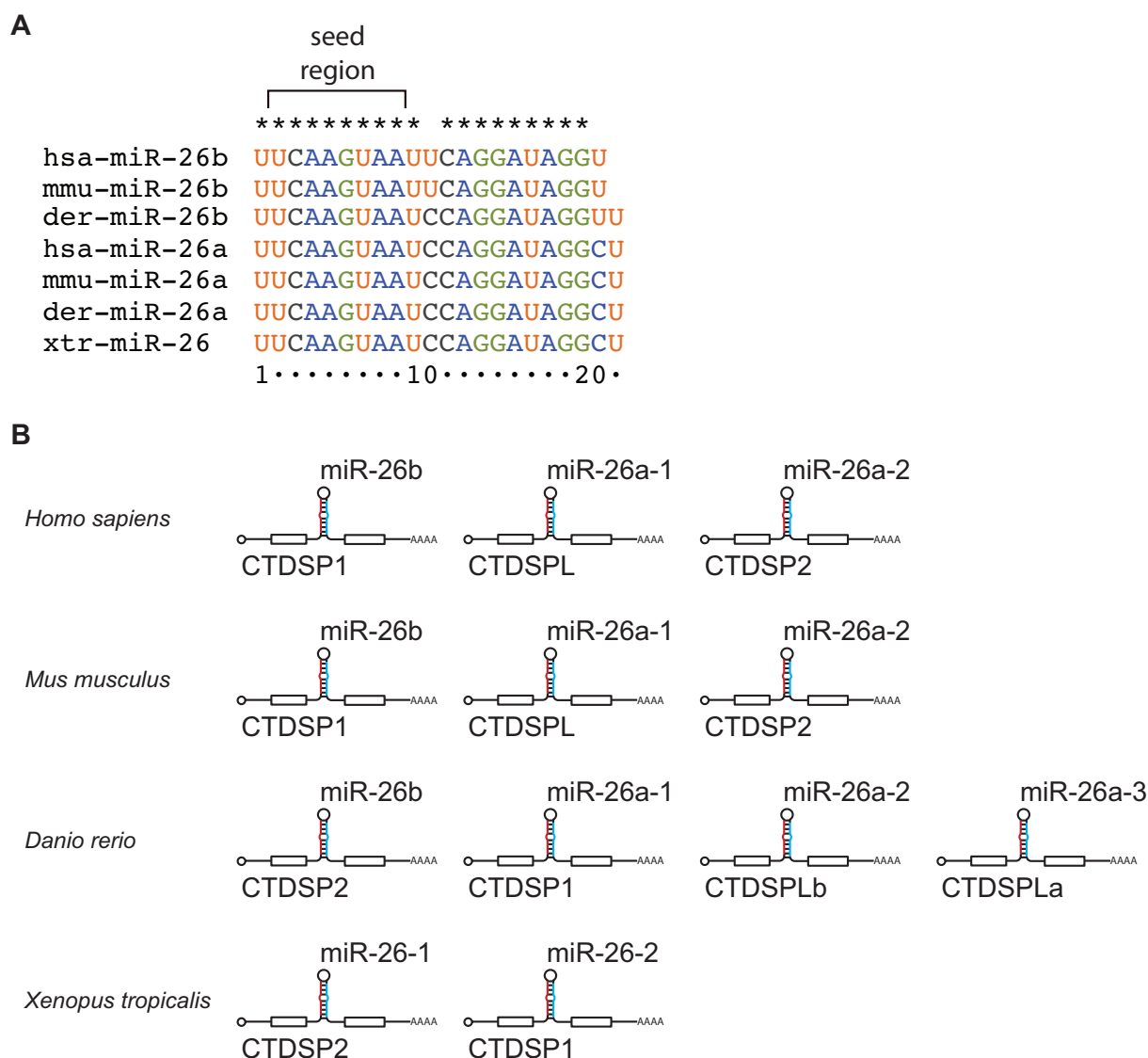


**Figure 9 The miR-26 family is highly conserved in vertebrates**

**A** Multiple sequence alignment of the miR-26 family members in human (hsa, *Homo sapiens*), mouse (mmu, *Mus musculus*), zebrafish (dre, *Danio rerio*) and *Xenopus* (xtr, *Xenopus tropicalis*). Conserved residues are indicated with an asterisk. The seed region is marked with a bracket. **B** Genomic localization of pre-miR-26 in its host gene CTDSP in indicated organisms.

Of note, not only the sequences are highly conserved in vertebrates but also their genomic localization. Thus, all miR-26 analyzed are intronically encoded in CTDSP genes. From earlier studies it has been known that miR-26 production is regulated through transcription of its host gene CTDSP and does not have an individual promoter<sup>108</sup>. While human and mouse have three miR-26 genes (26b, 26a-1 and 26a-2) in three CTDSP loci (ctdsp1, ctdspL and ctdsp2), zebrafish has four copies (26b, 26a-1, 26a2 and 26a-3) in 4 ctdsp loci (ctdsp2, ctdsp1, ctdsplb and ctdspla) and *Xenopus* has two copies (26-1 and 26-2) in two ctdsp loci (ctdsp2 and ctdsp1)(Figure 9A).

The conserved miR-26 sequences and the similar intronic encoding in CTDSPs in vertebrates strengthen the argument that also miR-26-associated, regulatory mechanisms are conserved. This enables the investigation of the miR-26 regulation and its impact on neural development in several vertebrate model organisms.

#### 4.2 pre-miR-26 nuclear export is indistinguishable from export of other miRs upon micro-injection into *Xenopus laevis* oocytes

In a first set of experiments, I tested whether miR26 processing is halted at the precursor level, because its nucleo-cytoplasmic transport is blocked. In this case, the miR would not reach the cytosolic compartment where canonical DICER processing takes place<sup>109</sup>.

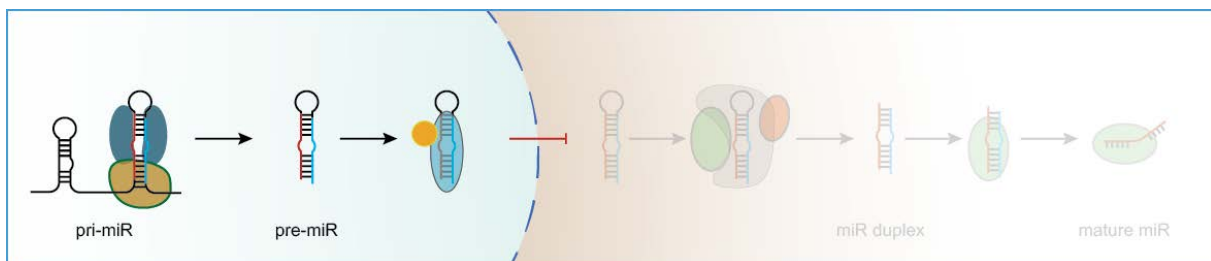


**Figure 10 Retained pre-miR export as pre-miR processing regulation**

Canonical miR processing with inhibition of export. Effected processing steps are shaded.

To analyze pre-miR-26 processing and transport, I chose microinjection experiments in *Xenopus laevis* oocytes, which is the classical model system to study export<sup>110</sup>. A mixture of radiolabelled RNA (dyed with dextran-blue) was injected into the nucleus of stage 5/6 oocytes. The mixture contained the pre-miR and also the U6 snRNA, which is retained in the nucleus, and a U1 snRNA mutant (termed U1 $\Delta$ Sm), which is rapidly exported via the Crm1 export pathway but not re-imported<sup>111</sup>.

The nucleus and the cytosol were isolated after 60 min incubation (Figure 4B) and RNA from either compartment was isolated, separated by denaturing gel electrophoresis and visualized by autoradiography (Figure 11A, C). In all experiments, the U6 snRNA remained entirely nuclear, indicating that the microinjection occurred precisely to the nucleus no leakage had occurred (Figure 11C). The U1 $\Delta$ Sm in contrast was exported to the cytoplasm showing that the oocytes were export competent (Figure 11C). Interestingly, not only control pre-miRs (-430b and -31b) were efficiently exported but also pre-miR-26b (Figure 11C). Of note, the export efficiency (Figure 11C) and kinetics (data not shown) were found to

be very similar for all injected pre-miR. These results rule out that blocked or delayed nucleo-cytoplasmic transport of pre-miR-26 is responsible for the processing delay during early development in *Xenopus laevis*. Given the high conservation of this miR (see 4.1, Figure 9) I hypothesize that this is also the case in other vertebrate systems.

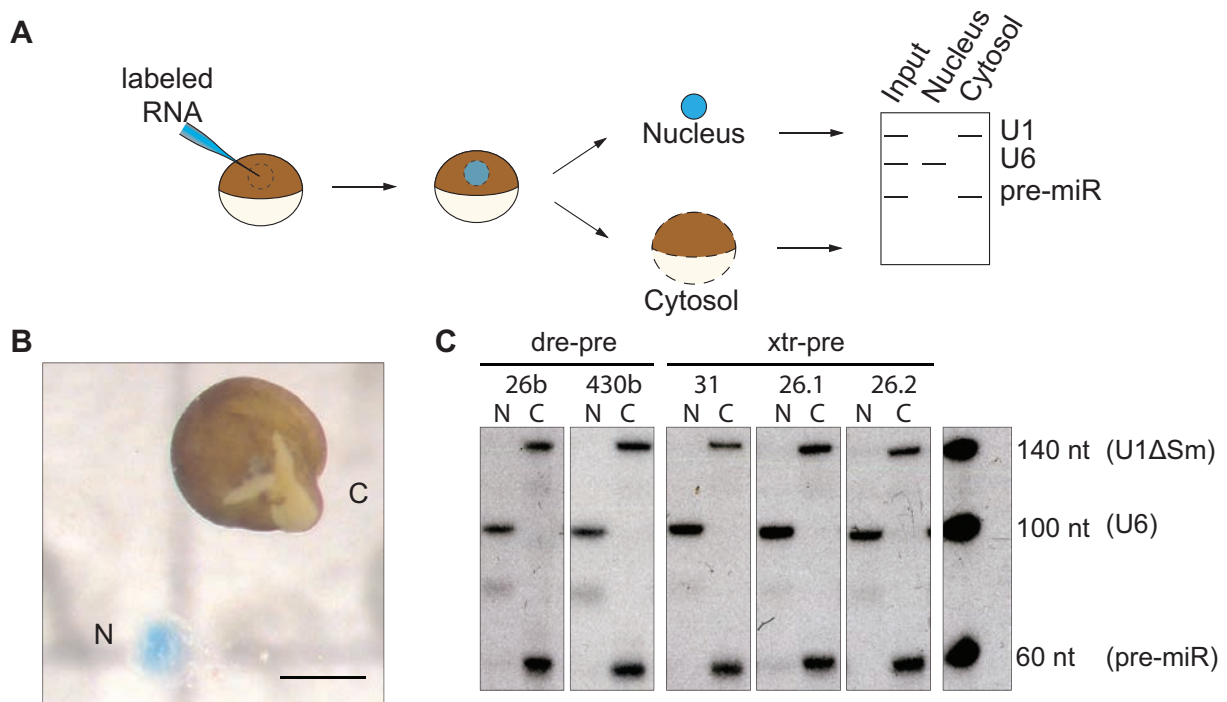


**Figure 11 pre-miR export assay**

**A** *Xenopus* nuclear injection strategy. A mixture of radiolabelled RNAs was injected into the nucleus of oocytes and manually dissected after incubation. The RNA is isolated from the fraction, separated and visualized. **B** Dissected oocyte showing the injected nucleus (N) and the cytosol (C). **C** Oocytes were injected with a mixture of radio-labeled zebrafish<sup>112</sup> pre-miR-26b, pre-miR-430b, *Xenopus* (xtr) pre-miR-31, pre-miR-26.1, pre-miR-26.2 and U1ΔSm and U6. The export was monitored 60 min after injection by separation of isolated RNA on a denaturing gel and autoradiography.

### 4.3 pre-miR 26b is not processed in early zebrafish embryos: indication for an inhibitor of miR-26 maturation

In the next set of experiments I tested the regulation of miR-26 processing. To elucidate whether the processing is regulated by a trans-acting factor or if DICER itself is inactive I investigated miR-26 maturation in early zebrafish embryos using a combination of *in vivo* and *in vitro* approaches (Figure 13A).

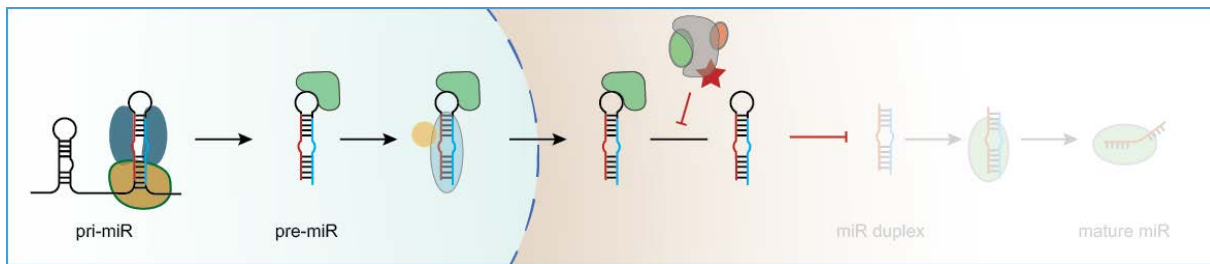


**Figure 12 pre-miR processing regulation by regulated pre-miR or DICER**

Canonical miR processing is inhibited by inhibition of DICER processing by either a pre-miR binding protein or by inactivated DICER. Effected processing steps are shaded.

First, DICER processing of pre-miRs was investigated in an *in vivo* assay. Radiolabelled pre-miR 26 and miR-430 as a positive control (miR-430 is processed in early embryogenesis<sup>113</sup>) were injected into one cell stage zebrafish embryos (20' after fertilization) and incubated for 30 and 60 min. Injected RNA was then isolated, separated by denaturing gel electrophoresis and visualized by autoradiography. Pre-miR-430 (Figure 13B) was efficiently processed as evidence by the appearance of RNA products with the length between 21 and 24 nucleotides shows.

This finding is consistent with the presence of mature endogenous miR-430 in the early zebrafish embryo. Very similar observations were made for pre-miR-9-1, pre-miR-124, pre-miR-92a, pre-miR-92b and the *Xenopus* pre-miR-451 (data not shown). In striking contrast, no processing of injected pre-miR-26 was observed (Figure 13B). This demonstrates that DICER is active in early zebrafish development and can process pre-miRs. However, pre-miR-26 is not available as a DICER substrate at this stage.

In my next set of experiments I tested whether the pre-miR-26 can be processed at later developmental stages. For this I incubated pre-miR-26b and pre-miR-430 *in vitro* in a lysate derived from 24 hours-old embryos. At this time point neurogenesis starts in zebrafish and maturation of endogenous pre-miR-26b was previously observed by northern blot analysis<sup>81</sup>. As shown in Figure 13C not only the exogenously added control miR-430 but also miR26b were processed with comparable efficiency.

These experiments show that DICER is active throughout the entire phase of early zebrafish development. The fact that pre-miR-26b is only processed in extracts from 24 hours old embryos but not at the single stage is consistent with the model where miR-26 processing is regulated by (a) trans-acting factor(s). These results strongly suggest that a maternal factor regulates miR-26 processing, most likely by binding



to the precursor molecule and preventing its processing by DICER similar to Lin28<sup>98,102</sup>.

Limiting AGO protein levels, however, is less likely to be responsible for the absence of mature miR-26<sup>114</sup>.

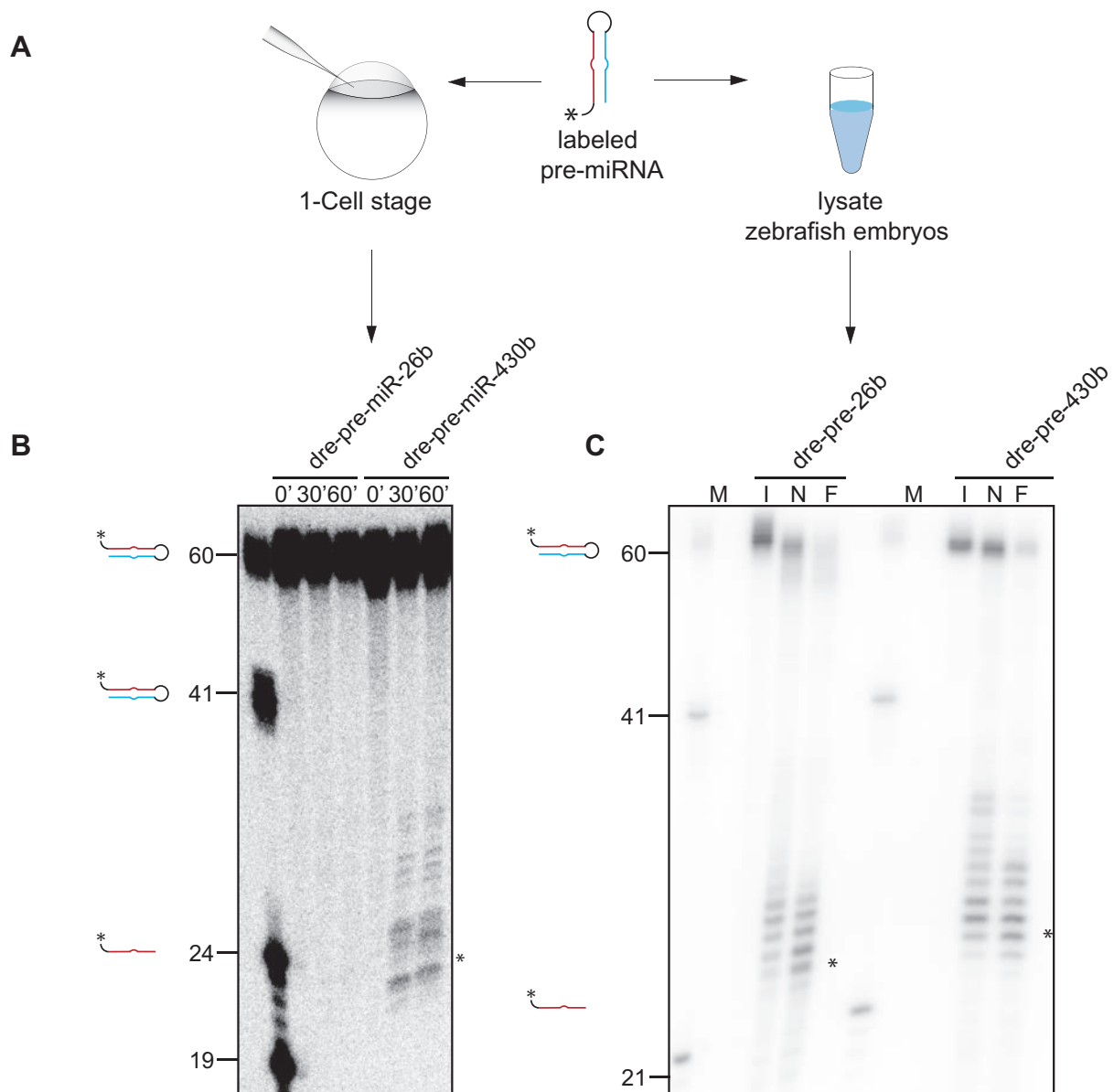


**Figure 13 Zebrafish *in vivo* and *in vitro* pre-miR cleavage assay**

**A** DICER cleavage assay strategy. *In vivo* assay: Injection of radiolabelled pre-miR in one cell stage zebrafish (left). *In vitro* assay: incubation of radiolabelled pre-miR in zebrafish lysate. **B** Autoradiograph of an *in vivo* processing assay of pre-miR-26b and pre-miR-430b. RNA was isolated and separated on a sequencing gel. **C** Autoradiograph of an *in vitro* processing assay of pre-miR-26b and pre-miR-430b. RNA was isolated and separated on a sequencing gel.

#### 4.4 Identification of miR-26 regulatory proteins

Based on the findings described above different affinity strategies were employed to biochemically isolate pre-miR-26 trans-acting regulatory factors from early embryo

extracts. To this end I immobilized zebrafish and murine pre-miR on streptavidin coated beads using two different but complementary strategies (Figure 14A).

In a first approach pre-miR with a short 5' extension was transcribed *in vitro*. A 3' biotinylated 2'-O-methyl-DNA hook, which is complementary to the extended 5' end of the pre-miR, was used to immobilize the precursor to the beads (Figure 14A, up)<sup>102,115</sup>. As a second strategy I directly bound the RNA on streptavidin beads using an RNA aptamer. I used either a S1 aptamer on the 5' end of the pre-miR (Figure 14A, middle)<sup>116</sup> or a S1m in the precursor loop (Figure 14A, down, see 6.2.6.15)<sup>117</sup>.

The different pre-miRs were immobilized on streptavidin beads and subsequently incubated with murine or zebrafish lysate for 30 and 60 min. After removing non-bound components by extensive washing, bound proteins were eluted and identified by mass spectrometry (Figure 14B).

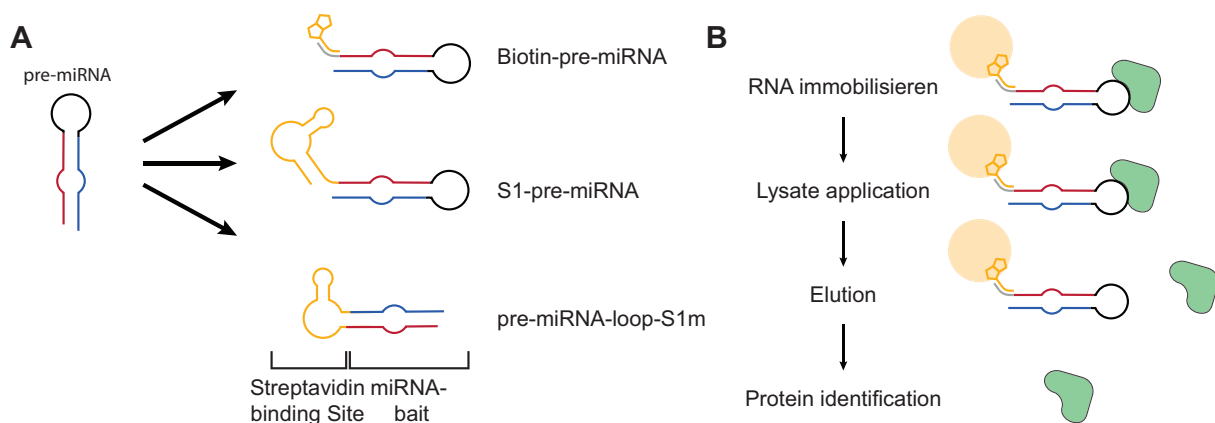


**Figure 14 Methods used for the identification of miR-26 regulatory proteins**

**A** RNA modification for streptavidin immobilization. 5' prolonged pre-miR with complimentary biotinylated hook<sup>118</sup>, 5' prolonged pre-miR with S1 aptamer (middle) or pre-miR with mS1 aptamer as loop (down). **B** Immobilization strategy: modified RNA is immobilized with streptavidin and incubated with lysate. Bound proteins were washed, eluted and identified.

#### 4.4.1 Identification of miR hairpin binding proteins using the indirect binding approach

In a first attempt to identify miR-26 binding factors by affinity chromatography, I used lysate of 6 hpf old zebrafish embryos since processing of pre-miR-26b is inhibited in these extracts<sup>81</sup> (see also above). The extract was incubated with beads carrying immobilized pre-miR-26, a pre-miR-26 loop mutant and pre-miR-430, miR-21 (hsa) and miR-let7 (hsa) as controls. After extensive washing, bound proteins were eluted and separated by SDS-PAGE (Figure 15A). A miR-26 binding factor is expected to be of low abundance so the non-specific background exceeds by far specific protein bands when analyzed on SDS gels.

---

Accordingly, the protein pattern among the different experiments was very similar and a more sophisticated analysis detecting also less abundant proteins was required. For this, we used a mass spectrometry based analysis. For every pre-miR used as a bait and the pre-cleared sample at least two technical replicates were generated. The proteomic data from the pull down experiments were ranked using the (blue heat map) values obtained by the mass spectrometry analysis. Identified proteins that also exhibited hits in both pre-clear samples were marked as unspecific binders and removed as well as proteins that were enriched in all samples. Candidate proteins with a potential affinity for a specific hairpin with multiple hits in the replicates were sorted by unsupervised hierarchical clustering (Figure 15B, see 6.2.6.15). The well-characterized let-7 pre-miR served as a positive control, because it has been shown previously to bind specifically to lin-28<sup>98,102</sup>. 10 candidates were identified that were enriched in the pre-miR-26 probes (Figure 15B). Out of these the protein ZNF346 was the most promising candidate due to its high score and its known RNA binding function<sup>119</sup>. ZNF346 was also enriched in purifications from a lysate obtained from 24 hpf old zebrafish (data not shown), when pre-miR-26 processing repression is still observed.

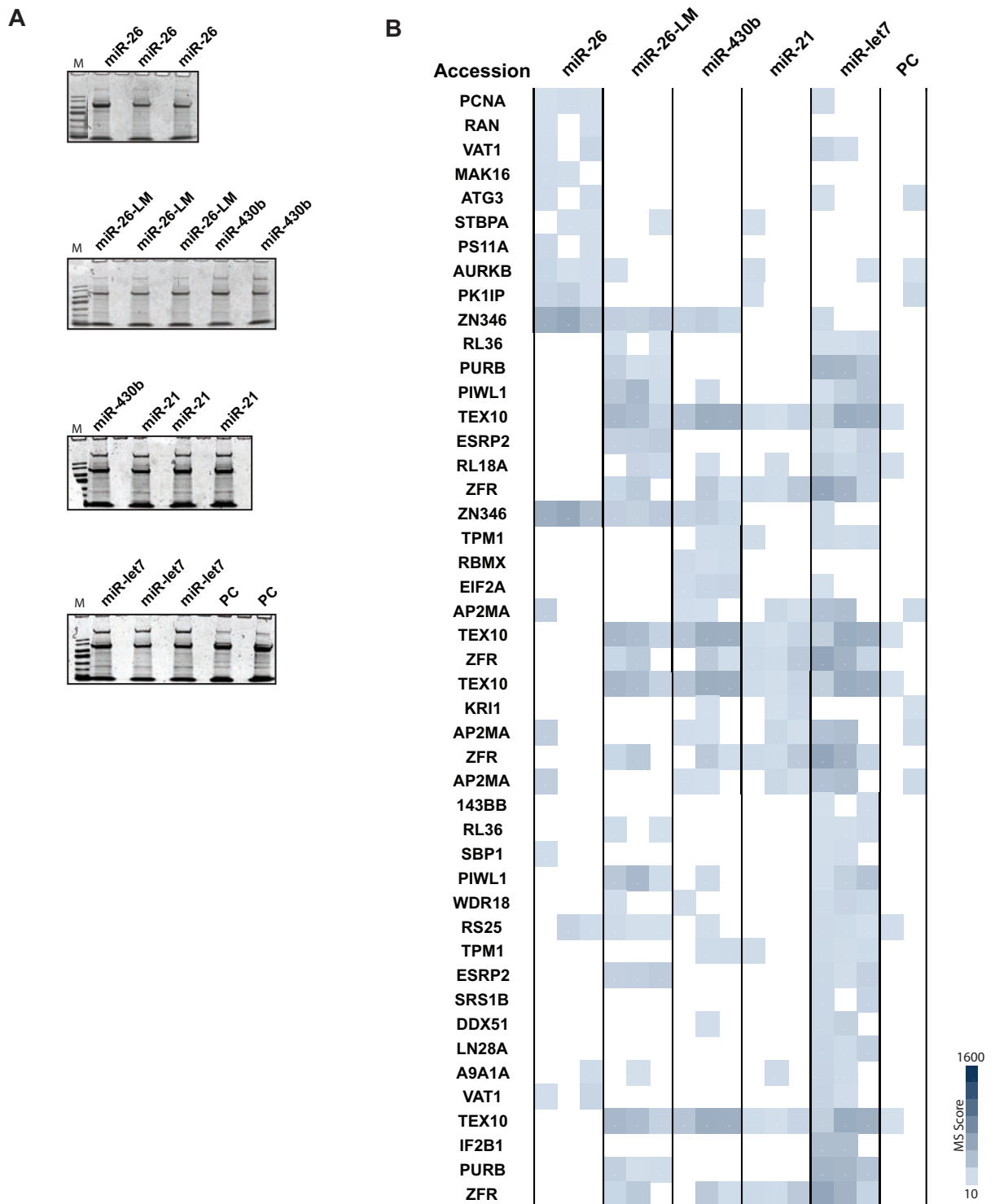


**Figure 15 miR Hairpin binding proteins in 6 hpf Zebrafish**

**A** Coomassie-stained SDS-PAGE of miRNPs of zebrafish miR-26b, loop mutated miR-26b, miR-430b and human let7 and miR-21. **B** Interacting proteins (gene symbols on the left) identified in 6 hpf zebrafish extracts using immobilized RNA hairpins, which are indicated on top. Mass spec score counts are indicated in blue.

In order to identify pre-miR-26b binding proteins in higher vertebrates I repeated the affinity purification in undifferentiated murine P19 cells. Like in early zebrafish development the miR-26b is halted at the precursor level in these cells<sup>81</sup> (see also

above). The experiment was performed as described above for the targets pre-miR-26a and pre-miR-26b and the controls pre-miR-29a1 and pre-miR-184-1 (Figure 16A). The bound proteins were further analyzed by mass spectrometry and scored according to their protein count, as described above. The affinity purification with immobilized pre-miR-26a hairpin showed 5 proteins with high scores, including ZNF346. Analogous experiments with the pre-miR-26b hairpin, however, failed to enrich this protein. Instead, pre-miR-26b bound specifically to 7 proteins with high score. Remarkably, 3 of these hits are the RNA binding proteins FMRP/FXR1/2, (Figure 15B), which had already been linked to miR biology<sup>120</sup>.

The combined data from the two affinity purification approaches yielded two candidates for further analysis. One is ZNF346 that has high scores in pre-miR-26 datasets in zebrafish and in pre-miR-26a datasets in murine P19 cells. The second is the FXR1/2/FMRP group, which was highly enriched in pre-miR-26b and P19 cell lysates. However, these proteins were not detected in the zebrafish system.

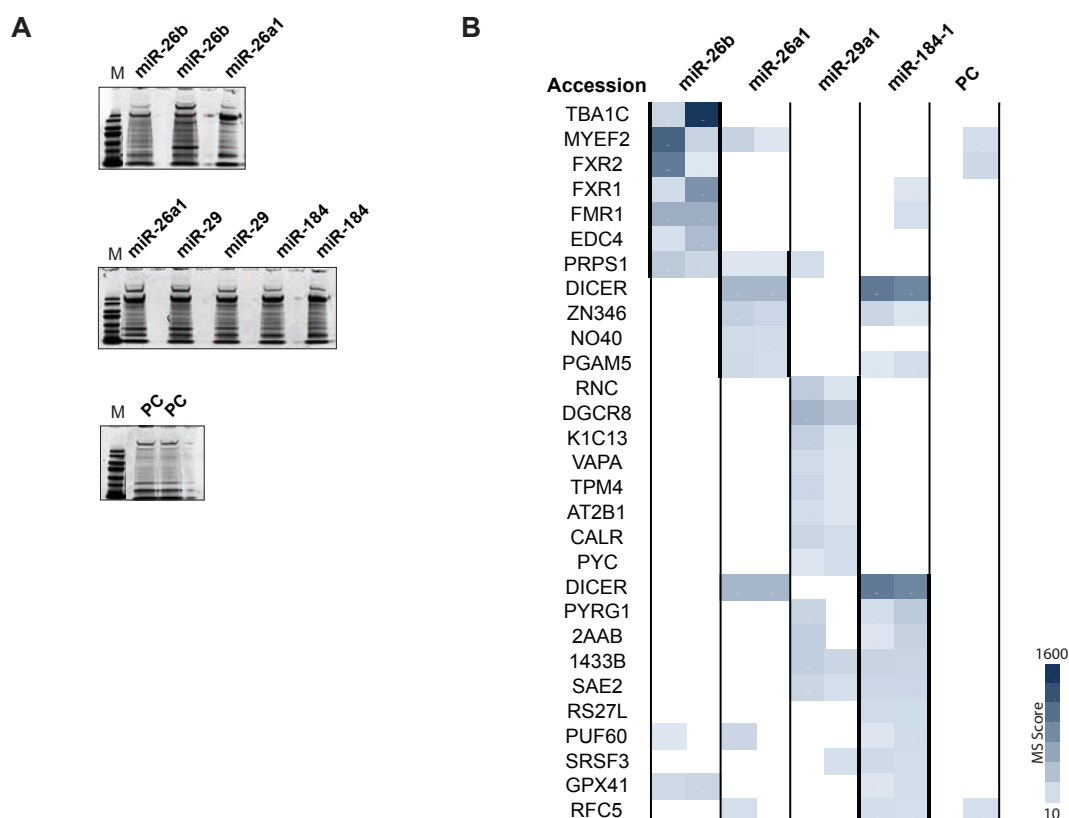


**Figure 16 miR hairpin-binding proteins in undifferentiated murine P19 cells**

**A** Coomassie-stained SDS-PAGE gel of affinity purifications using immobilized murine miR-26b, miR-26a1, miR-29a1 and miR-184 as baits. **B** Interacting proteins were isolated from 6 hpf zebrafish extracts using immobilized RNA hairpins, which are indicated on top. (gene symbols of isolated proteins on the left, the respective miRs are indicated on top of the diagram). Mass spec score counts are indicated in blue.

### **4.4.2 Investigation of pre-miR-26 processing regulation by the potential candidates**

As outlined above, potential candidates for the regulation of pre-miR-26 processing were identified by affinity approaches. Next, I wanted to test whether any of the identified factors is indeed the pre-miR26 processing factor. This factor is expected to meet the following criteria: It should be present in early embryonic cells (ESC or NPC, maternal factor in zebrafish) and specifically bind to pre-miR-26 in these cells but not in differentiated neurons. Upon binding the factor should interfere with maturation at the level of DICER processing or even at an earlier stage. The ablation of the factor would be expected to lead to increased levels of mature miR-26 in non-neuronal cells. In contrast, the overexpression of the factor should lead to prolonged repression of processing during cell differentiation and embryo development. In the following I describe experiments that I have performed in order to test whether one (or several) factor(s) meet these criteria and hence mediate the pre-miR-26 regulation.

#### **4.4.2.1 Analyzing the role of ZNF346 in miR26 maturation**

ZNF346 (also known as JAZ) is a double stranded RNA (dsRNA)-binding Zinc finger protein. It has very low affinity for DNA or single stranded RNA and so far no sequence specificity has been determined<sup>121</sup>. ZNF346 was recently discovered as a pri-miR binding protein, which binds the pri-miR-9 and -155 preferentially in A/U rich areas independent of dsRNA structure<sup>115</sup>. Zebrafish pre-miR-26b has a very similar A/U rich area as pri-miR-9-1, which makes ZNF346 a good candidate for pre-miR-26b processing regulation.

To see if Znf347 has an impact on pre-miR-26 processing, I initially overexpressed ZNF346 (via transcript injection) *in vivo* and measured the miR-26 levels by northern blotting. As a control, I also tested a transcript encoding MAK16, which showed only minor enrichments in the affinity purification experiment (Figure 15B). For overexpression of the mentioned proteins in zebrafish gene cassettes were constructed that express ZNF346:2A:eGFP or MAK16:2A:eGFP hybrid protein. These gene cassette form a pseudo-multicistronic cluster of the target protein (MAK16 or ZNF346) and a marker protein (eGFP). The 2A amino acid sequence is a self-cleaving peptide and cleaves the two proteins and leaves (initially) equal peptide levels. By this I was able to collect eGFP-positive embryos that co-express ZNF346.

From these clones a mRNA was transcribed *in vitro* and injected in one cell stage embryos.

I injected embryos with increasing RNA concentrations up to 2 µg/µl (3,6 µM). The eGFP intensity increased with higher concentrations of injected RNA (Figure 17A). Neither the MAK16-injected fish nor the ZNF346-injected fish showed any morphological changes (Figure 17A). To test if ZNF346 overexpression has an effect on miR-26 levels northern blots with embryonic RNA from ZNF346:2a:eGFP injected embryos were performed and probed for mature miR-26a and -26b (Figure 17B). Both miRs did not show changes of mature miR abundance after ZNF346 overexpression. Indicating that the overexpression of ZNF346 did not effect pre-miR-26 processing.

To see if ZNF346 binds directly to pre-miR-26, I produced recombinant ZNF346 and as a positive control the pre-let7-binding protein lin28 in *E. coli*. I incubated increasing concentration of lin28 and ZNF346 with constant levels of radiolabeled pre-miR-26b and pre-let7 and analyzed RNA binding via a dot-blot assay (Figure 17C/D). pre-miR-26 was found to specifically bind to ZNF346 but not to lin28 (lin28:  $K_D$  11,2 nM;  $r^2$  0,98; max. 15% binding; ZNF346:  $K_D$  4,9 nM;  $r^2$  0,97; max 80% binding). pre-let7 on the other hand was bound by lin28 and by ZNF346 (lin28:  $K_D$  2,4 nM;  $r^2$  0,99; max. 86% binding; ZNF346:  $K_D$  3,7 nM;  $r^2$  0,98; max 87% binding). This indicates that ZNF346 binds pre-miR non-specific *in vitro*.

The potential role of ZNF346 in pre-miR-26 processing was next investigated in murine cell culture. A system of embryonic stem cells was used that could be differentiated into neurons over NSCs. This work was performed in cooperation with Mark Sauer and Prof. Albrecht Müller (ZEMM, Würzburg).

First, we analyzed ZNF346 expression levels during neural differentiation by real time quantitative PCR (qPCR). ZNF346 levels decrease by approx. 40% from ESC to NSC and stayed at this level until NC (Figure 17E). This could point towards a negative regulation of ZNF346 during neuronal differentiation.

Overexpression of ZNF346 in zebrafish showed no effect on miR-26 levels. To further analyze the potential impact on miR-26 we stably knocked out ZNF346 in the murine cell culture systems using CRISPR technology (see 6.2.8.2). We analyzed heterogenetic (He) as well as homogenetic (Ho) KO clones in regard to their miR levels by qPCR at the ESC stage (Figure 9F). pre-miR-26b levels were reduced in all

## Results

clones but mature miR-26b levels were increased indicating an enhanced pre-miR-26b processing. The levels of the control pre-miR-124 did not change after KO of ZNF346. Surprisingly the levels of pre-miR-26a did not change as well.

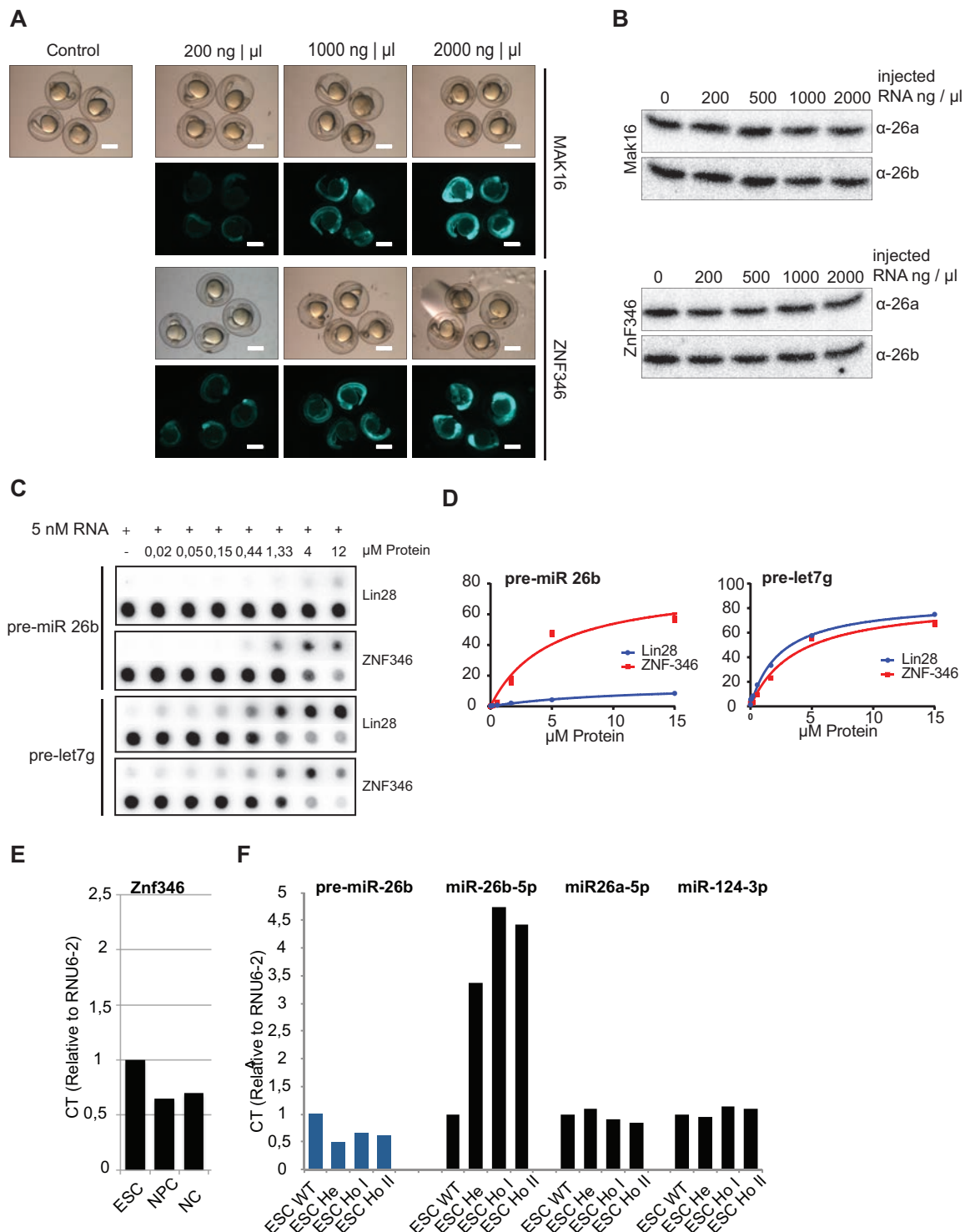


**Figure 17 Analyzing the role of Znf-346 in miR 26 in miR maturation**

**A** Bright-field and eGFP fluorescence images of zebrafish 24 hours after injection. Injected amounts of ZNF346:2A:eGFP and MAK16:2A:eGFP are indicated. **B** Northern blot of 24 hpf old injected fish probing for mature miR-26a and miR-26b. **C** Filter binding assay of recombinant lin28 and ZNF346 with radiolabelled pre-miR-26b and pre-let7. **D** Quantification of pre-miR filter binding assay. **E** qPCR of ZNF346 in differentiation murine ESCs to NCs. **F** qPCR of pre-miR-26b and the mature miR-26b, -26a and -124 after ZNF346 KO in murine ESCs. Analysis in E and F was done by Mark Sauer.



Taking together I could elucidate that ZNF346 can bind specifically to pre-miR-26b but its overexpression had no measurable effect on miR-26 levels in zebrafish. However, the knock out of ZNF346 led to increased miR-26b levels in the murine cells culture system exhibiting a negative effect on the pre-miR-26b processing. Due to the binding to the pre-miR-26b the effect could directly alter the processing through DICER. Further experiments are needed to investigate its exact role for miR processing.

#### **4.4.2.2 Analyzing the role FMRP/FXR1/2 protein family in miR26 maturation**

Fragile X mental retardation 1 protein (FMRP) and its paralogous family members fragile X mental retardation syndrome-related protein 1 and 2 (FXR1 and FXR2) are RNA binding proteins implicated in various aspects of RNA metabolism including post-transcriptional gene regulation. More recent work also revealed interactions of FMRP and FXR1 with DICER and other components of RISC, linking this protein family to miR processing<sup>122</sup>. Of note, transcriptional silencing of the FMR-1 gene, which encodes FMRP, leads to fragile X syndrome, a neurodevelopmental disorder and the most common genetic cause of intellectual disability<sup>123</sup>.

As FMRP and FXR1 and 2 were enriched in Neurons<sup>124</sup>, I wanted to investigate the role of these proteins in neurogenesis in more detail.

In an initial experiment I investigated the expression pattern of FMRP and FXR1/2 during zebrafish development. RNA was isolated from developing zebrafish embryos starting from 6 hpf to 48 hpf, and a semi quantitative PCR was performed. The overall expression of FMRP stayed on a similar level throughout early development but more isoforms emerged at later time points (Figure 18A). In contrast the levels of FXR1 and FXR2 declined during development, which would be consistent with a potential role as regulatory factors of pre-miR-26 processing.

To investigate the effect of FMRP and FXR1/2 miR-26 processing, expression of both genes was reduced by morpholino injection into the one-cell stage of zebrafish embryos.

Injection of a morpholino against FMRP, FXR1 or FXR2 alone showed no morphological effect zebrafish development (data not shown). This indicated that the proteins can make up the loss of a single family member. However, the simultaneous inhibition of FXR1 and 2 or even all three family members (i.e. FMRP, FXR1 and 2) led to a retardation of development (Figure 18B). This is most obvious for the

development of the head and tail regions, both of which were strongly reduced in size (Figure 18B).

Next I investigated whether the morpholino-injections impacted miR-26b abundance. Therefore, one-cell stage embryos were injected again with a single morpholino or mixtures of morpholinos targeting the FMR/FXR mRNAs. RNA samples of injected fish were collected 6 hpf and 24 hpf later and miR levels were determined by northern blotting. In non-injected 6 hpf old zebrafish embryos no mature miR-26b or -92b is detectable. The control miR-430b is detectable at both stages. This picture did not change after injection of the morpholinos (Figure 18C). In non-injected 24 hpf old embryos miR-430 is reduced and the miR-26 and miR-92b start to appear at the northern blots. Single morpholino injections did not change miR levels. However, like on the morphological level, double injections showed an effect. miR-26 levels but not in the control miR-430b levels were enriched with higher concentrated morpholinos (0,9 mM). In the triple morpholino injected samples with a concentration 0,9 mM the levels for miR-26b and the level of miR-92b are increased (Figure 18C). The increased levels of miR-26 in double and triple knock down embryos point toward a negative effect of FMRP and FXR1/2 on miR-26 processing.

The interaction of pre-miR-26 and FMRP/FXR1/2 was observed in the binding assay using murine cell lysate. I therefore analyzed whether binding likewise occurred in zebrafish. Due to difficulties in recombinant FMRP/FXR1/2 expression I designed an *in vivo* expression construct using again the 2A:eGFP reporter system (see 4.4.2.1). I generated HA-Flag-tagged FMRP and FXR1 and cloned it in front of the reporter (FMRP-HA-Flag:2A:eGFP and FXR1-HA-Flag:2A:eGFP). With the HA-Flag-tag I was able to immobilize the proteins for immune precipitation. Additionally, the tags were used to visualize binding of the proteins to pre-miRs by western blot. First I injected *in vitro* transcribed FMRP-HA-Flag:2A:eGFP and FXR1-HA-Flag:2A:eGFP mRNA into one cell stage zebrafish embryos, collected the embryos 24 hpf and prepared lysates. The lysates were incubated with anti-Flag beads, unbound factors were removed by washing and bead-bound material was eventually eluted with Flag peptide (Figure 18D). The RNA was isolated from the samples and analyzed by northern blotting. As shown in Fig. 11, I could detect no binding of miR-26 to any member of the FMRP/FXR family (Figure 18D). A reciprocal approach in which I immobilized the RNA on streptavidin beads (see 4.4.1) and incubated the beads with lysate from 24 hpf old FMRP-Flag-HA:2A:eGFP- or FXR1-Flag-HA:2a:eGFP-injected

embryos likewise showed no interactions as determined by western blotting (Figure 18E).

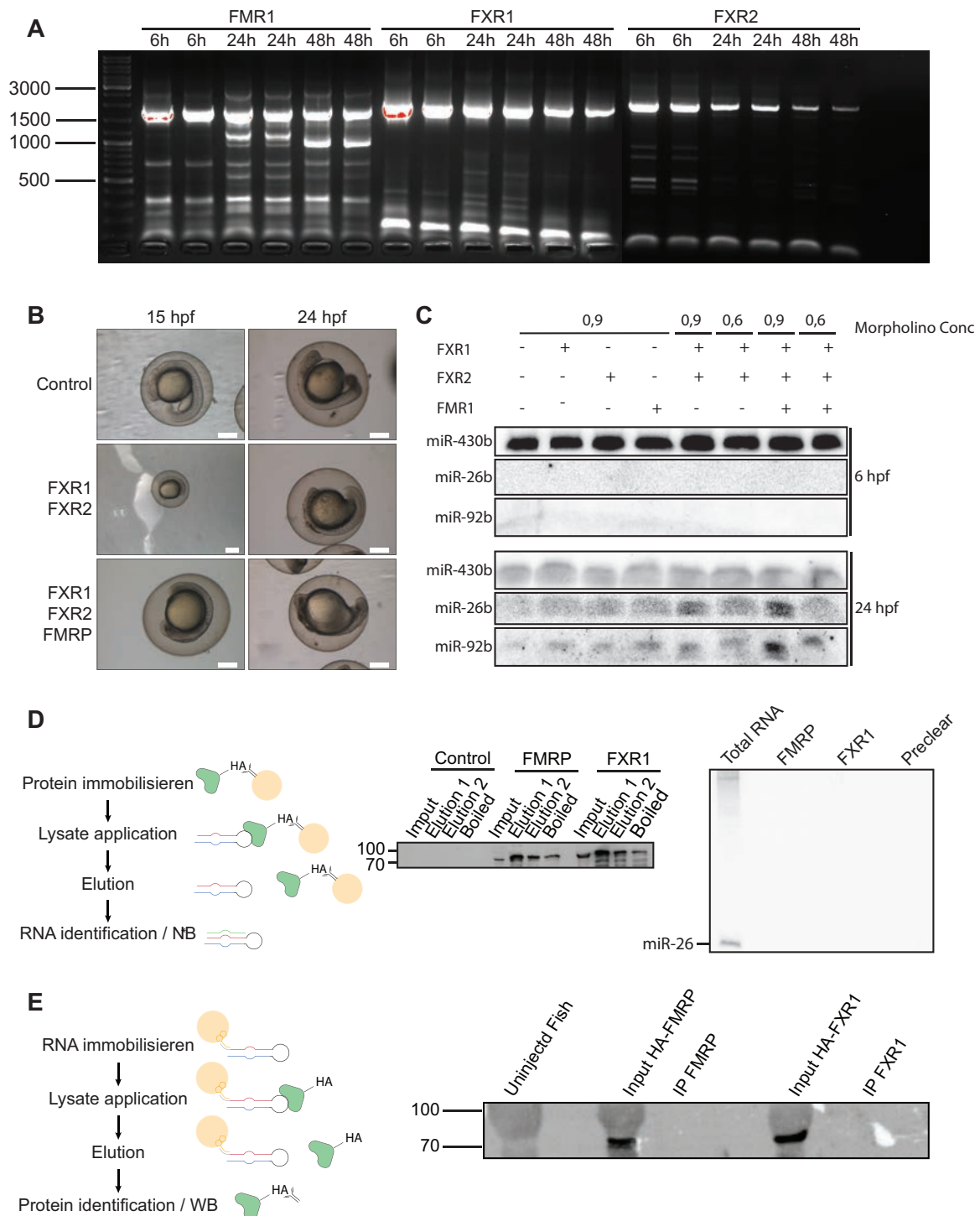


**Figure 18 Analyzing the role of FMRP/FXR1/2 in miR-26 maturation**

**A** Semi quantitative PCR of FMRP/FXR1/2 expression during early zebrafish expression. **B** Zebrafish after morpholino-mediated knock down of FXR1/2 and FMRP/FXR1/2. **C** Northern blot of zebrafish RNA against indicated miR after knock down of FMRP, FXR1 and FXR2 as indicated. **D** RNA IP of immobilized FMRP and FXR1. Experimental strategy (left), western blot of FMRP and FXR1 IP (middle), northern blot against miR-26 after FMRP- FXR1 RNA IP. **E** pre-miR pull down with lysate from FMRP-HA:2A:eGFP and FXR1-HA:2A:eGFP injected zebrafish. Experimental strategy (left), western blot after pull down (right).

FMRP and FXR1/2 show expression profiles during development that are compatible with a role as a negative regulator of pre-miR-26 processing. In line with this, the combined reduction of these proteins led to increased miR-26 levels. A direct interaction of these proteins with pre-miR-26, however, could not be detected. The role of these proteins in the miR-26 maturation pathway is therefore still unclear.

### **4.4.3 Identification of miR hairpin binding proteins using S1 aptamer approach**

Although the experiments described above revealed several candidates for miR-26 regulation, none of them met all criteria and hence their function remained unclear. I therefore decided to develop an alternative approach to identify miR-26 binding factors based on an altered RNA immobilization strategy. In this approach, I used the S1 aptamer fused to the pre-miR for immobilization (see 6.2.6.15). The pre-miR molecules were changed by adding a S1 aptamer to the 5' end of the pre-miR or by exchanging the loop by an S1m aptamer. The purification of miR-26 binding factors was performed as described (see 4.4.1) from lysates obtained from 6 hpf zebrafish embryos and murine ESCs. For purifications from zebrafish lysates pre-miR-26a-2, pre-miR-26b and pre-miR-430b were used as bait. For the pre-miR-26b and pre-miR-430b the pre-miR-S1m loop hybrids were used additionally. Purifications from mouse ESC extracts were performed with pre-miR-26a-2, pre-miR-26b and pre-miR-9b as bait. Again, for the pre-miR-26b and pre-miR-430b the pre-miR-S1m loop hybrids were used as well.

For each RNA lysate combination quadruplicates were generated. Proteins that bound to the respective affinity matrices were identified by mass spectrometry and the data sets were pooled and analyzed for protein quantification using MaxQuant<sup>125</sup>. Proteins identified as contaminants or not identified in at least three datasets were filtered out. Volcano plots were generated in which the fold change of individual proteins was calculated (x-axis) and plotted against the statistical probability (p-value) of these proteins (y-axis). The functionality of the assay was tested by blotting noRNA (preclear) data sets against pre-miR data sets (Figure 19A,D).

pre-miR-S1m loop baits bound factors did not show a potential candidate (data not shown). XRN1 was identified in all loop data sets, indicating the bait RNA was degraded, because XRN1 is 5'-3' RNA exonuclease and critical for eukaryotic RNA turnover<sup>126</sup>.

A comparison of pre-miR-26b-bound factors with the negative control (no RNA bound to beads) identified known general miR binding factors in the zebrafish extract

(DICER, DGCR8 and TRBP2; Figure 19A,D highlighted in blue). A very similar observation was done when pre-miR-9 binding factors were compared to the negative control in the murine system (Figure 19D). This indicated that the binding assay allowed isolation of miR interacting factors from either extract.

Next, I compared factors bound to pre-miR-26b and pre-miR-26a versus the pre-miR-430b and the no-RNA control. In this case, no factor that specifically binds to pre-miR-26 was found (Figure 19B,C).

In the binding assay with murine NSCs, however, the Eral1 protein was identified as a specific pre-miR-26 binder (Figure 19E,F highlighted in red) and was analyzed in more detail.

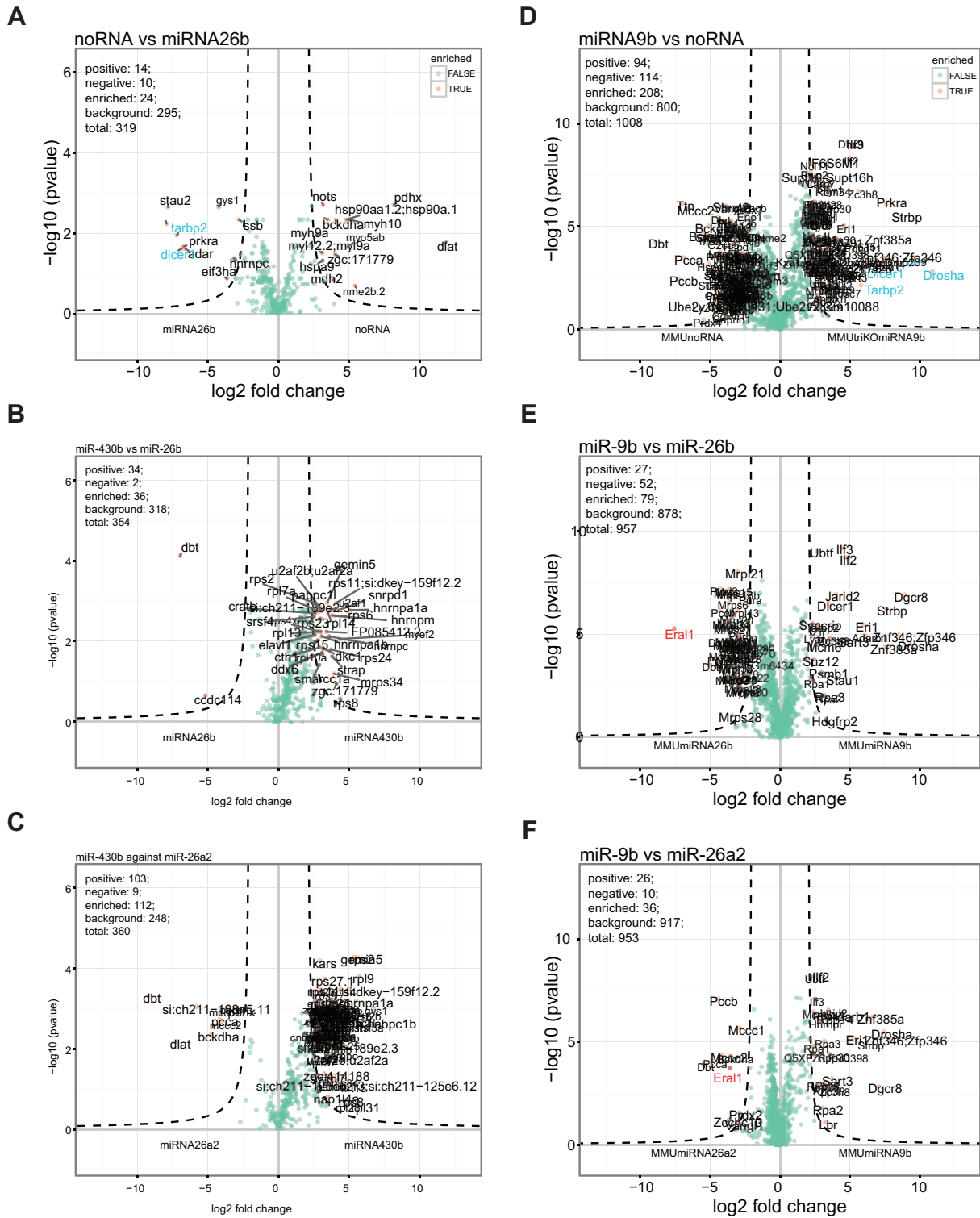


**Figure 19** Proteom of pre-miRNPs using aptamer pre-miR

Volcano plot after Aptamer-based pre-miR pull down. **A** noRNA versus pre-miR-26b. **B** pre-miR-430b versus pre-miR-26b. **C** pre-miR-430b and pre-miR262a. **D** noRNA versus pre-miR-9b. **E** pre-miR-9b versus pre-miR-26b. **F** pre-miR-430b and pre-miR26a2. **A-C** 6 hpf zebrafish lysate. **D-F** murine ESCs. Dotted line: two-dimensional cutoff with  $S_0=0.6$  and  $P<0.05$  (Welch's  $t$ -test)<sup>127</sup>. miRNA machinery associated proteins (blue). potential factor Eral1 (red).

#### 4.4.3.1 Analyzing the role of Eral1 in miR-26 maturation/regulation

Eral1 is a RNA chaperone and is involved in the assembly of the 28S small subunit of mitochondrial ribosomes<sup>128</sup>. Eral1 is a GTP binding protein and is reported to bind and stabilize 12S mt-rRNA in a regulated manner that involves a GTP/GDP cycle<sup>128</sup>.

To verify pre-miR binding by Eral1 in an independent experiment Eral1 was immunoprecipitated from NSC extracts using a monospecific antibody. This led to the specific enrichment of the protein, as confirmed by western blotting (Figure 20B). I analyzed by qPCR whether pre-miRs were specifically co-enriched in these IPs (Figure 20A). The experiment showed a strong enrichment of the most abundant miR-26 family member pre-miR-26a2. Minor enrichments were also found for pre-miR-26b, pre-miR-26a1 and the non-related pre-miR-290. Mature miRs-26a and miR-26b also showed an enrichment in the co-immunoprecipitation.

I could show that Eral1 binds pre-miR-26. It was shown in literature that Eral1 binds the lower stem of 12S mt-rRNA<sup>128</sup>. This stem shows sequence similarities with the lower stem of all pre-miR-26s (Figure 30). This makes Eral1 a good candidate that would be able to regulate all pre-miR-26. Additionally, the RNA binding function of Eral1 is regulated by a GTP/GDP cycle<sup>128</sup>, which could explain the regulation of potential inhibition of pre-miR-26 processing. In future experiment Eral1 will be knocked down or be overexpressed in zebrafish embryos and its impact on the mature-miR 26 levels will be analyzed.

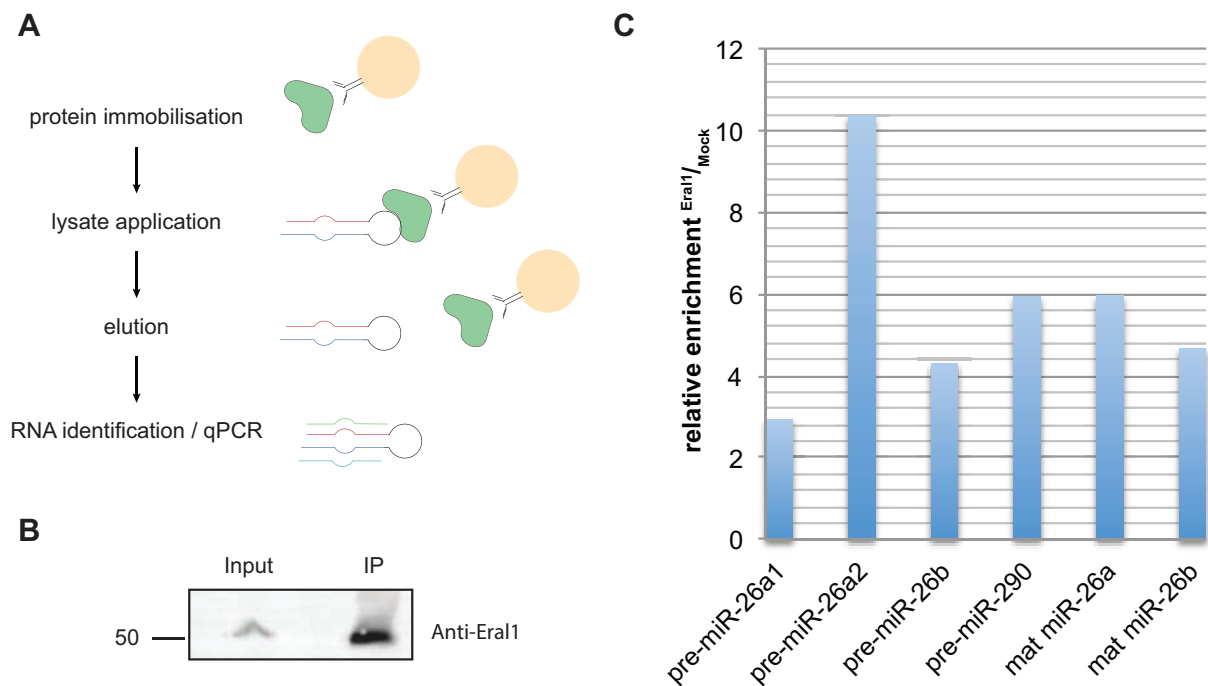


**Figure 20 Analyzing the role of Eral1 in miR 26 in miR maturation**

**A** Strategy of RNA IP with Eral1 antibody. **B** Eral1 IP with murine ESC lysate. **C** qPCR after Eral1 IP against murine pre-miR 26a1, pre-miR26a2 and pre-miR-26b and mature miR-26a and miR-26b.

It was previously shown, that miR-26 processing is halted in zebrafish development<sup>81</sup>. Nuclear-cytoplasmic transport experiments showed no alteration in pre-miR-26 export. Moreover, *In vivo* and *in vitro* experiments showed that pre-miR-26 is not processed in early zebrafish embryos but can be processed at later stages. This indicates that the processing is stalled at the precursor level by regulating proteins acting in *trans*. To identify *trans* acting factor we used two different set ups, which unfortunately yielded three different candidates. All the three candidates showed properties, which pointed toward miR-26 regulation. FMRR, FXR1 FXR2 and ZNF346 showed alteration in mature miR-26 levels upon knock down. And ZNF346 and Eral1 showed binding towards the pre-miR-26. However, at this point it cannot be said, if one of the candidates is the regulator and none of them can be excluded as candidate. Further experiments are needed to pin down the regulator.

#### 4.5 Analyzing the role of the miR-26 family in an murine *in vitro* neuronal differentiation system

The stepwise transition of embryonic stem cells (ESC) toward the neuronal fate to form neurons is a highly regulated process. The differentiation of ESC starts with the transition into a primitive ectodermal like stage followed by the formation of



neuroectoderm. A population of NPCs is formed from these cells, which will later gradually develop into neurons.

Morpholino-based knock down strategies initially allowed to investigate the role of miR-26 in developing zebrafish<sup>81</sup>. While zebrafish allowed to investigate neurogenesis in a developing organism it is not a suitable system for detailed studies at the different neurodevelopmental levels (NSCs, NCs) or for functional investigations of NCs.

We used a cell culture differentiation system that mimics neurogenesis. This allowed the efficient analysis of the neural differentiation process *ex vivo* using genetic and systematic approaches. It enables the generation of a defined pool of NPCs, which can be finally differentiated into neuronal cells (Figure 21A)<sup>129,130</sup>. As shown in various reports from different laboratories, this system faithfully recapitulates neurogenesis based on cell morphology criteria as well as expression profiles of established cellular and molecular markers<sup>129,130</sup>.

This work was performed in close collaboration with the graduate student Mark Sauer (laboratory of Prof. A. Müller, Institute for Medical Radiology and Cell Research (MSZ) in the Center for Experimental Molecular Medicine (ZEMM), University of Würzburg). Results that are part of the thesis of M. Sauer (not published yet) are marked and are only included in order to make the data collected in this joint research project better understandable for the reader.

Initially it was important to investigate whether the miR-26b-mediated Ctdsp feedback loop identified in zebrafish<sup>81</sup> could also be observed upon *ex vivo* ESC differentiation into neurons. The levels of the pre-miR-26, mature miR-26 and CTDSP were analyzed by qPCR at different differentiation stages. As expected, CTDSP expression increased upon differentiation from ESC to NPC but decreased in neuronal cells. The levels of pre-miR-26 were high relative to the mature miR-26 levels in NPC. However, the level of pre-miR-26 decreased in NC while the levels of mature miR-26 increased. This indicates that pre-miR-26 processing is repressed in undifferentiated cells but becomes activated when neurons are formed. In zebrafish it was shown, that CTDSP is negatively regulated by miR-26. The same could be shown for the cell culture system. The elevation of exogenous miR-26 via miR mimics led to decreased CTDSP levels (data not shown, personal communication Mark Sauer). Thus, the *ex vivo* cell differentiation system faithfully recapitulated key

events of miR-action during neurogenesis. This allowed us to systematically analyze the role of the miR-26 family in the differentiation process.

### **4.5.1 Knock out of the miR-26 family members in murine ESCs**

To investigate the impact on the miR-26 family on neurogenesis we used two strategies to inactivate miR-26. In one approach, this was achieved using antisense morpholinos in zebrafish, which typically lead to a reduction of the miR but not its complete removal. In addition, due to the sequence homology of miR 26a and b, this approach does not distinguish between those miRs. In a second approach, we deleted the miR locus in the genome by CRSPR/Cas9 technology, which generates a complete knockout in a murine *ex vivo* differentiation system (see 6.2.8.2).

miR-26b, miR-26a1 and miR-26a2 are encoded in introns of Ctdsp1, CtdspL and Ctdsp2 genes, respectively (see 3.4, Figure 9). All three miRs of the mouse genome have been deleted in ESCs and homozygous clones of either miR-26b alone (KO<sup>26b</sup>), of miRs-26a1 and -26a2 (dKO<sup>26a1/a2</sup>) or of miR-26b/26a1/26a2 triple KO (tKO<sup>26b/26a1/a2</sup>) have been generated (Figure 21B).

The pre-miR-26s loci were cut out of the genomic DNA by CRISPR/Cas9. To ensure that the pre-miR-26 sequences were deleted and the CTDSPs remain unaffected. For genotyping, genomic DNA of the KO cell lines was taken, miR-26 specific PCR was done and the target locus was characterized by sequencing (data not shown). KO<sup>26b</sup>, dKO<sup>26a1/a2</sup> and tKO<sup>26b/26a1/a2</sup> showed sufficient deletion with intact CTDSP exons. KO<sup>26b</sup>, dKO<sup>26a1/a2</sup> and tKO<sup>26b/26a1/a2</sup> cell cultures formed colonies of normal ESC-type morphology (Figure 21C). To analyze if the KO clones kept their pluripotency (potential to differentiate in any of the three germ layers) ESCs were analyzed by qPCR for pluripotency markers such as Oct4, Sox2, Nanog and Rex1. All KOs and the wild type cultures show unaltered expression of core pluripotency markers (data not shown).

### **4.5.2 The KO of miR-26 does not effect the differentiation to NPC but final neural differentiation**

The proliferation of wild type and knockout cells was analyzed by determining cumulative population doublings (CPD) and assessed cell numbers (data not shown). We observed no significant differences between all cell lines in proliferation (Figure 21C). Furthermore, similar numbers of NPC markers (Sox2 and Nestin) were

observed in wildtype and KO NPC cultures (Figure 21C). Thus, knockout of miR-26 family members does not affect the differentiation of ESCs to NPCs.

Differentiation of NPCs to NCs resulted in NC cultures with markedly increased frequencies of Sox2+ and Nestin+ cells numbers in the KO cultures (data not show) indicating that the KO cultures show higher amount of proliferating progenitors than differentiated wild type cultures. Mature neuronal markers such as Map2, Tau or Tuj1 were strongly reduced in all KO cultures (Figure 21C and data not shown).

A detailed analysis revealed that the KO of miR-26 resulted in cultures with markedly increased proliferating progenitor cells, which do not differentiate into neuronal cells any more. In addition, KO<sup>26b</sup> and the dKO<sup>26a1/a2</sup> alone are sufficient to reduce the number of neuronal marker positive cells suggesting that all miR-26 family members fulfill non-redundant functions.

## Results

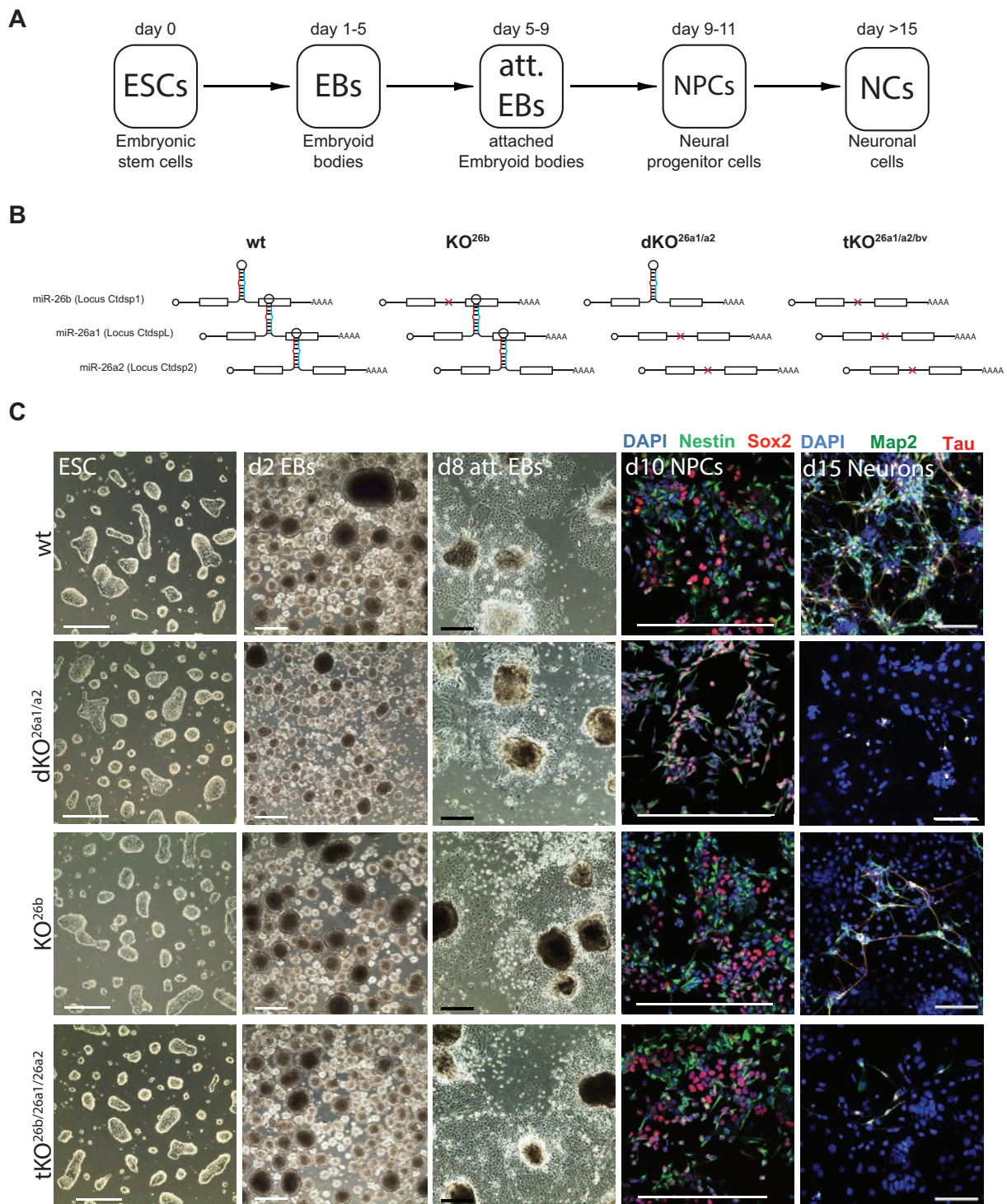


**Figure 21 Effect of miR-26 KO on neuronal differentiation**

**A** Scheme of individual stages of *in vitro* differentiation of ESCs into NCs over NPCs. **B** KO overview of  $KO^{26b}$ ,  $dKO^{26a1/a2}$  and  $tKO^{26b/26a1/a2}$  cell lines. miR-26 localization as indicated. **C** Phase contrast panels show representative morphological changes during neuronal differentiation from undifferentiated ESCs via embryoid bodies (EBs) to attached EBs and to NPCs. Sox2- and Nestin-specific immunostainings of NPC cultures (4<sup>th</sup> column). Representative immunostainings of differentiated NCs (day 15 of culture) with neuronal markers (Map2, Tau) (5<sup>th</sup> column). Scalebar 100  $\mu$ m. All analysis was done by Mark Sauer

#### 4.6 Transcriptome analysis of miR-26 KO cell lines

As shown above, deletion of the miR-26 family does not impede the formation of NPCs but interferes with later steps of neurogenesis. Indeed, this phenotype was observed not only in the triple knockout (tKO<sup>26b/26a1/a2</sup>) but also in cells in which individual miR-26 family members have been deleted. To gain insight into the molecular events that led to this phenotype the gene expression profiles of wild type and miR-26 deficient cells were systematically analyzed by RNA deep sequencing.

Deep sequencing of RNA reverse transcribed to complementary DNA (cDNA) refers to the multiple sequencing of transcripts. This enabled us to measure gene expression and analyzes changes of the transcriptome by comparing two datasets (KO vs. wt). It also enabled us to look for alternative spliced transcripts or posttranscriptional modifications. We sequenced long, poly(A)-tailed RNAs (mRNAs, long non-coding RNAs), that were depleted of ribosomal RNAs and small RNAs, where the RNAs are separated by size and only small RNA were further sequenced. (for more information see 4.7).

Two individual purified total RNA samples from two independent clones for each homozygous miR deletion and four individual purified total RNA samples from wild type cells were used for sequencing. RNAs samples were taken from each ESCs and d15 cultured cells (referring to NCs).

cDNA libraries of the RNA were generated and deep sequenced using an Illumina HiSeq3000 system in the laboratory of M. Hafner (NIH, Bethesda, USA)(See MM for additional Information). To analyze the changes of mRNA expression levels obtained sequence reads were mapped to the murine genome (GRCm38/mm10) using the Tuxedo suite algorithms<sup>131</sup> and the relative expression levels were calculated (performed by Markus Hafner, NIH, USA). The relative expression was compared between the individual KO cell lines and the wild type neuronal cells. Each sequencing reaction yielded 40-60 Million reads per sample, which is sufficient for quantitative mRNA expression analysis<sup>132</sup> (see Illumina webpage).

I analyzed, if the pre-miR-26 deletions led to alteration of the CTDSP transcripts. One clone of the KO<sup>26b</sup> cells showed reduced expression (compared to wild type) in the CDTSP1 exons upstream and downstream of the miR-26b cut out sites and were removed from further analyses. All other clones were included in the analysis.

For analyzing the impact of miR-26 on the expression profile in neurogenesis I compared the transcriptome of the KO clones and wild type cells. As miR-26 is not

## Results

active in ESCs I focused these studies on NCs. The changes in gene expression levels were displayed by plotting the  $\log_2$  values of the ratio between KO and wild type cells for each sample. Nearly the same number of up- and downregulated genes was found (Table 1; Figure 22A).

**Table 1 Up- and downregulated Genes in KO cell line over wild type cell lines**

KO Line	Upregulated	Downregulated
KO <sup>26b</sup>	11508	11697
dKO <sup>26a1/a2</sup>	11573	11443
tKO <sup>26b/26a1/a2</sup>	12599	10778

For further studies only transcripts were analyzed that were at least 4 times up- or downregulated (Figure 22A, down red, up green). dKO<sup>26a1/a2</sup> showed the highest amount of changed transcripts (down 2300, up 1346) whereas KO<sup>26b</sup> (down 439, up 550) and tKO<sup>26b/26a1/a2</sup> (down 543, up 943) showed milder changes in transcript abundance (Figure 22A).

Next, I analyzed whether a similar set of transcripts was affected in the different KO cell lines. These results are displayed in Venn diagrams that illustrates that the amount of commonly regulated genes is quite low while the KOs have relative high amounts of uniquely regulated genes (Figure 22B). This is quite surprising, because they all show the same phenotype (4.5.2). Analyzing the intersected downregulated genes showed neuronal terms in gene ontology (GO) analysis (data not shown). However, the upregulated genes showed no similarity in GO terms (data not shown). To understand what happened in the individual KO lines condition I analyzed the changed transcripts individually and performed GO analysis (Figure 22C).

For all KO clones no GO term tendency could be observe for upregulated genes. For the tKO<sup>26b/26a1/a2</sup> downregulated genes 9 of 15 GO terms belonged to neural terms (Figure 22C, red). The same could be seen for dKO<sup>26a1/a2</sup> (data not shown). For the KO<sup>26b</sup> cells this was not as obvious, but reducing the threshold to at least two fold downregulated exhibited the same effect for this KO (data not shown).

Taken together the transcriptome analyses showed that upon inactivation of miR-26 neuronal genes are globally downregulated. This finding is consistent with our finding that these cells are blocked in neurogenesis at the stage of NPCs. However, due to a missing tendency of common biological processes in upregulated genes it could not be concluded to which differentiation fate the cells are committed. It also showed that

the KO<sup>26b</sup> displayed the mildest effect and that the dKO<sup>26a1/a2</sup> and tKO<sup>26b/26a1/a2</sup> showed more severe effects.

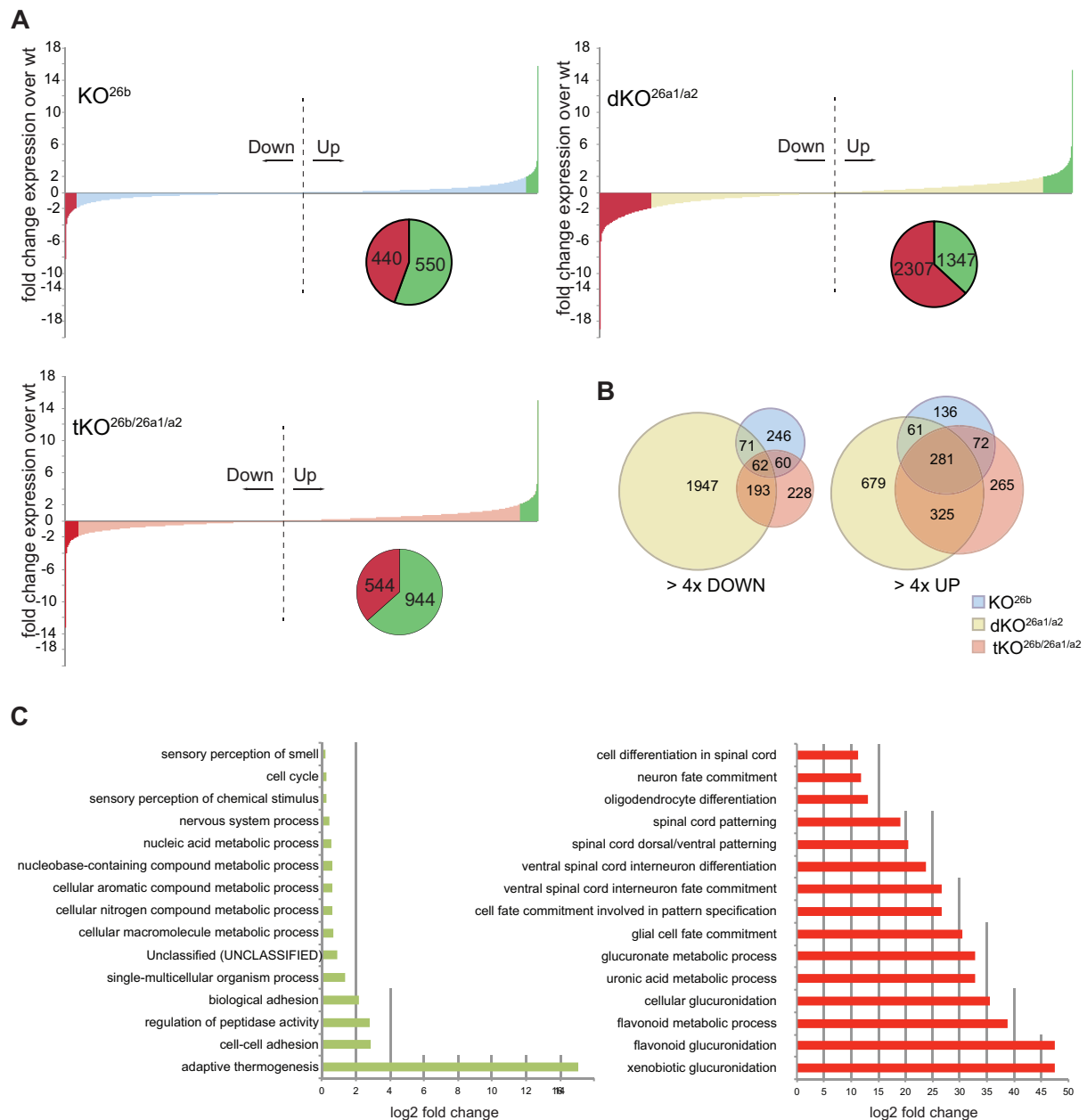


**Figure 22 Transcriptome analysis of miR-26 KO cells.**

**A** Down- and upregulated genes in KO<sup>26b</sup>, dKO<sup>26a1/a2</sup> and tKO<sup>26b/26a1/a2</sup> cell lines over wild type cells. Genes differently expressed with a factor more than 4 times are indicated (up green; down red). Pie diagrams indicate the relation between up- and downregulated genes. **B** Venn diagram of the distribution of transcripts that exhibit at least 4 times changed in KO cell lines (downregulated, left; upregulated, right). **C** GO terms of represented gene sets of up- (red) and downregulated (green) genes. ESC to NC differentiation and RNA purification was performed by Mark Sauer.

#### 4.7 REST regulated miR show target sites in mRNAs of REST complex members

As illustrated in the preceding section a global downregulation of neuronal genes was observed in miR-26 deficient NCs. We next asked how this transcriptional

deregulation was evoked at the molecular level. As the REST complex had been described to represses the transcription of neural genes we speculated that alterations in its activity might be primarily responsible for this phenotype.

The REST complex does not only regulate the expression of neuronal proteins it also represses the transcription of non-coding transcripts, like long non-coding RNAs or small non-coding RNAs (lncRNAs, miRs)<sup>133,134</sup>. Studies on miRs that are under regulation of the REST complex are summarized in Table 2. Potential REST-regulated miRs were predicted by analyzing the genomic background for RE1 in a window of up to 20 kb up- and downstream of the miRs<sup>134,135</sup>. With this prediction around 40 miRs have been identified. For 14 out of these 40 miRs REST-binding could be shown by chromatin immunoprecipitation (ChIP)<sup>77,136</sup>. For this thesis only these confirmed 14 miRs (REST-miRs) were used (Table 2).

**Table 2** Known & predicted miRs that are under REST complex regulation. Evidence for regulation: ChIP, chromatin immunoprecipitation; RE1, REST target prediction.Pub, relevant publication

miR	Pub	Evidence	miR	Pub	Evidence	miR	Pub	Evidence
miR-9	77,134,136	Chip, RE1	miR-455	134	RE1	miR-602	135	RE1
miR-124	77,134,136	Chip, RE1	miR-7-2	135	RE1	miR-637	135	RE1
miR-132	77,134,136	Chip, RE1	miR-7-3	135	RE1	miR-940	135	RE1
miR-9*	46	Chip, RE1	miR-129-2	135	RE1	miR-1179	135	RE1
miR-29a	134,136	Chip, RE1	miR-137	135	RE1	miR-1208	135	RE1
miR-29b	134,136	Chip, RE1	miR-146b	135	RE1	miR-1224	135	RE1
miR-95	134	RE1	miR-147	135	RE1	miR-1249	135	RE1
miR-135	134,136	Chip, RE1	miR-184	135	RE1	miR-1253	135	RE1
miR-139	134,136	Chip, RE1	miR-203	135,136	Chip, RE1	miR-1255	135	RE1
miR-153	134	RE1	miR-204	135,136	Chip, RE1	miR-1257	135	RE1
miR-212	134,136	Chip, RE1	miR-328	135	RE1	miR-1267	135	RE1
miR-218	134,136	Chip, RE1	miR-375	135	RE1	miR-1301	135	RE1
miR-346	134,136	Chip, RE1	miR-422a	135	RE1	miR-330	136	Chip, RE1

miR-9 and miR-124 have been shown to be important for proper neurogenesis<sup>137</sup> and are able to reprogram somatic cells into neurons<sup>138</sup>. Their expression is regulated by the REST complex<sup>46,77,78</sup>, but simultaneously they also negatively regulate the REST complex forming a negative feedback loop<sup>46,77,78</sup>. The neuronal miR-132, which is regulated by the REST complex, can act against the complex associated protein MeCP2<sup>77,79</sup>.

To test, if the other potentially REST-regulated miRs might form negative feedback loops with the REST complex I performed target scans of all the 14 REST complex



associated miRs (REST-miRs) *in silico* using TargetScan (Release 7.1,<sup>139</sup>) and analyzed the 3' UTR of the mRNAs of REST complex associated proteins (Figure 31). Interestingly, all 14 REST-miRs have target sites in at least two subunits of the REST complex (Figure 23). Only HDAC1/2 and LSD1 do not have target sites for REST-miRs. This goes along with their role in other chromatin remodeling mechanisms<sup>140-143</sup>.

These biocomputational considerations suggest that the REST complex does not only negatively regulate a specific subset of miRs at the transcriptional level. Rather, the complex itself is a target of negative regulation by REST-controlled miRs. That implies that upon downregulation of REST complex activity the complex levels will decline more and more in a self regulating manner.

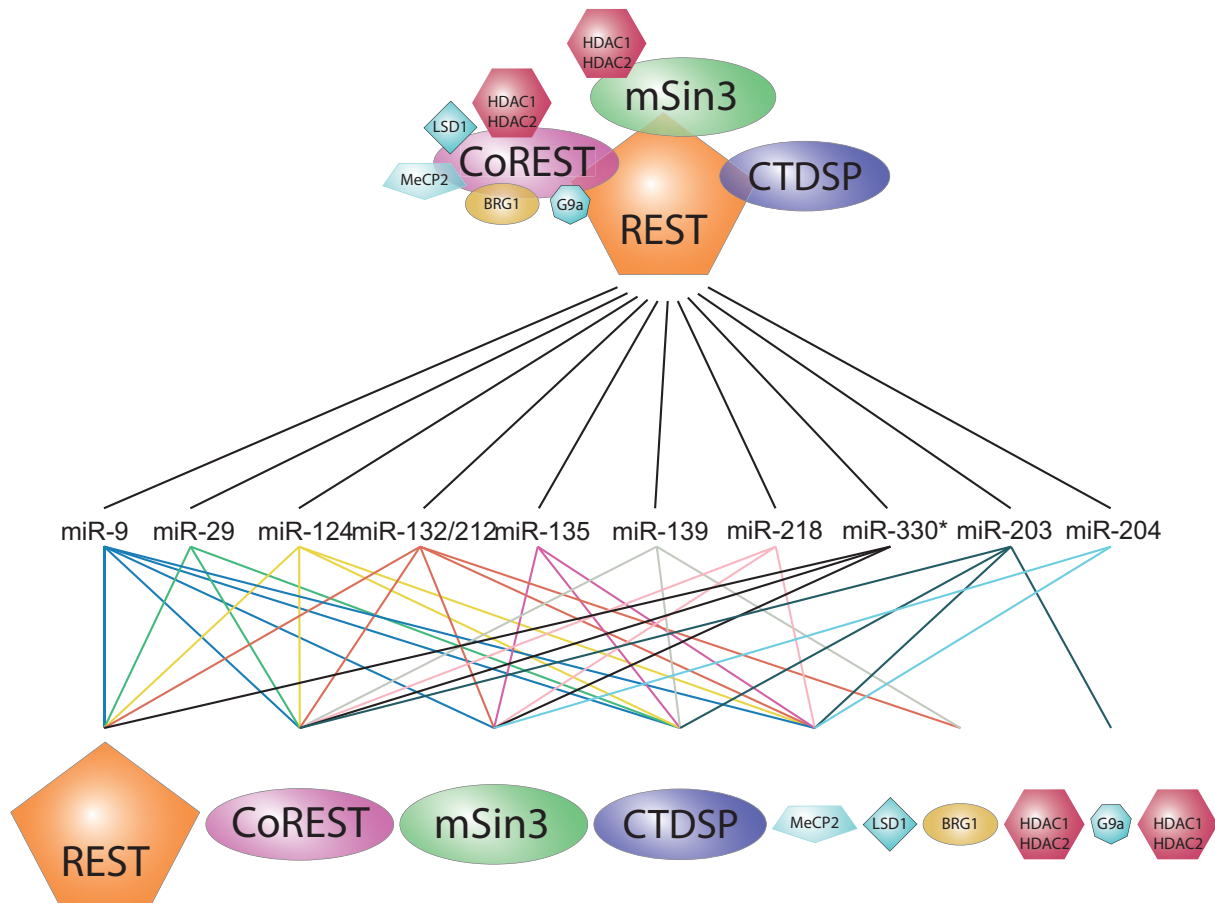


**Figure 23 REST to miR/miR to REST regulation.**

The REST complex represses the expression of the shown miRs (REST-miRs). All of these miRs themselves can attack several parts of the complex, showing the miR-REST feedback loops.

#### 4.8 The majority of REST-miRs are down regulated in miR KO cell lines

As shown before, miR-26 acts against its host gene CTDSP (Figure 7)<sup>81</sup>. miR-26 has target sites in REST, coREST, mSin3a and MeCP2 (Figure 31), but is itself not under REST regulation. This raises the possibility that miR-26 functions as an initial trigger for REST complex regulation. One prediction from this consideration is, that the 14 REST-miRs form negative feedback loops with the REST complex. If the miR-26 acts such a factor it should alter the REST-miR levels after KO.

I analyzed the effect of miR-26 on general miR abundances in the three KO cell lines by small RNA sequencing. cDNA libraries of small RNAs were generated, deep sequenced and aligned to known miRs genes (miRseq, performed by Markus Hafner, NIH, Bethesda, USA). I compared miR levels that were at least 20% down- or upregulated (KO over wildtype) and plotted their distribution. In contrast to the transcriptome analysis (Figure 22) the KO cell lines show a high overlap of down- and upregulated miRs (Figure 24A). In the KO cell lines around 600 miRs were regulated (KO<sup>26b</sup>: 606; dKO<sup>26a1/a2</sup>: 615; tKO<sup>26b/26a1/a2</sup>: 628) and the majority were upregulated (KO<sup>26b</sup>: 69% 606; dKO<sup>26a1/a2</sup>: 69% 615; tKO<sup>26b/26a1/a2</sup>: 66%) (Figure 24 A/C).

I selectively plotted the 14 REST-miRs (Figure 24B) in the 3 different KO cell lines (Figure 24C). In contrast to the overall miRs, the majority of the REST-miRs are downregulated in all KO cell lines (KO<sup>26b</sup>: 65% 606; dKO<sup>26a1/a2</sup>: 70% 615; tKO<sup>26b/26a1/a2</sup>: 76%). The upregulated miRs are mainly the 6 copies of miR-29 (miR-29a, miR-29b, miR-29c, miR-29a\*, miR-29b\* and miR-29c)(Figure 24C).

In conclusion, the absence of miR-26 has a huge negative impact on REST-miRs. The downregulation of the individual miRs might not be so high but downregulation of the REST-miR together should have a major effect on the REST complex.

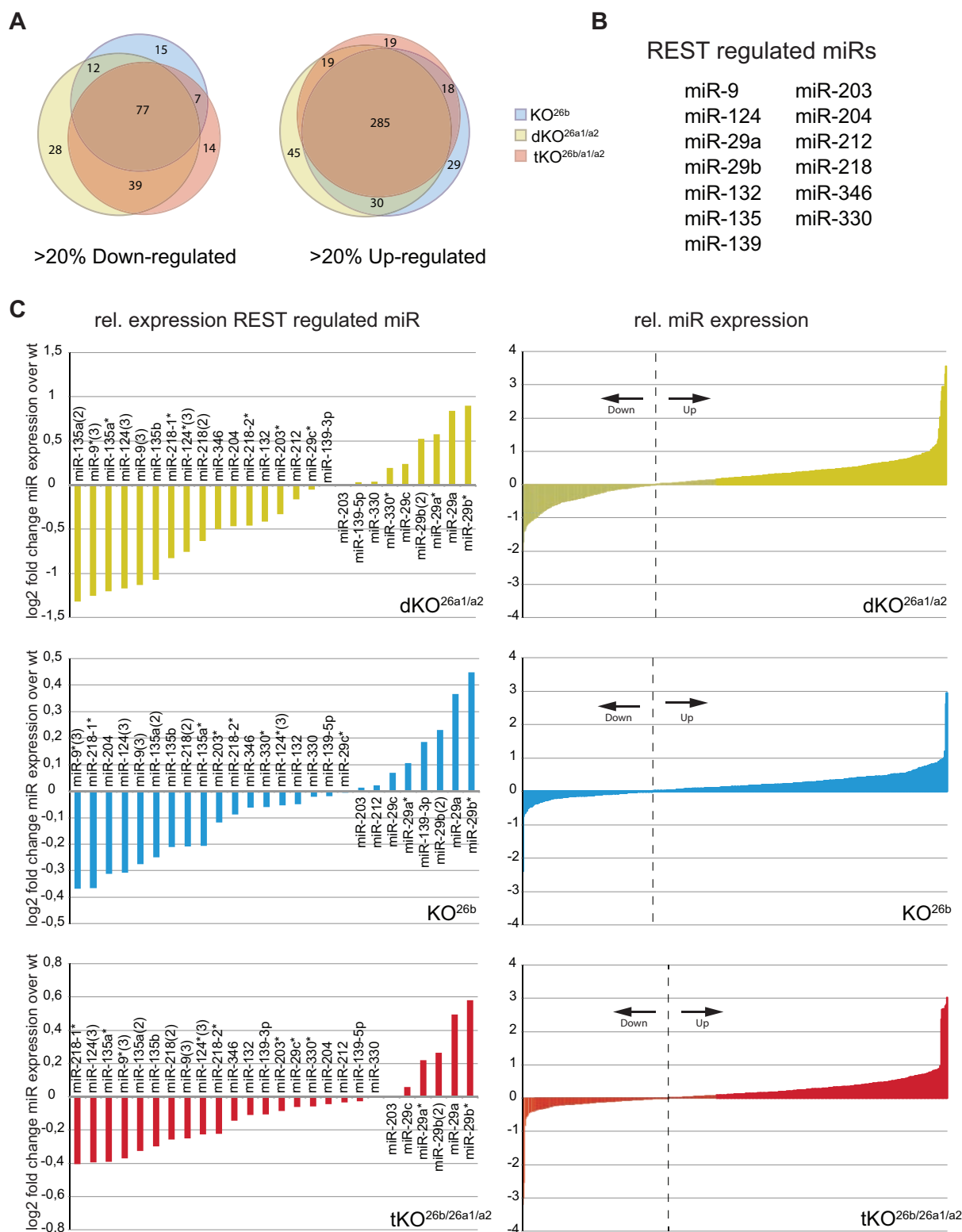


**Figure 24** Impact of miR-26 on REST-miRs.

**A** Venn diagram of the distribution of changed miR levels ( $\geq 20\%$  changed) in KO cell over wt cells (downregulated, left; upregulated, right), cell lines as indicated. **B** List of investigated REST-miRs. **C** Down- and upregulated REST-miRs in KO<sup>26b</sup>, dKO<sup>26a1/a2</sup> and tKO<sup>26b/26a1/a2</sup> cell lines over wild type cells (left). All down- and upregulated miRs in KO<sup>26b</sup>, dKO<sup>26a1/a2</sup> and tKO<sup>26b/26a1/a2</sup> cell lines over wild type cells (right). ESC to NC differentiation and RNA purification was performed by Mark Sauer.

#### 4.9 miR-26 initiates the activation of the REST-miRs

As shown above, the KO of the miR-26 family led to reduced amounts of neurons and decreased REST-miRs levels in differentiated cells. To see if these effects are due to the KO of miR-26 and not due off target effects of the KO preparation rescue experiments were performed. For this the tKO<sup>26b/26a1/a2</sup> cells at the NPC stage were transfected with miR-26a, miR-26b and miR-124 mimics and the miR levels of miR-9, miR-124, miR-218 and miR-135a were measured 72h post transfection by qPCR. The levels of all the tested miRs were reduced in the tKO<sup>26b/26a1/a2</sup> cells (Figure 25A). These decreased levels can be partially rescued by the transfection of miR-26a or miR-26b mimics and nearly completely rescued by a miR-124 mimic. This mimic transfection is also able to rescue the amount of neuronal marker positive cells (Tuj1) in tKO<sup>26b/26a1/a2</sup> differentiated cells. These results show that the KO effects are due to loss of miR-26. The fact that the miR-124 shows similar rescue effects goes along with our hypothesis of the impact of miR-26 on the REST-miRs by affecting the REST complex.

To see if miR-26 is sufficient to induce the REST miR expression and initiates the multiple REST regulation feedback loops, miR mimic experiments in wild type cells were performed. For this, wild type NPCs were transfected with miR-26a and miR-26b mimics and the miR-REST levels of miR-9, miR-124, miR-218 and miR-135a were measured by qPCR (Figure 25C). The transfection of both miR-26a and miR-26b led to enrichment of all tested REST-miRs (Figure 25C).

The transfection of miR-26 led to the enrichment of miR-124. We could show that miR-124 could rescue the miR-26 KO. We tested, if miR-124 acts on miR-26 and the REST-miRs expression in wild type cells. Wildtype NPCs were transfected with miR-124 and the abundance of the miRs-26a, miR-26b, miR-9, miR-218 and miR-135a was measured by qPCR. While the REST-miRs were enriched after miR-124 transfection miR-26a and miR-26b were not affected (Figure 25D).

Taken these results together we concluded that miR-26 can trigger REST-miR expression and is also necessary for proper activation of the REST-miRs and subsequent neuronal differentiation.

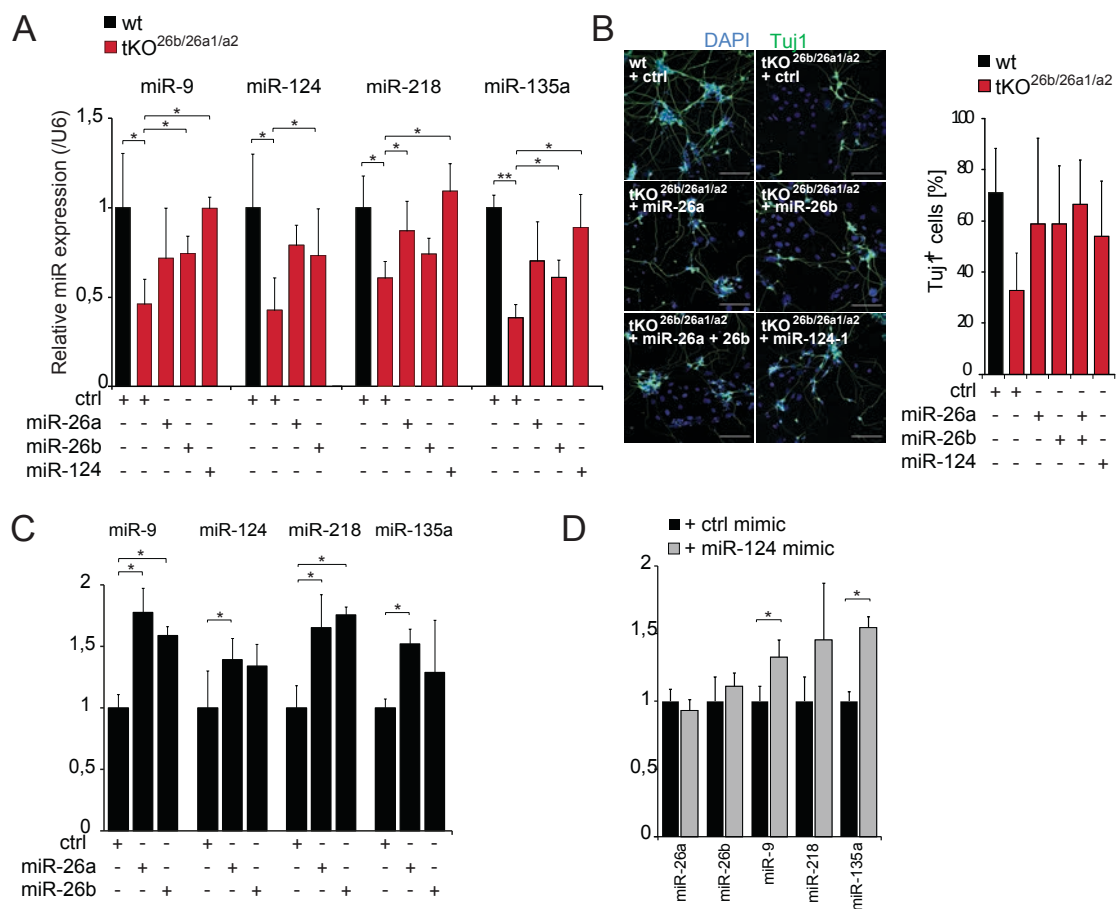


**Figure 25 miR-26 induce REST-miRs.**

**A** qPCR analysis of indicated REST-miRs after control-miR, miR-26a, miR-26b and miR-124 mimic transfection of wild type and tKO<sup>26b/26a1/a2</sup> NPCs. **B** Tuj1 staining of wild type and tKO<sup>26b/26a1/a2</sup> NCs (d15 in culture) 6 days after control-miR, miR-26a, miR-26b and miR-124 mimic transfection. Scale bars 100  $\mu$ m. **C** qPCR analysis of indicated REST-miRs after miR-26a and miR-26b mimic transfection of wild type NPCs. **D** qPCR analysis of indicated miRs after transfection of wild type NPCs with miR-124 mimics. tKO<sup>26b/26a1/a2</sup> cells red, wild type cells black bars. All analysis was done by Mark Sauer



## 5 Discussion

A complex gene regulation network controls formation of terminally differentiated neurons from multipotent ESC. In ESC (or non-neuronal cells), the REST complex represses the transcription of neuronal genes. This neuronal gene silencing is achieved through the remodeling of chromatin and formation of heterochromatin (inactive condensed DNA) or by directly manipulating the RNA Pol II activity. The REST activity is carried out by its cofactors such as C-terminal domain small phosphatases (CTDSPs). It has been shown that the genes encoding CTDSP and its paralogues carry members of the miR-26 family in their introns. These miRs are post transcriptionally regulated, modulate the expression of their hosts and hence have a direct impact on REST activity. Processing of miR-26 family members is halted in early developmental stages of embryogenesis at the level of DICER processing. Processing is activated just prior or concomitantly to the onset of neurogenesis.

In this thesis, I performed experiments that addressed two key questions related to the miR-26-regulated onset of neurogenesis: First, I performed a series of biochemical experiments aimed at identifying factors that regulate the processing of miR-26 family members. Second, an *ex vivo* model of neurogenesis was established as part of a collaboration with the laboratory of Prof. A. Müller to investigate how miR-26 affects the gene expression program using a systems biology approach and how this relates to the formation of neurons.

### 5.1 Role of miR-26 is conserved in vertebrates

Studies in zebrafish had clearly shown a role of miR-26b in the final stages of neurogenesis, i.e. the differentiation of neuronal precursor cells into neurons<sup>81</sup>. While these studies linked miR-26 to neurogenesis it remained an open question whether this is a general function of this family. I therefore performed a comprehensive bioinformatic approach to analyze miR-26 family members in vertebrates.

These data revealed that all miR-26 family members can only be found in vertebrates and, more importantly, that all of them are encoded in introns of CTDSPs. While the precursor molecules show no structure (folding) similarities (Figure 30), the mature miR is conserved in all vertebrates (Figure 9), suggesting similar functions in different vertebrates. This is also strengthened by the fact that in vertebrates the miR-26 family has predicted target mRNAs that encode for components of the REST complex (Figure 31). A target scan analysis showed that miR-26 has sites broadly

conserved among vertebrate mRNAs in REST, coREST and CTDSP2 and poorly conserved sites for Sin3a and MeCP2. This strongly suggests that miR-26 regulates the activity of the REST complex, most likely in a negative way. miR-26 and the respective host gene CTDSPs are not regulated by RE1.

Interestingly, the miR-26 based REST complex regulation seems to differ in vertebrates. In lower vertebrates, like zebrafish or *Xenopus laevis*, more target sites could be identified in CTDSP. In higher vertebrates, like mammals, there are fewer target sites in CTDSP mRNAs (Figure 31). In REST mRNA, however, it is the other way around. Here, more target sites could be identified in REST mRNA in higher vertebrates and none could be found in lower vertebrates. That could be due to the fact that the early development is much faster in lower vertebrates. Maybe in lower eukaryotes the REST complex acts more over the CTDSP regulation during early development and needs advanced regulation. This indicated that different effectors of the REST complex might have different activity during neurogenesis and a different role in cell development. This complex regulation might have changed over evolution. Therefore, studying the influences of miR-26 on single REST complex members could give insights in REST complex functionality during development and neurogenesis.

### **5.2 pre-miR-26b shows normal nucleo-cytoplasmic transport**

The initial question that I addressed regarding the role of miR-26 is how it is spatio-temporally controlled in the course of neurogenesis. Earlier studies had shown that miR-26 was expressed throughout development but kept in its inactive precursor form until the onset of neurogenesis. This suggested that a factor controls miR-26 maturation and hence determines whether a neuronal stem cell develops into a mature neuron. To gain insight into this process I investigated at which step in the biogenesis pathway the miR-26 is halted. As DICER processing is believed to occur exclusively in the cytoplasm, it seemed to be a plausible scenario that the miR is retained in the nucleus after DROSHA cleavage. However, microinjection studies in *Xenopus laevis* oocytes indicated that this was not the case. Specifically, I could show that the pre-miR-26 is exported to the cytoplasm with an efficiency and kinetic that was indistinguishable from the export of control miRs such as pre-miR-430 or pre-miR-31. These results rule out that nuclear retardation of miR-26 accounts for its processing delay in development in *Xenopus laevis*. Because of the similarity of the



miR-26 regulation between mouse, zebrafish and *Xenopus*, it is likely that this conclusion applies to vertebrates in general.

### **5.3 pre-miR-26 shows stage specific processing in zebrafish development**

As the export of pre-miR-26 was ruled out to account for the processing delay of miR-26b, the possibilities of inactive DICER or of a trans acting factor, which prevents the pre-miR-26 from further maturation, was assessed. In microinjection experiments I tested if pre-miR-26 can be processed in early developmental stages. The pre-miR-26b did not show any processing products whereas the control pre-miR-430b was processed efficiently. This not only demonstrated that DICER is active in early zebrafish but it also showed that pre-miR-26b processing is selectively repressed.

In *Xenopus leavis* it has been shown that AGO is limited during early developmental stages<sup>114</sup> which leads to reduced formation of mature miRs. It is, however, unlikely that this accounts for the block in miR-26 processing in early embryogenesis as the control miR-430 is processed under the same conditions efficiently.

To test if this repression is ongoing throughout development I further analyzed pre-miR processing at a developmental stage with ongoing neurogenesis. Both, the control pre-miR-430b and pre-miR-26b, showed processing with comparable efficiency at *in vitro* incubation in zebrafish lysate derived from 24 hpf old zebrafish.

These results underline that the regulation of miR-26 processing takes place at the level of pre-miR maturation. These results also suggest a maternal factor regulating the miR-26b biogenesis. This regulation most likely prevents DICER processing.

There are several factors known that specifically bind pre-miRs and inhibit DICER processing. For example, the pre-miR-151 is bound and edited (converting adenosine (A) to inosine (I)) by ADAR<sup>144</sup>. This editing is sufficient to prevent DICER cleavage and leads to accumulation of pre-miR-151 RNAs<sup>144</sup>. Another example for such a regulation is lin-28, which inhibits pre-let7 processing. Lin-28 inhibits nuclear DROSHA processing<sup>100,101</sup> and is able to block the cytosolic DICER processing<sup>98,99</sup>. Lin-28 interacts with a conserved GGAG motive of the let-7 stem loop. Hereby, it does not only block the processing, but it also recruits the terminal uridylyltransferase TUT4, which destabilizes the let-7 precursor by adding uridines (U) to its 3' end<sup>102</sup>.

## 5.4 Identification of pre-miR-26 binding proteins

Based on the experiments described in sections 5.2 and 5.3 the presence of a trans acting factor that regulates pre-miR-26 processing appeared the most plausible scenario. According to my data this hypothetical factor was further predicted to act as a repressor, rather than an activator, and would bind at early stages of development (i.e. before onset of neurogenesis) to the pre-miR. Consequently, affinity-based strategies were applied to isolate such factor(s) from zebrafish and mouse embryonal cell extracts.

I applied two complementary strategies to isolate and characterize pre-miR-26b binding partners. In one approach, the precursor was immobilized directly via an intermolecular S1 aptamer to a stationary phase. In an alternative approach the precursor was indirectly immobilized. For this, the 5'-end of the precursor was prolonged and a biotinylated DNA adapter molecule with a complimentary prolonged sequence was used as a hook. These approaches resulted in 3 potential candidates, which will be discussed in the following sections.

Such strategies were successfully used before to identify pre-miR binding proteins. The well-known let-7 interacting proteins lin-28 and TUT4 have been identified as miR biogenesis suppressors by RNA affinity purification<sup>102</sup>. Also the pre-miR-134 localization mediated by DHX36 has been identified with such an approach<sup>145</sup>. Most recently, an extended database of around 180 pre-miR-binding proteins was built by such a RNA affinity approach for more than 70 miR (excluding miR-26) in a large number of human cell lines<sup>115</sup>.

### 5.4.1 ZnF346

Using zebrafish lysate (6 hpf) and the indirect RNA affinity chromatography (Figure 15), the zinc finger protein ZnF346 was isolated as a promising miR-26 binding factor. ZnF346 is a known dsRNA binding protein<sup>121</sup>.

The overexpression of ZnF346 in developing zebrafish was not sufficient to alter the mature miR-26 abundance. This does not exclude ZnF346 as a potential factor. A second factor might be needed for regulation or ZnF346 needs to be modified to regulate the processing. Recombinant ZnF346 binds to pre-miR-26 as good as to a control pre-miR (let7). The binding affinity toward dsRNA might predominate the sequence specificity towards miR-26 in this experiment. However, complete suppression of ZnF346 expression in murine ESC is sufficient to increase mature miR-26 abundance, indicating a negative regulating effect on pre-miR-26 processing.

Whether this can also be observed in zebrafish early development remains to be analyzed. In order to analyze whether ZnF346 required co-factors for its activity, the ZnF346 interactome would need to be analysed. ZnF346 was shown lately to bind to the pri-miR-9 and -155 in A/U-rich areas independent of dsRNA structure<sup>115</sup>. A specific function of ZnF346 on pri-miR-9 and -155 was not described so far. Maybe its function on this pri-miR is only detectable in differentiating or differentiated neurons. Our cell culture system is perfect to analyze the impact of ZnF346 on this pri-miR in neurogenesis and will be used in the near future.

In summary, the role of ZNF346 in miR biology in general and in the regulation of miR-26 in particular remains an open question. Whereas some experiments suggest a role in the process of questions, others appear to contradict such model. Clearly, further studies are required to further investigate the impact on miR-26 and general miR processing in developing zebrafish and differentiating neuronal cells.

#### **5.4.2 FXR1, FXR2 and FMRP**

As described in 5.1 miR-26 is highly conserved in vertebrates (regarding sequence, targets and most likely regulation). I therefore performed the indirect RNA affinity chromatography using murine undifferentiated P19 cell lysate. The same murine P19 cell line was used to describe the pre-miR-26 retardation in mice<sup>81</sup>. By this set up the fragile X related protein family was identified as potential miR-26 processing regulators.

This family has three members, the fragile X mental retardation 1 protein (FMRP) and its paralogous fragile X mental retardation syndrome-related protein 1 and 2 (FXR1 and FXR2). Of note, transcriptional silencing of the FMR-1 gene, which encodes FMRP leads to fragile X syndrome, a neurodevelopmental disorder and the most common genetic cause of intellectual disability<sup>123</sup>. All members possess two KH domains and C-terminal arginine-glycine-rich regions, which are all known to bind RNA<sup>146</sup>. As FMRP and FXR1 and 2 were enriched in neurons<sup>124</sup> and their absence impairs proper neuronal function, an impact on neurogenesis seems likely. In zebrafish it was shown that the downregulation of FMRP leads to enriched neurite length and branching in motor neurons<sup>147</sup>, which display the opposite phenotype of the miR-26 knock down in zebrafish, where secondary motoneurons were reduced in size<sup>81</sup>. FMRP and FXR1 were shown to interact with DICER and a component of RISC linking them to the miR machinery<sup>148-150</sup>. While FXR1 is needed for efficient miR-9 and miR-124 processing, loss of FMRP and FXR2 in combination leads to

enriched levels of miR-9 and mir-124<sup>120</sup>. As miR-9 and miR-124 are REST regulated<sup>46,78</sup>, this forms a connection to miR-26. Also miR-26 was identified to be bound by FXR1 and FMRP using RNA-protein crosslinking in combination with affinity chromatography (PAR-CLIP)<sup>146</sup>.

Taking this information together makes the fragile X related protein family a good candidate as a miR-26 regulating factor.

I first tried to analyze the impact of these proteins in developing zebrafish. Although all three proteins of the FMRP/FXR family are present in the developing zebrafish, their expression levels differ considerably. The level of FMRP increases during development, whereas the levels of FXR1/2 decrease. The knock down of individual proteins of the family failed to show effects on zebrafish morphology or miR-26 processing. However, the simultaneous knock down of FXR1 and 2 or of FMRP, FXR1 and 2 lead to retardation of development especially of the head and tail regions and to increased levels of mature miR-26. Under these conditions I observed also enriched formation of mature miR-92b, i.e. a micro-RNA that is activated during neurogenesis<sup>151</sup>. This implies that miR-26 is able to increase miR-92b expression.

Unfortunately, I was not able to validate the binding of FMRP and FXR1/2 with pre-miR 26b in zebrafish. However, a clear impact on miR-26b processing could be shown. If this is due to a direct regulation of miR-26-processing or due to a general influence of FRMP/FXR1/2 on the miR-machinery cannot be said at this point. To further investigate the impact of FRMP/FXR1/2 on miR-26, on pre-miR-26 binding and on general miR processing in developing zebrafish as well as in differentiating neuronal cells additional studies are needed.

### 5.4.3 Eral1

The factors described above (5.4.1, 5.4.2) showed some criteria arguing for miR-26 regulation but also showed some deficits. To identify additional candidates direct S1 RNA affinity chromatography was performed. By using lysate from murine ESC cells (Figure 19) Eral1 was identified as potential regulating factor.

Eral1 (ERA (*E. coli* RAS like protein) like protein, human analogue also known as H-ERA), is a mitochondrial RNA chaperone and is involved in the assembly of the 28S mitochondrial small ribosomal subunit by binding and stabilizing the 12S mitochondrial rRNA via its KH-domain<sup>128</sup>. The 12S rRNA forms a stem loop where Eral1 binds. The lower part of this stem is similar to the lower stem of all pre-miR-26 (Figure 30)<sup>128</sup>, which makes Eral1 an interesting candidate for a pre-miR-26

processing regulator. The activity of Eral1 is regulated through its GTP binding domains. It is inactive if bound to GDP and active if bound to GTP<sup>152</sup>. This could also function as a releasing mechanism of pre-miR-26 upon neurogenesis initiation.

Binding of pre-miR-26 was shown to be highly specific as the immunoprecipitation of Eral1 co-enriched pre-miR-26 as shown by qPCR.

Although Eral1 is nuclear encoded, its primary function and localization is in mitochondria, which is not compatible with potential regulation of miR-26b processing.

However, the N-terminal mitochondrial localization signal of Eral1 is encoded in exon1. Interestingly, in mouse and zebrafish potential alternative translation start codons can be found, which are in frame and both upstream of the GTP binding domain. Isoforms missing exon 1 would be localized in the cytosol but still active. Eral1 regulation of miR-26 could still be a possible function. However isoform profiles have to be analyzed and a potential cytosolic localization has to be shown, to account as a miR-26 regulating factor.

#### **5.4.4 Alternative approaches for detection of pre-miR factors**

I am aware of the possibility, that the used affinity approaches might not be suitable for the identification of regulatory factors, maybe because the factor interacts only transiently to pre-miR-26 or the binding conditions that were used did not allow efficient interactions. An alternative approach might be UV crosslinking, which would allow the identification of transient interactions and also would allow more stringent washing. This would remove the high background that was always a problem in my purifications. For example, *in vivo* mRNA binding by OSCAR, a well known RNA localization molecule, could only be shown after crosslinking the protein to its mRNA<sup>153</sup>.

miR regulation often comes along with precursor modifications that inhibit processing by DICER or DROSHA. Such modifications can occur at the 5' or 3' end, at internal position or the RNA sequence itself is edited. As mentioned above ADAR edits RNA by converting adenosine to inosine by deamination<sup>144</sup>. Another example is TUT4 that uridylates the 3'-end of pre-let7<sup>102</sup>. It might be helpful to first analyze the retained pre-miR-26 molecules for RNA editing or modification. For the analysis the precursor RNA would have to be captured first and then analyzed. If a modification would be identified, the pool of potential factors would be reduced to a manageable group,

which then could be knocked out or down and subsequently the miR-26 levels could be analyzed.

Another possible regulator would be an RNA based regulator in form of a non coding RNA. Such a regulator could be identified by affinity chromatography approaches used for protein regulators with subsequent sequencing instead of mass spectrometry.

### **5.5 miR-26 KO cells show loss of neural identity**

Neurogenesis is the formation of neuronal cells from neuronal progenitor cells, which derive from embryonic stem cells. This differentiation depends on tightly regulated gene regulation programs<sup>1,2,75</sup>. As shown before, the miR-26 plays a role in neuronal formation most likely through its regulation on its host and on REST complex member CTDSF. To better understand the role of miR-26 during neurogenesis the function of miR-26 was analyzed in a murine *ex vivo* neural differentiation system. In this system ESC differentiate into NC via NPC. It allows systematic analysis of protein and gene expression during neurogenesis. This cell system also enables studies with knockout cells generated by the CRISPR-Cas9 system.

To analyze miR-26 in neurogenesis, the three genomic loci of miR-26 (miR-26a-1, miR-26a-2 and miR-26b) were deleted individually and in combination and three cell lines were generated (KO26, dKO26a1<sup>/a2</sup> and tKO<sup>26b/26a1/a2</sup>).

As mentioned above, miR-26 (4.1) is inactive in ESC and NSC but gets active in further differentiation. Missing miR-26 should not affect the neurogenesis until the NSC state. As expected, all KOs had no effect on ESCs and showed no significant effect during differentiation until the cultures reach the NSC state. Further differentiation into NCs, however, was massively restricted in all KO conditions. Surprisingly, the KO of a single member (a or b) is already sufficient to impair the formation of neurons. This would indicate a level-dependent regulation, which needs a specific threshold for neurogenesis.

The effect of miR-26a KO is more dramatic than the miR-26b KO (Figure 22, 23). This is most likely, because the miR-26a is more abundant (based on our small RNA seq analysis, data not shown). Unexpectedly, the dKO<sup>26a1/a2</sup> shows also stronger phenotypes than the tKO<sup>26b/26a1/a2</sup> (Figure 22, 23). We found no rational explanation for this phenomenon. It seems that there is a miR-26 concentration-dependent control mechanism that is activated in the tKO<sup>26b/26a1/a2</sup> but is not active in the dKO<sup>26a1/a2</sup>. Another possibility would be that the targets of miR-26a are different from

miR-26b. This should not be the case, because there are no differences in the guide sequence of the two miRs. A third option would be that there are minor differences in the temporal expression of the 3 miRs. For more information, the expression of the three pre-mi-26 and their CTDSP hosts would need to be measured during neurogenesis in shorter time-intervals.

To understand the molecular mechanisms, that are affected by the miR-26 KO and generate such a strong phenotype, the transcriptome of differentiated KO and wild type cells was compared. Gene ontology (GO) analysis of downregulated genes showed that neuronal GO terms are reduced in all KO conditions. This indicates that the KO cannot fully differentiate to NCs and lost its neuronal fate. On the other hand could not be identified, which differentiation outcome the cells reach, because upregulated genes did not show a tendency for specific biological processes in differentiated KO cells. The cells seem to stay on a NPC level or a further intermediate differentiation state.

Interestingly, in all knock out cell cultures there are still a few neurons, which have differentiated. It would be interesting to analyze the difference of these neurons. They might differentiate to a different subculture that might have a different neurogenesis gene regulation.

## **5.6 miR-26 KO affects the REST – REST-miR feedback loop**

The REST complex represses neuronal genes in non-neuronal cells. The target genes are not only protein-coding but may also encode regulatory RNAs such as miRs. The best-studied miRs under REST regulation are miR-132, miR1-24 and miR-9/9\*. These miRs have been shown to regulate REST complex members such as, REST, CoREST, CTDSP and MeCP2<sup>46,77-79</sup>. A literature survey revealed approx. 40 miRs, which are potentially regulated by the REST complex and out of those 14 have been validated (REST-miRs). Each of these REST-miRs have target sites in at least two mRNAs encoding REST complex factors and thus might form multiple negative regulatory feedback loops (Figure 26). This regulation is likely to be functional in all vertebrates, because not only the regulating miRs are conserved but also the target sites in REST components.

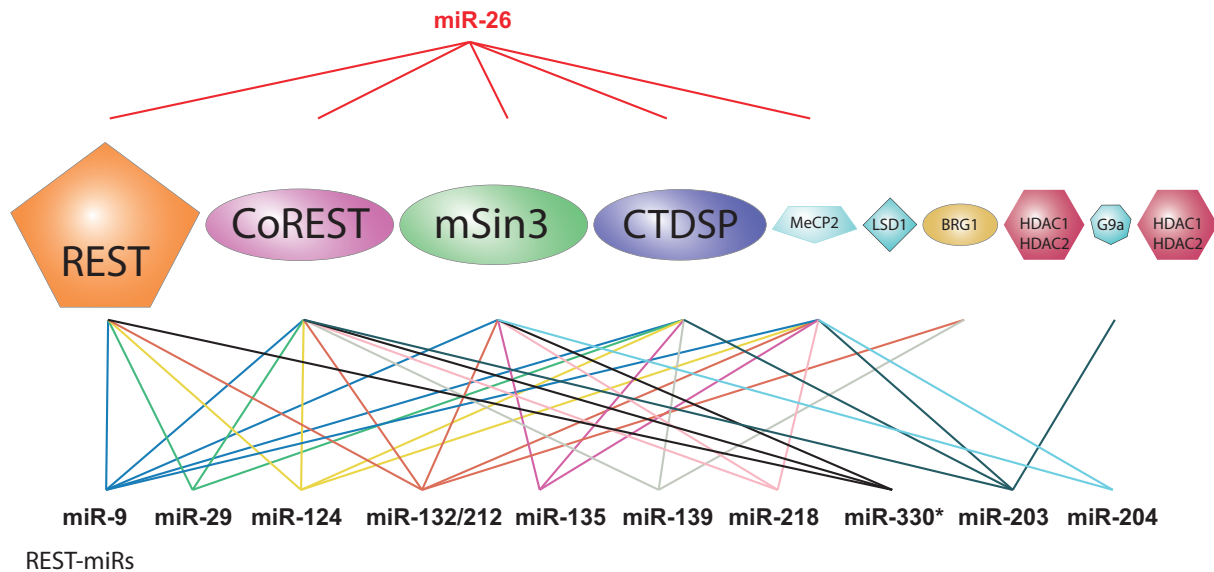


**Figure 26 REST to miR; miR to REST regulation.**

miR-26 regulates complex members, but is not under REST control. The REST complex represses the expression of the shown miRs (REST-miRs). All of these REST-miRs themselves can attack several parts of the complex, indicating potential feedback loops.

A miR that targets parts of the REST complex but is not regulated by the complex itself is miR-26 (Figure 26). miR-26 might initiate a potential feedback loops. To analyze this hypothesis we examined the miR levels in differentiated KO and wild type cultures. Indeed, small RNA sequencing showed that the concentrations of the majority of the REST-associated miRs are decreased. I could also show that the activation of miR-26 initiates the expression of REST-miRs. This might trigger a cascade of REST-miR feedback loops, which gradually enhances the down regulation of the REST complex.

Our observation that the lack of miR-26 results in reduced formation of neurons might indeed be explained by the lack of the REST-miR initiation. We assume that the miR-26 regulates multiple REST complex members and not only CTDSP as shown by Dill et al<sup>81</sup>. A prove for this model would be a rescue experiments of tKO<sup>26b/26a1/a2</sup> by inactivation the REST complex (or members thereof) or by altering their miR-26 target site. However, such an experimental strategy appears not feasible because miR-26 is acting against multiple REST complex members simultaneously and hence the inactivation of individual REST subunits is likely not to be sufficient to rescue tKO<sup>26b/26a1/a2</sup> cells. The inactivation on the other hand of multiple REST complex factors is expected to lead to major cell survival impairments.

The transcriptome of ESCs and NCs was also sequenced in KO and wild type cells. The impact of miR-26 on REST complex members could not be seen in either mRNA



sequencing data. This is most likely due to the fact that ESC sequencing data were acquired from a time point where miR-26 is not yet active. The miR-26 related activity should be at the transition from NPC to NCs, which is reached at d9 – d15. The data acquired from d15-differentiated cells, in contrast, are likely to be already too late to see the impact on the REST complex components.

To further investigate the connection between miR 26b and REST complex factors the sequencing of additional differentiation time points would be needed. If candidate proteins are identified it is also possible to analyze the REST factors by western blot during differentiation.

### **5.7 REST-miR function aside REST regulation**

miRs can target several hundred mRNA. It is no surprise that also REST-miRs regulate other targets. Especially the miR-9 and -124 are known to be important regulators during neurogenesis. Tlx is described as an essential regulator of NSC proliferation<sup>154</sup> and can be inhibited by miR-9 during differentiation. In turn, Tlx is able to transcriptionally repress miR-9<sup>155</sup>. Also the other arm of the miR-9 is active. The miR-9\* together with the miR-124 change the BAF complex composition from the neural progenitor specific BAF complex to the neural specific BAF complex via the down regulation of BAF53a<sup>137</sup>. This complex composition switch is essential for the expression of neural genes and neural commitment during neurogenesis<sup>156</sup>. Another function of miR-124 is regulation of neuron specific alternative splicing. miR-124 downregulates the splicing regulator Ptbp1. This leads to an increase of the splicing regulator Ptb2, which in turn enables the neuron specific splicing program.<sup>157</sup>

The impact of the miR-9 and -124 on neurogenesis is so significant, that the induction of these two miRs can reprogram somatic cells into neurons<sup>138</sup>. Even if they are sufficient to induce neurogenesis they still need to be activated and for this the miR-26 is an important factor.

### **5.8 The Role of miR-26 in neurogenesis**

Based on the findings described in this thesis and the already published knowledge about the miR-26, the REST-complex and the REST-miRs, a model for the role of miR-26 in neurogenesis can be put forward. In ESC, or non-neuronal tissues cells, the REST complex is active, whereas the pre-miR-26 is, although being expressed, not active as it is retained in the unprocessed stage. In this situation, the REST complex represses the expression of neuronal genes including REST-miR genes. At

the transition from NSC the miR-26 starts to become processed and the mature miR-26 can act against CTDSP and other REST member mRNAs. This leads to reduced REST activity and REST-miRs are slowly expressed. As the differentiation to NCs proceeds the REST-miR-REST feedback loop leads to increased miR-REST activity and REST complex downregulation. This leads to more and more expression of neuronal genes until the cell reaches a neuronal state.

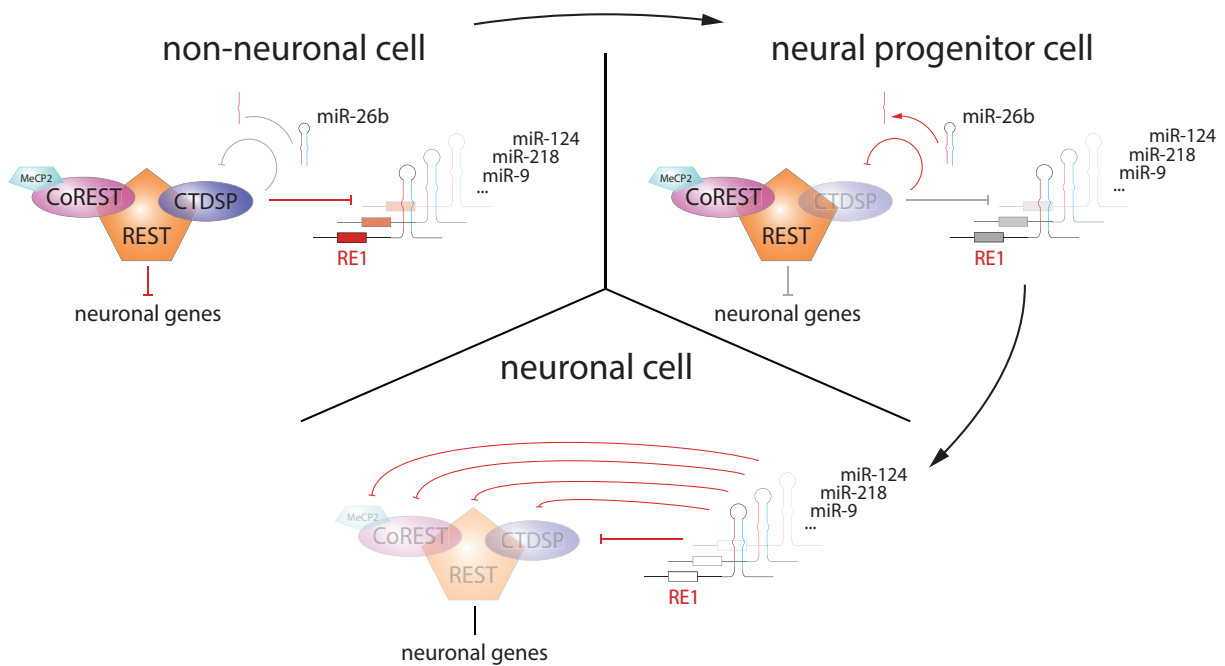


**Figure 27 Model: role of miR-26 in neurogenesis**

**Non neuronal cell:** REST repress neuronal genes and REST-miRs, miR-26 processing is halted. **Neural progenitor cell:** Mature miR-26b is acting against CTDSP, partial inactivation of the REST complex leads to partial expression of neuronal genes and REST-miR. **Neuronal cell:** Activation of REST-miR initiated feedback loop regulation which further inactivates REST-complex and eventually leads to its complete shut-off.

## 6 Material & Methods

### 6.1 Materials

All used chemicals were purchased from Merck, BD Biosciences, Serva, Sigma-Aldrich, Riedel-de Haen, Boehringer Ingelheim and Roth. Laboratory consumables were obtained from Hartenstein, Macherey-Nagel, Eppendorf, Sarstedt, Satorius stedim, Dispomed and Geiner. Radiochemicals were purchased from Hartmann Analytic.

#### 6.1.1 Nucleotide and Protein Ladders

GeneRuler™ DNA Ladder Mix	Thermo Scientific
GeneRuler™ 100 bp DNA Ladder	Thermo Scientific
PageRuler™ Prestained Protein Ladder	Thermo Scientific
PageRuler™ Unstained Protein Ladder	Thermo Scientific

#### 6.1.2 Buffers and Solution

DNA loading buffer (6x)	30% (v/v) Glycerol 0,25% Bromophenol blue 0,25% Xylene cyanol FF
Native loading buffer (5x)	50% (v/v) Glycerol 0,5x TBE 0,02% (w/v) Bromophenol blue
5x Tris/EDTA/borate (TBE)	445 mM Tris-HCl, pH 8.3 445 mM Boric acid 10 mM Na <sub>2</sub> EDTA
10x Lämmli	250 mM Tris-Base 1,92 M Glycine 35% SDS

## Material & Methods

---

10x NET buffer	500 mM Tris-Base 50 mM NaEDTA 1,5 M NaCl 0,5% Triton-X 100
NET-Gelantine	2,5 g Gelantine 1x NET Buffer
10x Phosphate buffered saline (PBS)	1,4 M NaCl 27 mM KCl 100 mM Na <sub>2</sub> HPO <sub>4</sub> 18 mM KH <sub>2</sub> PO <sub>4</sub>
6x Protein sample buffer	300 mM Tris-HCl, pH 6.8 12% (w/v) SDS 30% (v/v) Glycerol 600 mM DTT 0,04% (w/v) Bromophenol blue
CaCl <sub>2</sub> -Buffer	60 mM CaCl <sub>2</sub> 15% (v/w) Glycerol 10 mM PIPES pH 7,0
10x T7 Transcription buffer	400 mM Tris-HCl (pH 7.9) 10 mM Spermidine 260 mM MgCl <sub>2</sub> 0,1% Triton X
RNA Stop Mix	8 M Urea 50 mM EDTA 0,03% (w/v) Bromophenol blue 0,03% (w/v) Xylene Cyanol

---

RNA loading buffer	95% Formamide 50 mM EDTA 0,03% (w/v) Bromophenol blue
RNA gel elution buffer	0,5 M NH <sub>4</sub> OAc 0,1 mM EDTA 2 mM MgCl <sub>2</sub> 0,1% SDS opt. 0,1 mg/ml tRNA
Proteinase K resuspension buffer	25 mM Tris-HCl pH 8 10 mM CaCl <sub>2</sub> 50% Glycerol
10x Proteinase K buffer	100 mM Tris-HCl pH 8,0 50 mM EDTA pH 8,0
MMR 1	50 mM Hepes pH 7,8 100 mM NaCl 20 KCl 1 mM MgSO <sub>4</sub> 1 mM Na <sub>2</sub> HPO <sub>4</sub> 20 mM CaCl <sub>2</sub> 1 mM EDTA
OR-I	5 mM Hepes pH 7,6 82,5 mM NaCl 2,5 mM KCl 1 mM MgCl <sub>2</sub> 1 mM Na <sub>2</sub> HPO <sub>4</sub>

OR-II	5 mM Hepes pH 7,6 82,5 mM NaCl 2,5 mM KCl 1 mM MgCl <sub>2</sub> 1 mM Na <sub>2</sub> HPO <sub>4</sub> 1 mM CaCl <sub>2</sub> 0,1 mg/ml Gentamycin
Zebrafisch lysate buffer	300 mM NaCl 30 mM Tris/HCl pH 7,0 5 mM MgCl <sub>2</sub> 5 mM DTT 0,5% Igepal 1:1000 Protease inhibitor
0,3% Danieaus Medium	17,4 mM NaCl 0,21 mM KCl 0,12 mM MgSO <sub>4</sub> 0,18 mM Ca(NO <sub>3</sub> ) <sub>2</sub> 1,5 mM Hepes pH 7,5 0,0001% Methylenblue
<b>6.1.3 Bacterial culture Media</b>	
Luria broth (LB)	1,0% (w/v) Tryptone 1,0% (w/v) NaCl 0,5% (w/v) Yeast Extract
Super broth (SB)	3,5% (w/v) Tryptone 0,5% (w/v) NaCl 2,0% (w/v) Yeast Extract set pH to 7,5 using NaOH

Selection media was prepared by combination of antibiotics (100 µg/ml Ampicillin (Roth), 50 µg/ml Kanamycin (Sigma), 50 µg/ml Chloramphenicol (Sigma)) and media. Agar plate were made by addition of 2% (w/v) Agar.

### 6.1.4 Bacterial Cells

Strain	Chromosomal genotype	Supplier
<i>E. Coli</i> DH5 $\alpha$	F- $\Phi$ 80lacZ $\Delta$ M15 $\Delta$ (lacZYA-argF) U169 recA1 endA1 hsdR17 ( $r_k^-$ , $m_k^+$ ) phoA supE44 $\lambda^-$ thi-1 gyrA96 relA1 $\lambda^-$	Invitrogen
<i>E. Coli</i> BI-21-Rosetta	thi hsdR17 ( $r_k^-$ $m_k^+$ ) glnV44 relA1 lac F-ompT hsdS <sub>B</sub> ( $r_B$ $m_B$ ) gal dcm pRARE (Cam <sup>R</sup> )	GE Healthcare

### 6.1.5 Zebrafisch Cell lines

*TLF* (Tüpfel long fin) is one of the used wild type strains with dotted pigment patterns.

*WIK* (Wild India Kalkutta) Wild type strain with striped pigment pattern.

*TÜ* (Tübingen strain) Another striped wild type strain called.

### 6.1.6 Antibodies

#### 6.1.6.1 Primary Antibodies

6.1.6.1.1.1.1.1.1 y	Antibod	6.1.6.1.1.1.1.1.2 er	Suppli	6.1.6.1.1.1.1.1.3 n	Dilutio
FLAG		Sigma (A2220)		1:1000	
HA		HISS (MMs-101R)		1:1000	
FMRP		Linder et al 2008 <sup>158</sup>		1:500	
FXR1		Merck (6BG10)		1:200	
FXR2		Thermo Scientific (A42)		1:200	
Eral 1		PA5-41800		1:500	

#### 6.1.6.2 Secondary Antibodies

6.1.6.2.1.1.1.1.1 y	Antibod	6.1.6.2.1.1.1.1.2 er	Suppli	6.1.6.2.1.1.1.1.3 n	Dilutio
$\alpha$ -mouse glgG		6.1.6.2.1.1.1.1.4	Sigma	6.1.6.2.1.1.1.1.5 0	1:500
$\alpha$ -rabbit glgG		6.1.6.2.1.1.1.1.6	Sigma	1:5000	
		(A6514)			

### 6.1.7 Plasmid Vectors

Plasmid	Description	Cloning	Reference
---------	-------------	---------	-----------

## Material & Methods

			Supplier
pcDNA3.1			Addgene
pcDNA3.1:ZNF346:P2A:eGFP	IVT, dre- Injection	Not1/Xho1	This study
pcDNA3.1:Mak16:P2A:eGFP	IVT, dre- Injection	Not1/Xho1	This study
pcDNA3.1:PK1IP:P2A:eGFP	IVT, dre- Injection	Not1/Xho1	This study
pcDNA3.1:FMRP:P2A:eGFP	IVT, dre- Injection	Not1/Xho1	This study
pcDNA3.1:FXR1:P2A:eGFP	IVT, dre- Injection	Not1/Xho1	This study
pT-28(a)	Protein purification		Novagen
pT-28(a):ZNF346	Protein purification	EcoR1/Xho1	This study
pT-28(a):Lin28	Protein purification	BamH1/Xho1	This study
pGEX-6P-1	Protein purification		GE Healthcare
pGEX-6P-1:ZNF346	Protein purification	EcoR1/Xho1	This study
pGEX-6P-1:Lin28	Protein purification	BamH1/Xho1	This study
pGEX-6P-1:FMR1	Protein purification	EcoR1/Xho1	This study
pGEX-6P-1:FXR1	Protein purification	EcoR1/Xho1	This study
pGEX-6P-1:FXR2	Protein purification	EcoR1/Xho1	This study
puC19:U1ΔSm-T7	IVT	BamH1	Neuenkirchen et al 2015 <sup>159</sup>
puC19:U6-SP6	IVT	BamH1	Neuenkirchen



### 6.1.8 DNA nucleotides

All DNA nucleotides were purchased from Sigma-Aldrich.

#### 6.1.8.1 DNA nucleotides for cloning

Oligo name	Sequence (5'-3')
Mak16 EcoRI for	GATTCGGAATTCATGCAACACGACGACGTTATATGG
Mak16 XhoI rev	GTACTTCTCGAGCTATGTGGCCTTGCTTTTCTGAG
ZNF346 EcoRI forw	GATTCGGAATTCATGGAGAGGCTTGTTTCAGCG
ZNF346 XhoI rev	GTACTTCTCGAGTCACTCGTAGGCCACGTTGAA
PK11P EcoRI forw	GATTCGGAATTCATGAGCGAGTGTTTTACAGTCATG
PK11P XhoI rev	GTACTTCTCGAGTTATTGAACCTTTTGCCTTTTCTTCTTT
Lin28 BamHI for	GTACCTGGATCCATGCCCCGGCAAATCCG
lin28 XhoI rev	GATCTTCTCGAGCTAATCAGTGCTCTCTGGCAG
Fmr1- For EcoR1	GATTCGGAATTCATGGACGAGCTCGCGGTGGA
FMR1-xho1-rev	GTACTTctcgagCGAAACGCCGTTCACTACGG
Fxr1- For EcoR1	GATTCGGAATTCATGGAGGAACTGACGGTGGAGGTCC
FXR1-xho1-rev	GTACTTctcgagCGAGACTCCGTTGACCACGGC
Fxr2- for EcoR1	GATTCGGAATTCATGGACGGGTTGGCGGTGGAGG
FXR2-xho1-rev	GTACTTctcgagGGAGACGCCGTTACCATGGC
FMR1 Hygro For	TCCAGCACAGTGGCGGCCGCCACCATGGACGAGCTCGCGGTGGAA
FMR1 Hygro Rev	CAGAGAGAAGTTCGTGGCCGAAACGCCGTTCACTACGGC
FMR1 Hygro P2A for	GCCGTAGTGAACGGCGTTTCGGccacgaacttctctctg
FXR1 Hygro For	TCCAGCACAGTGGCGGCCGCCACCATGGAGGAACTGACGGTGGAGG TCC
FXR1 Hygro Rev	CAGAGAGAAGTTCGTGGCCGAGACTCCGTTGACCACGGCT
FXR1 Hygro P2A for	AGCCGTGGTCAACGGAGTCTCGGccacgaacttctctctg
FXR2 Hygro For	TCCAGCACAGTGGCGGCCGCCACCATGGACGGGTTGGCGGTGGAGG
FXR2 Hygro Rev	CAGAGAGAAGTTCGTGGCGGAGACGCCGTTACCATGGCC
FXR2 Hygro P2A for	GGCCATGGTGAACGGCGTCTCCGccacgaacttctctctg
Hygro eGFP Rev	TAAACGGGCCCTCTAGACCTCGAGTCACTTGTACAGCTCGTCcatgccga gagt
3.1 For ZnF 346	TCCAGCACAGTGGCGGCCGCCACCATGGAGAGGCTTGTTTCAGCGCAT GTATTGT
3.1 Rev ZnF 346	CAGAGAGAAGTTCGTGGCCTCGTAGGCCACGTTGAAGCTGTCCCAC T
3.1 For ZnF 246 egfp /	TTCAACGTGGCCTACGAGGCCACGAACTTCTCTCTGTTAAAGCAAGCA

## Material & Methods

---

mcherry	
3.1 For P21	TCCAGCACAGTGGCGGCCGCCACCATGAGCGAGTGTTTTACAGTCAT GGGGGAT
3.1 Rev P21	CAGAGAGAAGTTCGTGGCTTGAACCTTTTGCCTTTTCTCTTTTTTCC
3.1 For P21 egfp / mcherry	AAAAGGCAAAGGTTCAAGCCACGAACTTCTCTCTGTTAAAGCAAGCA
3.1 For MAK16	TCCAGCACAGTGGCGGCCGCCACCATGCAACACGACGACGTTATATG GGACCTT
3.1 Rev MAK16	CAGAGAGAAGTTCGTGGCTGTGGCCTTGCTTTTCTGAGCTGGTTCTGT
3.1 For MAK16 egfp / mcherry	CAGAAAAGCAAGGCCACAGCCACGAACTTCTCTCTGTTAAAGCAAGCA
FLAG/HA-IVT-For FMR1-REV-HA	TAATACGACTCACTATAGGGAGACCCAAGCTGGC CTAAGCGTAATCTGGAACATCGTATGGGTATGATCCTGATCCCGAAAC GCCGTTCACTACGGCC
FXR1-REV-HA	CTAAGCGTAATCTGGAACATCGTATGGGTATGATCCTGATCCCGAGAC TCCGTTGACCACGGCT
FXR2-REV-HA	CTAAGCGTAATCTGGAACATCGTATGGGTATGATCCTGATCCGGAGAC GCCGTTCACTACGGCC
FMR1-REV-FLAG	CTACTTGTCATCGTCGTCCTTGTAGTCTGATCCTGATCCCGAAACGCC GTTCACTACGGCC
FXR1-REV-FLAG	CTACTTGTCATCGTCGTCCTTGTAGTCTGATCCTGATCCCGAGACTCC GTTGACCACGGCT
FXR2-REV-FLAG	CTACTTGTCATCGTCGTCCTTGTAGTCTGATCCTGATCCGGAGACGCC GTTCACTACGGCC
FLAG-HA-FMR-FOR	GTAATTGGTACCGCCACCatggactacaaggacgacgatgacaagtaccatacgatgtt ccagattacgctggatccATGGACGAGCTCGCGGTGGAA
FLAG-HA-FXR1-FOR	GTAATTGGTACCGCCACCatggactacaaggacgacgatgacaagtaccatacgatgtt ccagattacgctggatccATGGAGGAACTGACGGTGGAGGTCC
FLAG-HA-FXR2-FOR	GTAATTGGTACCGCCACCatggactacaaggacgacgatgacaagtaccatacgatgtt ccagattacgctggatccATGGACGGGTTGGCGGTGGAGG
U6 T7 add forward	TTAATACGACTCACTATAGGGTGCTCGCTTCGGCAGC
U6 T7 add reverse	AAAAATATGGAACGCTTCACGAATTT

### 6.1.8.2 DNA Nucleotides for Northern Blot

Oligo name	Sequence (5'-3')
NB-miR-26b	ACCTATCCTGGATTACTTGAA
NB-dre-pre-miR-26b	GTAACCAAGAATAGGCCGTA TAGTGGGAACT
NB-miR-430b	CTACCCCAACTTGATAGCACTTT
NB-dre-pre-miR-430b	CTACTTTGCTTAAAAGAAAGATGCTAAAGTTAGAGT
NB-der-miR-9-1	ACTTTCGGTTATCTAGCTTTA
NB-dre-pre-miR-9-1	AGAATGAATAACACTCATAACAGCTAGATAACCAAAGA

NB-dre-miR-92a-1	ACAGGCCGGGACAAGTGAATA
NB-dre-pre-miR-91a-1	ACACACAGCATTGCTACCAATCCCAACCT
NB-dre-miR-92b	GGAGGCCGGGACGAGTGAATA
NB-dre-pre-miR-92b	GAGATTGAACAACACTGCACA ACATCCCACA

### 6.1.8.3 DNA nucleotides for *in vitro* transcription

Oligo name	Sequence (5'-3')	Comment
dre-26b-HH	GAAACAAGTAACCAAGAATAGGCCGCTACTAGTGGGAACT AACCTATCCTGGATTACTTGAAGACGGTACCGGGTACCG TTTCGTCCTCACGGACTCATCAGTTCAAGTAATCCAGTC TCTCTCTCTCTCCCTATAGTGAGTCGTATTAA	IVT-ribozyme
dre-430b1-HH	CTACCCCAACTTGATAGCACTTTCTACTTTGCTTAAAAGA AAGATGCTAAAGTTAGAGTGACGGTACCGGGTACCGTTT CGTCCTCACGGACTCATCAGACTCTAACTTTAGCTCTCT CTCTCTCTCTCCCTATAGTGAGTCGTATTAA	IVT-ribozyme
xtr-31a1-HH	GATGGCAATAGGTTGGCACAACCTGGTTTCAGATGCAACA GCTATGCCAACATCTTGCCTGACGGTACCGGGTACCGTT TCGTCCTCACGGACTCATCAGAGGCAAGATGTTGGTCTC TCTCTCTCTCTCCCTATAGTGAGTCGTATTAA	IVT-ribozyme
xtr-26-1-HH	GAAACAAGTAATCAAGAGTAGGCCGCTGCTTTGAGGAAAC AGCCTATCCTGGATTACTTGAAGACGGTACCGGGTACC GTTTCGTCCTCACGGACTCATCAGTTCAAGTAATCCAGT CTCTCTCTCTCTCCCTATAGTGAGTCGTATTAA	IVT-ribozyme
xtr-26-2-HH	GTCCCAAGTAATCGAGAAAAGGCTGACAGGAGACATTAC AGCCTATCCTGGATTACTTGAAGACGGTACCGGGTACC GTTTCGTCCTCACGGACTCATCAGTTCAAGTAATCCAGT CTCTCTCTCTCTCCCTATAGTGAGTCGTATTAA	IVT-ribozyme
TO-dre-miR 26b	GAAACAAGTAACCAAGAATAGGCCGCTACTAGTGGGAACT AACCTATCCTGGATTACTTGAACCTATAGTGAGTCGTATT AA	IVT
TO-dre-miR 430b	CTACCCCAACTTGATAGCACTTTCTACTTTGCTTAAAAGA AAGATGCTAAAGTTAGAGTCCTATAGTGAGTCGTATTAA	IVT
TO-xtr-miR 31a1	GATGGCAATAGGTTGGCACAACCTGGTTTCAGATGCAACA GCTATGCCAACATCTTGCCTCCTATAGTGAGTCGTATTA A	IVT
TO-xtr-miR 31a1 Lund	GGCAATAGGTTGGCACAACCTGGTTTCAGATGCAACAGCT ATGCCAACATCTTGCCTATAGTGAGTCGTATTAA	IVT
TO-xtr-miR 26.1	GAAACAAGTAATCAAGAGTAGGCCGCTGCTTTGAGGAAAC AGCCTATCCTGGATTACTTGAACCTATAGTGAGTCGTATT AA	IVT

## Material & Methods

---

TO-xtr-miR 26.2	GTCCCAAGTAATCGAGAAAAGGCTGACAGGAGACATTAC AGCCTATCCTGGATTACTTGAACCTATAGTGAGTCGTATT AA	IVT
dre-miR-26b- RNaseH	GAAACAAGTAACCAAGAATAGGCCGTAAGTGGGAACT AACCTATCCTGGATTACTTGAAGTCGATCTTGTACGTCC CTATAGTGAGTCGTATTAA	IVT-RNase
dre-miR-430b- RNaseH	CTACCCCAACTTGATAGCACTTTCTACTTTGCTTAAAAGA AAGATGCTAAAGTTAGAGTGTGCGATCTTGTACGTCCCTA TAGTGAGTCGTATTAA	IVT-RNase
xtr-pre-miR-31a-R NaseH	GATGGCAATAGGTTGGCACAACCTGGTTTCAGATGCAACA GCTATGCCAACATCTTGCCTGTGCGATCTTGTACGTCCCT ATAGTGAGTCGTATTAA	IVT-RNase
xtr-pre-miR-31aLu nd-RNaseH	GGCAATAGGTTGGCACAACCTGGTTTCAGATGCAACAGCT ATGCCAACATCTTGCCGTCGATCTTGTACGTCCCTATAG TGAGTCGTATTAA	IVT-RNase
xtr-pre-miR-26.1- RNaseH	GAAACAAGTAATCAAGAGTAGGCCGTGCTTTGAGGAAAC AGCCTATCCTGGATTACTTGAAGTCGATCTTGTACGTCC CTATAGTGAGTCGTATTAA	IVT-RNase
xtr-pre-miR-26.2- RNaseH	GTCCCAAGTAATCGAGAAAAGGCTGACAGGAGACATTAC AGCCTATCCTGGATTACTTGAAGTCGATCTTGTACGTCC CTATAGTGAGTCGTATTAA	IVT-RNase
xtr-pre-miR-451	CAGAACCCTTACCATTACTAACTCAGTAATGGTAACGG TTTGTGCGATCTTGTACGTCCCTATAGTGAGTCGTATTAA	IVT-s
dre-pre-miR-9-1- RNaseH	TACTTTTCGGTTATCTAGCTTTATGAAGAATGAATAACACT CATACAGCTAGATAACCAAGAGTCGATCTTGTACGTCC CTATAGTGAGTCGTATTAA	IVT-RNase
dre-pre-miR-92a-1- RNaseH	ACAGGCCGGGACAAGTGCAATACCTTCAAACACACAG CATTGCTACCAATCCCAACCTGTGCGATCTTGTACGTCCC TATAGTGAGTCGTATTAA	IVT-RNase
dre-pre-miR-92b- RNaseH	GGAGGCCGGGACGAGTGCAATATTGGCGGGAGATTGAA CAACACTGCACAACATCCCACACCTGTGCGATCTTGTACG TCCCTATAGTGAGTCGTATTAA	IVT-RNase
dre-pre-miR-124-1- RNaseH	TTGGCATTACCGCGTGCCTTAATTGAAATACAATAAATC AAGGTCCACTGTGAACACGGTCGATCTTGTACGTCCCTA TAGTGAGTCGTATTAA	IVT-RNase
dre-pre-miR-137-1- <b>RNaseH</b>	CTACGCGTATTCTTAAGCAATAACAACGAGAGCCGTATT ATCCACCCAAGAATACCCGTGTGCGATCTTGTACGTCCCT ATAGTGAGTCGTATTAA	IVT-RNase
pre-dre-26b-S1- Temp	GAAACAAGTAACCAAGAATAGGCCGTAAGTGGGAACT AACCTATCCTGGATTACTTGAACCCGGCCCGCGACTATC TTACGCACTTGCATGATTCTGGTCCGTCTATAGTGAGT	S1-RNA-Pull- down

	CGTATTAA	
pre-dre-26b-S1- Loop-Temp	GAAACAAGTAACCAAGAATAGGCGCCGACCCGCGACTA TCTTACGCACTTGCATGATTCTGGTCGGCACCTATCCTG GATTACTTGAATTGATACCTATAGTGAGTCGTATTAA	S1-RNA-Pull- down
pre-dre-26a1-S1- Temp	GAACCAAGTCATCCCGAATAGGCTTCCGGACATCACAA GCCTATCCTGGATTACTTGAACCCGGCCCGCGACTATCT TACGCACTTGCATGATTCTGGTCGGTCCTATAGTGAGTC GTATTAA	S1-RNA-Pull- down
pre-dre-26a2-S1- Temp	AGTGCAAGTAATCATGAATAGGCCTCCAGGACAGACAG CCTATCCTGGATTACTTGAACCCGGCCCGCGACTATCTT ACGCACTTGCATGATTCTGGTCGGTCCTATAGTGAGTCG TATTAA	S1-RNA-Pull- down
pre-dre-26a3-S1- Temp	AGTGCAAGTAACCAAGAACAGGCCAACCCCTAGTCCACAA AGCCTATCCTGGATTACTTGAACCCGGCCCGCGACTATC TTACGCACTTGCATGATTCTGGTCGGTCCTATAGTGAGT CGTATTAA	S1-RNA-Pull- down
pre-dre-430b1-S1- Temp	CTACCCCAACTTGATAGCACTTTCTACTTTGCTTAAAAGA AAGATGCTAAAGTTAGAGTCCCGGCCCGCGACTATCTTA CGCACTTGCATGATTCTGGTCGGTCCTATAGTGAGTCGT ATTAA	S1-RNA-Pull- down
pre-dre-430b1-S1- Loop-Temp	CTACCCCAACTTGATAGCACTTTGCCGACCCGCGACTAT CTTACGCACTTGCATGATTCTGGTCGGCAAAGATGCTAA AGTTAGAGTTTGATACCTATAGTGAGTCGTATTAA	S1-RNA-Pull- down
pre-mmu-26b-S1- Temp	GAGCCAAGTAATGGAGAACAGGCTGGTCAGCACCACAA CCTATCCTGAATTACTTGAACCCGGCCCGCGACTATCTT ACGCACTTGCATGATTCTGGTCGGTCCTATAGTGAGTCG TATTAA	S1-RNA-Pull- down
pre-mmu-26b-S1- Loop-Temp	GAGCCAAGTAATGGAGAACAGGCGCCGACCCGCGACTA TCTTACGCACTTGCATGATTCTGGTCGGCACCTATCCTG AATTACTTGAATTGATACCTATAGTGAGTCGTATTAA	S1-RNA-Pull- down
pre-mmu-26a1-S1- Temp	CGTGCAAGTAACCAAGAATAGGCCCTTGGGACCTGCA CAGCCTATCCTGGATTACTTGAACCCGGCCCGCGACTAT CTTACGCACTTGCATGATTCTGGTCGGTCCTATAGTGAG TCGTATTAA	S1-RNA-Pull- down
pre-mmu-26a2-S1- Temp	GAAACAAGTAATCAAGAACAGGCCTCATGGACGGACAC AGCCTATCCTGGATTACTTGAACCCGGCCCGCGACTATC TTACGCACTTGCATGATTCTGGTCGGTCCTATAGTGAGT CGTATTAA	S1-RNA-Pull- down
pre-mmu-9a-S1- Temp	ACTTTCGGTTATCTAGCTTTATGACGGCTCTGTGGCACT CATAAGCTAGATAACCAAGACCCGGCCCGCGACTAT CTTACGCACTTGCATGATTCTGGTCGGTCCTATAGTGAG	S1-RNA-Pull- down

	TCGTATTAA	
pre-mmu-9a-S1-	ACTTTTCGGTTATCTAGCTTTATGAGCCGACCCGCGACTA	S1-RNA-Pull-
Loop-Temp	TCTTACGCACTTGCATGATTCTGGTCGGCTCATACAGCT	down
	AGATAACCAAAGATTGATACCTATAGTGAGTCGTATTAA	

### 6.1.9 Morpholino Oligos

Morpholinos were purchased from GeneTools.

Morpholino oligo name	Sequence 5' to 3'
FXR1	CCACCGTCAGTTCCTCCATGTTGAG
FXR2	CAACCCGTCCATGTTGTCGTC
TDRD3	GCGCCGAGCTTAAATCGCACATCTT
top3b	CACCATTAACACAGTCCTCATCGCT
FMR1	AGCTCGTCCATGACGCCAGTAATTT

## 6.2 Methods

### 6.2.1 Molecular methods

#### 6.2.1.1 Polymerase chain reaction

DNA fragments of interest were amplified by PCR reaction using by the Phusion High Fidelity PCR Master Mix (Thermo Scientific) and DNA oligonucleotides (see material section oligos). Following reaction mix was used for PCR:

DNA template	>50 ng
2x Master mix	1x
Forward primer	1 $\mu$ M
Revers primer	1 $\mu$ M

The mixture was transferred to a thermo cycler and the following program was run.

Program	Temp	Time	Cycles
Initiation	95°C	5'	1
Denaturing	95°C	1'	
Annealing	50-60°C	30''	30 -35
Elongation	72°C	30'' per KB	
Final elongation	72	2 x Elongation	1

The melting temperature of the primer was calculated with the nearest neighbor algorithm by <http://biotools.nubic.northwestern.edu/OligoCalc.html><sup>160</sup> and 2°C less were always taken as the annealing temperature. If the primer consists of additional sequences like restriction sites or homologous regions, the program was expanded with an additional denaturing-annealing-elongation cycle:

Program	Temp	Time	Cycles
Initiation	95°C	5'	1
Denaturing	95°C	1'	
Annealing	45-55°C	30''	5
Elongation	72°C	30'' per KB	
Denaturing	95°C	1'	
Annealing	55-65°C	30''	35
Elongation	72°C	30'' per KB	
Final elongation	72	2 x Elongation	1

#### 6.2.1.2 Agarose Gel electrophoreses

To separate nucleotides by size, agarose gel electrophoresis was applied. The agarose gel with a concentration of 0.5-2% (dependent on the size of the DNA of interest) was produced by heating the agarose in 1x TBE.

#### 6.2.1.3 Purification of DNA from agarose gels or PCR-reaction

For DNA-fragment purification from agarose gels or PCRs the NucleoSpin Gel and PCR Clean-up (Macherey-Nagel) was used as per manufacturer's instruction.

#### 6.2.1.4 Restriction digestion and dephosphorylation of DNA

For cloning purposes, DNA fragments (100-500 ng) and plasmid vectors (1-10 µg) were hydrolyzed by restriction endonucleases (Thermo Scientific, NEB). Restriction was carried out in the buffers recommended by the manufacturer with 1-5 U of enzyme for 1-16 h depending on enzyme activity and amount of DNA. After digestion plasmids were dephosphorylated with Shrimp Alkaline Phosphatase (SAP, Thermo Scientific) by adding 1 µl SAP to the restriction digestion reaction and incubating 1 h at 37°C. The digested DNA was purified as described in 6.2.1.3.

#### **6.2.1.5 Ligation of DNA-fragments**

Digested fragments and linearized vectors were ligated by T4 ligase (NEB) over night at 14°C or for 2 h at room temperature at a ratio of 1:1, 1:3 or 1:5 (plasmid: insert) with 100 ng of plasmid. For calculation the NEB online tool was used. (<http://nebiocalculator.neb.com/#!/main>). The ligation reaction was subsequently transformed in competent *E. coli*.

#### **6.2.1.6 Preparation of competent *E. coli* strains**

For the generation of chemically competent *E. coli* strains, a starting bacteria culture was grown in 50 ml of LB without antibiotics over night at 37°C with 180 rpm. 4 ml of the culture was transferred to fresh 400 ml of LB and incubated likewise until reaching an OD of 0,375. After incubation on ice for 10 min the cells were centrifuged at 1600 g for 2 min at 4°C and the pellet was re-suspended in 80 ml of CaCl<sub>2</sub>-Buffer. This step was repeated and the cells re-suspended in 20 ml of CaCl<sub>2</sub>-buffer. Finally, 100 µl aliquots were prepared, snap frozen and stored at -80°C.

#### **6.2.1.7 Transformation of chemically competent *E. coli* strains**

For transformation, Chemically competent cells were transformed with desired vector by heat shock. The cells were thawed on ice for 5' and 5-10 µl of ligation reaction or 100 ng of plasmid-vector were added. The cells were gently mixed and were put back on ice for 30'. After incubation, a 42°C heat shock was applied for 90" and immediately 1 ml of ice-cold media was added to the cells. The cells were then incubated at 37°C for 1 h shaking (1000 rpm). 10% or 90% of the cells were then plated on agar plates, containing antibiotic corresponding to the vector-encoded resistance gene.

#### **6.2.1.8 Colony screening of transformed bacteria**

To test positive cloning results, transformed bacteria colonies growing on selection agar plates with vector specific antibiotics were picked and put in 4 ml of LB and incubated over night at 37°C. The plasmids were purified (6.2.1.9) and the plasmids were digested by restriction enzymes and the resulting fragments analyzed by gel electrophoresis (6.2.1.2). Construct-positive clones were further analyzed by sequencing (eurofins).



### 6.2.1.9 Purification plasmids-vectors derived from bacteria

Bacteria derived plasmid vectors were purified by using the NucleoSpin Plasmid QuickPure Kit (Macherey-Nagel) as per manufacturer's instruction.

### 6.2.1.10 Bacterial cryo-stock preparation

To prepare long time storage bacterial cryo-stocks, 500 µl of overnight bacterial culture was mixed with 500 µl 50% sterile glycerol, snap frozen and stored at -80°C.

### 6.2.1.11 Site directed mutagenesis

To generate or eliminate mutation in vector-plasmids site directed mutagenesis by PCR were applied. This is based on a two-step PCR. The primer used, caring the site of mutation and flanking regions of the site where used separately in two different tubes for the first step.

DNA template	50-200 ng
10x Buffer	1x
dNTPs	10 mM
Primer (for <u>or</u> rev)	10 pMol
Pfu-Pol (Genaxxon)	1 U

The mixture was incubated and the following program was run in a thermo cycler:

Program	Temp	Time	Cycles
Initiation	95°C	5'	1
Denaturing	95°C	30''	
Annealing	55°C	1'	5
Elongation	72°C	2' per KB	

After the first step half of the sense and antisense were mixed a 1 additional U of Pfu-Pol was added. The same program as described before was run, except that 12-16 cycles were performed. Subsequently the maternal DNA was digested with 1 U of DpnI (Thermo Scientific) at 37°C for 1 h. 10-20% of the mixture was afterwards transformed into *E. coli* (6.2.1.7). Positive colonies were tested for positive mutants by sequencing (6.2.1.8).

### 6.2.1.12 DNA sequencing

DNA sequencing was performed by Eurofins Germany.

## 6.2.2 Biochemical Methods

### 6.2.2.1 Bradford assay

Protein concentrations in solution were determined by Bradford method. For Bradford 2 µl of sample were mixed with 998 µl of 1x Bradford solution (Biorad) and the absorbance at 595 nm was measured and compared against a standard curve.

The standard curve was made using BSA (Sigma) of known concentration 0,5 µg, 1 µg, 2 µg, 4 µg and 5 µg.

### 6.2.2.2 SDS-Page

Size separation of proteins was achieved by denaturing (SDS) polyacrylamide gel electrophoresis (SDS-Page). SDS-Page was run in 1x Lämmli-buffer at a constant current of 65-75 mA.

Composition of a typical 10% Gel:

#### Separation Gel

Rotipherese Gel 30 (Acrylamide:Bisacrylamid 37:1)	10 ml
1,5 mM Tris-HCl, pH 8,8	5,5 ml
ddH <sub>2</sub> O	14,5 ml
APS	67 µl
Temed	67 µl

#### Stacking Gel

Rotipherese Gel 30 (Acrylamide:Bisacrylamid 37:1)	1,65 ml
1,5 mM Tris-HCl, pH 8,8	2,45 ml
ddH <sub>2</sub> O	5,9 ml
APS	67 µl
Temed	67 µl

### 6.2.2.3 Coomassie staining of SDS-gels

SDS-Page separated proteins were non-specifically stained with Coomassie blue staining solution (20% (v/v) Isopropanol, 10% Acidic acid, 0,15% Serva blue R) for 30'. After staining the left over solution was washed away with ddH<sub>2</sub>O and the gel

were de-stained with 20% EtOH. This removes the background and let the protein bands became visible.

#### **6.2.2.4 Silver staining of SDS-gels**

Another way for staining SDS-Page separated proteins is Silver staining. Therefore SDS-gels were fixated with 50% (v/v) methanol, 12% (v/v) acidic acid and 0,5 ml/l formaldehyde (37%) for 1 h. After fixation the gels were washed three times for 20' with 50% (v/v) Ethanol and incubated with 0,2 g/l sodium thiosulfate for 1'. After fixation the gels were washed 3 times in ddH<sub>2</sub>O and incubated for 30' in silver staining solution (2 g/l AgNO<sub>3</sub>, 0,5 ml/l formaldehyde (37%)) and again washed twice in in ddH<sub>2</sub>O. Protein bands were then visualized by incubating the gels in developing solution (60 g/l Na<sub>2</sub>CO<sub>3</sub>, 0,5 ml/l formaldehyde (37%)). The development was stopped by adding solution containing 50% (v/v) methanol, 12% (v/v) acidic acid.

#### **6.2.2.5 Purification of recombinant protein**

For the expression for recombinant proteins, coding vectors were transformed in *E.coli* BL21 Rosetta 2. Cells were grown in 100 ml SB medium supplemented with antibiotics at 37°C to OD<sub>668</sub> of 0,6. Expression was induced with 0,5 mM IPTG and carried out at 18°C for 4 h. Then cells were harvested by centrifugation and re-suspended in lysis buffer (20 mM Hepes pH7,5, 300 NaCl, 10%Glycerol, protease inhibitor 1:1000, 5 mM Imidazole, 1 mM DTT (HIS) or 5 mM β-Mercaptoethanol (β-Me)(GST). The lysates were then sonified and clarified (1 h; 30000 rpm; 4°C) in a Beckman 45Ti rotor. The cleared lysate was then incubated for 1 hour with either Ni-NTA (His-tag) agarose (Qiagen) or Glutathion-Sepharose (GST) beads (GE Healthcare) at 4°C. Beads were then washed 3 time with lysis buffer and 3 times with lysis buffer containing 10 mM Imidazole. Proteins were freed from beads by either elution (20 mM Hepes pH 7,5, 300 NaCl, 10% Glycerol, protease inhibitor 1:1000, 5 mM Imidazole, 1 mM DTT (HIS) or 5 mM β-Mercaptoethanol (β-Me)(GST, 300 mM Imidazole or 20 mM Glutathione) or cleavage (GST; 4 U/μl PreScission protease(GE Healthcare). If the protein were eluted, Imidazole and Glutathione were removed by dialysis with 3500 kDa cut of membranes in 5 l buffer without imidazole or Glutathione over night at 4°C. Subsequently proteins were run on a Superdex 75 Akta column and different fractions were further used.

### **6.2.3 Zebrafisch Methods**

#### **6.2.3.1 Zebrafisch keeping**

The zebrafish breeding and keeping was done as described in “Zebrafisch – A practical Approach” (Oxford University Press, 2002).

#### **6.2.3.2 One cell stage injection**

Male and female fish were kept overnight in one tank, but separated by a divider. The next morning the fish were brought together and the fertilized eggs were collected 15 min later. The collected eggs were transferred to an injection plate with 1.5% agarose in Danieau's media buffer. The excess media was removed and the eggs were injected immediately using a pneumatic picopump PI/820 (WPI) and a Micromanipulator from Narishige. Injection mix always contained 100 mM KCl and phenol red. Injection parameters (injection time, injection pressure,) was adjusted for every single needle to have an injection volume of 0,5 nl.

#### **6.2.3.3 Glass capillary preparation**

The used capillaries (1.0 mm OD x 0.78 mm ID, Harvard Apparatus LTD) were pulled using a Sutter P 87 Flaming/Brown Micropipette Puller (Sutter Instruments) (pulling conditions: heat 646, pull 80, velocity 75, time 90, pressure 300).

#### **6.2.3.4 Zebrafisch lysate preparation**

Embryos were collected in eppendorf tubes at several developmental stages or time points, the liquid was removed, the collections snap frozen in liquid nitrogen and stored until needed. When needed the embryos were that on ice and 2 µl lysis buffer per embryos was added. The embryos were homogenized through pestle and mortar. The lysate was further homogenized by sonication (micro tip, 5 time 30', level 3, 30% output). After lysis 100 µl of heptane (v/v) was added, vortexed 5 times and centrifuged 30' at 15000 g. The liquid phase between the pallet and the heptane was transferred to a fresh tube and the protein concentration determined. Glycerol was added to final concentration of 10%.

### **6.2.4 Cell lysate preparation**

Cells were washed with ice cold PBS, scraped from the plate and transferred to falcon flasks. After centrifugation at 3000 g at 4°C the supernatant was removed. Now the cell have been stored after snap freezing at -80°C or the lysate was

proceeded. For lysis one volume of cell lysis buffer was added and the pelleted cells re-suspended. If the volume was less than 300  $\mu$ l the cells were homogenized by passing through a 27G needle six times. Higher volume was solicited on ice (2 x 20 pulses, 50%, level 2-3). After lysis cell debris was pelleted by centrifugation (high-speed, 15 min) and the cleared lysate was transferred to fresh tube.

## **6.2.5 Immunobiological methods**

### **6.2.5.1 Antibody based immune precipitation (IP)**

Immunoprecipitation was performed with 25  $\mu$ l of  $\alpha$ -Flag M2 Agarose (Sigma) or 30  $\mu$ l of magnetic Dynabeads (Protein A or Protein G, Invitrogen.) For IP cells or zebrafish lysate was prepared (6.2.3.4, 6.2.4). Beads were equilibrated by washing 3 times in washing buffer. Dynabeads were incubated with 5  $\mu$ g of Antibody at 4°C for one hour and washed three times with lysis buffer. The beads were incubated with 5 mg of lysate protein at 4°C for 3 h. The beads were washed 3 times in lysis buffer (without protease inhibitors) and one time washed in PBS with transferring the beads to fresh tubes twice. Dynabeads were boiled for elution in 1x protein loading buffer. Flag-beads were eluted by two elution steps using one bead volume of 200 ng/ $\mu$ l flag-peptide (10', 4°C, rotating, each) or boiling in 1x protein loading buffer. The eluate was analyzed by western blot or silver staining.

### **6.2.5.2 Western blotting**

To detect proteins of interest separated on SDS gels western blotting was performed using protein- or tag-specific antibodies. For this the protein content of the gel was transferred to a PDVF-membrane (450  $\mu$ m, GE Healthcare) in a semidry blotting chamber. Therefore, three layers of Whatman paper were covered with fitting PVDF-membrane. The gel was placed in the membrane and again with three layers of Whatmann paper. The whatman paper was previously soaked in transfer buffer (1x towbin, 20% Methanol) and the membrane was previously activated in 100% methanol. The blotting procedure was carried out at 0,8 mA/cm<sup>2</sup> of the gel for 2 h. The membrane was blocked (5% milk powder in 1x TBE) for 45'. After three times of washing the membrane was incubated with the primary antibody (in 1x NET-galantine, 1:1000 sodium azide) overnight at 4°C. The next day, the membrane was washed three times in 1x TBS-T for 5 min each and incubated with the horseradish peroxidase-coupled secondary antibody (1:1000 in 1x TBT) for 3 h at room temperature. Subsequently the membrane was washed again three times with 1x

TBS-T for 5 min each and the blot was developed with enhanced chemiluminescence system (ECL). 10 ml of ECL I-solution (1,25 mM Luminol; 100 mM Tris-HCl pH 8,5) were mixed with 100 µl of ECL II-solution (6,8 mM p-Cumeric acid in DMSO) and 10 µl of H<sub>2</sub>O<sub>2</sub> and the blot was incubated for 1' with the solution. The chemiluminescence was visualized using a Gel Doc Gel Documentation System (Biorad).

### **6.2.6 RNA methods**

#### **6.2.6.1 RNA Isolation and purification**

##### **6.2.6.1.1 Total RNA isolation**

For RNA isolation, 100 zebrafish embryos were put in RNase free 1,5 ml eppendorf tubes and the Danieau's medium was removed. 500 µl of Trizol reagent (Invitrogen) was added and the embryos were roughly homogenized by pestle. For fine homogenization the embryo lysate was pipetted up and down through 1000 µl and 200 µl tips. Afterwards additional 500 µl trizol was added and the tubes were placed on 55°C for five to ten minutes. The lysate was centrifuged with 5000 g at 4°C and the supernatant transferred to a new tube and 200 µl chloroform was added. The mixture was put to room temperature for 10 min and afterward centrifuged at 15000 g for 15 minutes. The aqueous phase was carefully transferred to a new tube and precipitated with 500 µl isopropanol at room temperature for 15 min. The RNA was pelleted at 18000 g for one hour. The pellet was washed with 75% ethanol. After removing the ethanol the tubes were centrifuged again for one minute and leftover ethanol was removed. The pellets were air-dried for approximately 10 min at room temperature and resuspended in ddH<sub>2</sub>O. The samples were stored at -20°C for short time storage or at -80°C for long time storage.

If the main focus was the capture of small RNAs, precipitation was done with more isopropanol over night at -20°C and washing steps were carried out with 85% EtOH.

##### **6.2.6.1.2 RNA isolation for nuclear export assay's**

For protein digestion the nuclear and cytosol fractions were treated with proteinase K (1 g/ml, in 1x Proteinase K buffer, 0,1 mg/ml tRNA) for 1 h at 55°C in a volume of 200 µl. After Digestion 200 µl P:C:I was added, the samples vortexed five times and centrifuged at room temperature at 15000 g. The aqueous phase was transferred to fresh tubes and 1 ml 100% EtOH and 30 µl 3 M NaOAc. The samples were then

centrifuged for 15 min at >15000 g at 4°C, the supernatant was discarded and the pellets washed with 70% EtOH and air dried for 10 min afterwards. 20 µl of Stop mix was added and the samples boiled at 95°C for at least 10 min shaking (1400 rpm). The samples were loaded on 12,5% Urea denaturing gel or stored at -20°C.

#### **6.2.6.1.3 RNA purification from solutions**

To purify RNA from solutions Phenol: Chloroform: Iso-amylalcohol (P:C:I; 25:24:1; pH 4) was used. Equal volumes of P:C:I were added to the samples and mixed by vortexing. The samples were centrifuged with 15000 g at room temperature for 15 min and the RNA containing aqueous phase was collected in a fresh tube. Equal volume of Chloroform: Iso-amylalcohol (C:I; 24:1) was added to remove traces of phenol and the centrifugation was repeated. The aqueous phase was mixed with 1/10 volume of 3 M NaOAc (pH 5.2) and 3 volume of 100% EtOH. The solution was cooled at 4°C for 30 min and centrifuged at 15000 g for 30 min. The pellet was air-dried and resuspended in ddH<sub>2</sub>O. The samples were stored at -20°C for short time storage or at -80°C for long time storage.

#### **6.2.6.2 Reverse transcription for cDNA synthesis**

cDNA was synthesized by RNA Superscript II first strand synthesis kit (Invitrogen) as per manufacturer's instruction. After synthesis cDNA was stored at -20°C.

#### **6.2.6.3 Denaturing RNA polyacrylamide gels**

RNA was separated by size through denaturing (~8 M Urea) polyacrylamide (PAA) gel. Denaturing gels were prepared using the Rothiphorese Sequencing gel system as per manufacturer's instruction. Depending on size of the RNA 10-15% of PAA was used.

Samples were mixed with RNA loading buffer and boiled for 5'. The gels were pre run for 45' and the samples were loaded. Regular 1 mm thick gels were run at 30 W for 1 h in 1 x TBE and sequencing 0,4 mm gels were run for 2h at 65 W.

Radioactive RNA was visualized on X-ray film. Non-radioactive RNA was visualized by UV (260 nm) shadowing against a F-254 DC kieselgel plate.

#### **6.2.6.4 Elution of RNA from denaturing polyacrylamide gel electrophoresis**

RNA bands of interest were cut out and the gel pieces were put on -80°C for at least 1 h. Afterwards, 1 volume of RNA elution buffer was added and the mixture was placed at -20°C over night and the RNA precipitated (see 6.2.6.1.3).

### 6.2.6.5 Northern Blot

30 µg of total RNA from embryos was separated on a 1 mm 10% PAA denaturing gel (6.2.6.3) and transferred to a charged nylon membrane (Hybond-N<sup>+</sup>, GE Healthcare) by electro-blotting in 1x TBE for 1 h with 400 mA. The membrane was UV(254 nm)-cross-linked with 1200 mJ after blotting. The membrane was then pre-hybridized with Rapid-hyb Buffer (GE Healthcare) at 40°C for 45'. Hybridization was then carried out in Rapid-hyb Buffer for at least 3 h with radiolabelled DNA probes. After hybridization the membrane was washed with 50 ml pre-warmed 2xSSC/1%SDS for 30 min at 40°C and then washed with 25 ml pre-warmed 0,2xSSC/1%SDS for 30 min. The membrane was then wrapped in saran wrap and exposed on phosphorimager screen. For stripping, the membrane was washed 3 time with boiling 0,1xSSC/0,5% for 2' and re-probed.

### 6.2.6.6 Radioactive labeling of nucleotides

#### 6.2.6.6.1 5' end labeling of DNA

DNA oligos has been synthesized by Sigma with a 5' OH. Meaning that the oligos can be end-labeled directly by T4 polynucleotide kinase (PNK; Thermo Scientific) using <sup>32</sup>P γ-ATP. The reaction mix was prepared:

DNA	30 pmol
<sup>32</sup> P γ-ATP	40 µCi
10x T4 PNK Buffer (forward)	1x
PNK	10 U

The mixture was heated to 95°C for 30' and snap cooled on ice and spun down quickly, before adding the PNK. The reaction was carried out for 30 min at 37°C. The reaction was stopped by adding 1,5 volume of EDTA (30 mM, pH 8). The DNA was purified on a G-25 column (GE Healthcare). The residual PNK was inactivated by incubation at 95°C for 30''.

#### 6.2.6.6.2 5' end labeling of RNA

5' labeling was done by T4 PNK phosphorylation's using <sup>32</sup>P γ-ATP. All used RNA was crated by *in vitro* transcription (6.2.6.12.1). This creates phosphorylated 5'-ends. Due to less effective exchange reaction of the T4 PNK, the RNA needed to be dephosphorylated prior to labeling. The dephosphorylation was done by Fast-AP (Thermo Scientific) in the fallowing reaction mix.



RNA	20 pmol
10x Fast AP Buffer	1x
Fast Ap	1 U

The mixture was heated to 95°C for 30' and snap cooled on ice and spun down quickly before adding the Fast AP. The reaction was carried out for 30' at 37°C and inactivated with heat shock by incubating at 75°C for 5 min. Then the following mix was prepared:

Dephosphorylated RNA (in Fast AP reaction mix)	
10x PNK buffer	1x
(forward)	
<sup>32</sup> P γ-ATP	25 μCi
PNK	1U

The mixture was heated to 95°C for 30' and snap cooled on ice and spun down quickly, before adding the Fast AP. The reaction was carried out for 15' at 37°C. To ensure proper 5' end phosphorylation cold ATP (final concentration 10 mM) was added and the reaction was prolonged for 5 min. Afterwards the reaction was inactivated by adding 1 volume stop mix. The RNA was purified by denaturing gel electrophoreses (6.2.6.3), elution and precipitation (6.2.6.4).

#### 6.2.6.7 RNaseH digestion

Transcripts that need RNaseH trimming were gel purified after IVT (6.2.6.12). For the reaction 0,25 nMol of RNA were incubated with 0,55 nmol DNA in the following buffer 20 mM Tris-HCl (pH 7,5), 0,1 M KCl, 10 mM MgCl<sub>2</sub>, 0,1 mM DTT, 5% (w/v) sucrose, with 1 U of RNaseH (Invitrogen) for 1 h at 37°C. The reaction was up scaled according to need with longer incubation time and more units of RNaseH. After digestion the RNA was again gel purified.

#### 6.2.6.8 RNA annealing

For processing assays it is important that all pre-miR are correctly folded. For this the precursor were put in annealing buffer (100 mM NaCl, 30 mM Tris-HCl pH 7,5, 2 mM MgCl<sub>2</sub>) and heated to 95°C for 1' follow by 1 h incubation at 37°C. The folded pre-miR were then directly used or stored at -20°C.

#### **6.2.6.8.1 Backbone labeling of RNA**

For backbone labeling RNAs were transcribed as described (6.2.6.12.1), with additional 30  $\mu\text{Ci}$  of  $^{32}\text{P}$   $\alpha\text{-UTP}$ .

#### **6.2.6.9 *In vivo* Zebrafisch DICER assay**

To investigate the processing of pre-miR in early development the  $\text{P}^{32}$  labeled pre-miR were injected in one cell stage zebrafish embryos (6.2.3.2). The embryos were incubated for 30', 60' and 120' at 28°C and 5-10 embryos were collected per time point and directly snap frozen in liquid nitrogen. If all time points of all pre-miR injections were collected the RNA was purified (6.2.6.1.1) and analyzed on a sequencing gel (6.2.6.3).

#### **6.2.6.10 *In vitro* Zebrafisch DICER assay**

To investigate the processing of pre-miR in later development, the  $\text{P}^{32}$  labelled pre-miR were incubated in zebrafish lysate (6.2.3.4). Pre-miR were incubated with zebrafish lysate with the following conditions for 30', 60' or 120' at 28°C.

Proteinconc.	2 mg/ml
Pre-miR	400 fmol
NaCl	75 mM
MgCl <sub>2</sub>	2 mM
Glycerol	10%

After incubation the RNA purified (6.2.6.1.3) and analyzed via RNA sequencing Gel (6.2.6.3).

#### **6.2.6.11 Precursor export assay**

Export assays were performed using stage 5 and 6 *Xenopus* oocytes. *Xenopus* ovary's carrying the oocytes were provided by Prof. Dr. Marie-Christine Dabauvalle from the department for cell and developmental biology of the university of Würzburg. The ovary was gently divide by forceps and put into OR-I media containing 0,5 mg/ml collagenase A1 (Sigma). The Ovary was shaking in the dark for 60' to 120' at room temperature and pipetted up and down using 2,5 ml plastic pipettes. This will free the Oocytes, which were then washed three times in OR-II containing 1 g/l BSA (Sigma). Finally the oocytes were placed into OR-II and kept at 18°C for a maximum of two days.

For injection, the oocytes were placed on a grid with the animal pole upside. The injection mixture was pulled into a glass needle and the needle was pierced to the

animal pole and 20 nl was injected. The injected oocytes were transferred in a new petridish containing OR-II and incubated for 60' to 120' at 18°C. After incubation, nuclei and cytoplasm were isolated from individual oocytes by manual dissection. The RNA was then isolated (6.2.6.1.2) and investigate on denaturing PAA gels (6.2.6.3).

The components of the mixture are 3 different radiolabeled RNAs. As a negative control served the small nuclear RNA (snRNA) U6. U6 is not exported out of the nucleus. As positive control served a modified capped snRNA U1ΔSm, which is exported but can not be imported back. As the RNA to investigate pre-miR were injected. As a control of accuracy for the nuclear injection and dissection dextran blue was added to the mix.

#### **6.2.6.12 *In vitro* transcription**

##### **6.2.6.12.1 *In vitro* transcription of small RNAs**

*In vitro* transcription of small RNAs was performed using home made T7 RNA polymerase. T7 transcription is a run off transcription, meaning that the transcription will start directly after the priming sequence and no ligation takes place. For initiation, a DNA double strand with the priming sequence is needed. For transcription three sorts of templates were used:´.

- 1) Single stranded DNA-Oligo
- 2) PCR product
- 3) Linearized plasmids

For all templates the antisense sequence is fused to a T7 promoter. If a single stranded DNA-oligos is used the addition of a T7 primer is needed to gain the double stranded start region. If plasmids are used it is important to linearize the plasmids properly. Once started, the transcription is very stable and circular plasmids would yield in long transcripts and low yield of the desired short transcript. The following reaction mix was used to synthesize RNA:

10x Buffer	1x
DTT	5 mM
GTP	8 mM
ATP	5 mM
CTP	5 mM
UTP	2 mM

T7 RNA POL	10% of finale Volume
DNA template	1) 1 $\mu$ M of top and bottom Strand
	2) 1/5 of PCR reaction
	3) 100 ng of Plasmid DNA

The usual reaction volume was 200  $\mu$ l. This can be up or down scaled as desired. The reaction was incubated at 37°C for 2 hours and the reaction was stopped by adding 1 volume of stop mix and boiled for 1 min at 95°C. To maximize the yield of transcriptions 0.4 U/ml thermostabile inorganic pyrophosphatase (Thermo Scientific) was added. RNA was separated on 10% PAA Urea Denaturing gel (6.2.6.3), eluted (6.2.6.4) and stored at -80°C.

### 6.2.6.12.2 In vitro transcription of capped RNA and capping of RNA

If the RNA was capped transcriptionally the transcription was set up as described in 6.2.6.12.1 except no GTP was added to mixture. Instead 5 mM m<sup>7</sup>G cap analogue was placed in the mix. The mixture was put on 37°C for 15 min for incubation with the cap analogue and then 1 mM GTP was added to the mixture for active transcription and the mixture was placed for additional 2 h at 37°C. The resulting RNA was purified as describe in 6.2.6.12.1.

If the RNAs were capped post-transcriptionally the ScriptCap™ m<sup>7</sup>G Capping System kit (Epicentre Biotechnologies) was used as per manufacturer's instruction.

### 6.2.6.12.3 In vitro transcription of mRNAs

For transcription of mRNAs which later were injected in zebrafish the mMMESSAGE mMACHINE™ T7 ULTRA Transcription Kit (Ambion) was used as per manufacturer's instruction. With this kit the RNA is poly-A tailed and capped with an ARCA cap-analogue. This special cap-analogue leads to higher translation rate<sup>161,162</sup>.

### 6.2.6.13 Different *in vitro* transcription strategies for pre-miR syntheses

For *in vitro* and *in vivo* experiments of pre-miR processing, the correct appearance of the 2 nt 3' overhang is crucial<sup>38,39</sup> (see 3.2, Figure 4).

All pre-miR were synthesized by *in vitro* run-of transcription using phage T7-RNA polymerase and linearized DNA templates (6.2.6.12.1). To ensure efficient T7 transcription 2 guanines nucleotides were always included after the T7 promoter region.

To provide optimized templates for pre-miR transcription the sequence of the pre-miR was altered. The 5' arm starts with 2 Gs. In order to not change the 2 nt 3'

overhang the first two nucleotides were also exchanged (Figure 28A left). This template gives high yield but a pre-miRs with a modified/changed sequence (Figure 28B left).

To circumvent the problem of modified pre-miR sequences a chimeric RNA construct was designed. This construct contains a hammerhead ribozyme in its 5' region followed by the pre-miR sequence (Figure 28A middle)<sup>163,164</sup>. The self-processing of the hammerhead-containing transcript occurs co-transcriptional with high activity. Unfortunately, the ribozyme folds very fast and cleavage can occur before the transcription is finished which results in premature termination of transcription in our buffer conditions. This leads to a relatively low yield of pre-miR (Figure 28B middle).

In a third strategy to obtain a higher yield of correct pre-miR the precursor sequence was prolonged at their 5' end with a linker sequence that started with two Gs. For this linker sequence a complementary DNA-oligo was designed (Figure 28A right). The DNA oligonucleotides and the pre-miR transcript were annealed and RNaseH was added (6.2.6.7). RNaseH digests RNA in a RNA-DNA hybrid leaving the correct pre-miR (Figure 28B right).

Correct pre-miR molecules are important for the processing experiments, because of the correct formed end for DICER processing (see above). High efficiency is also important to get sufficient yield for processing experiments for better detection of cleavage product. With the RNaseH-based approach both is given.

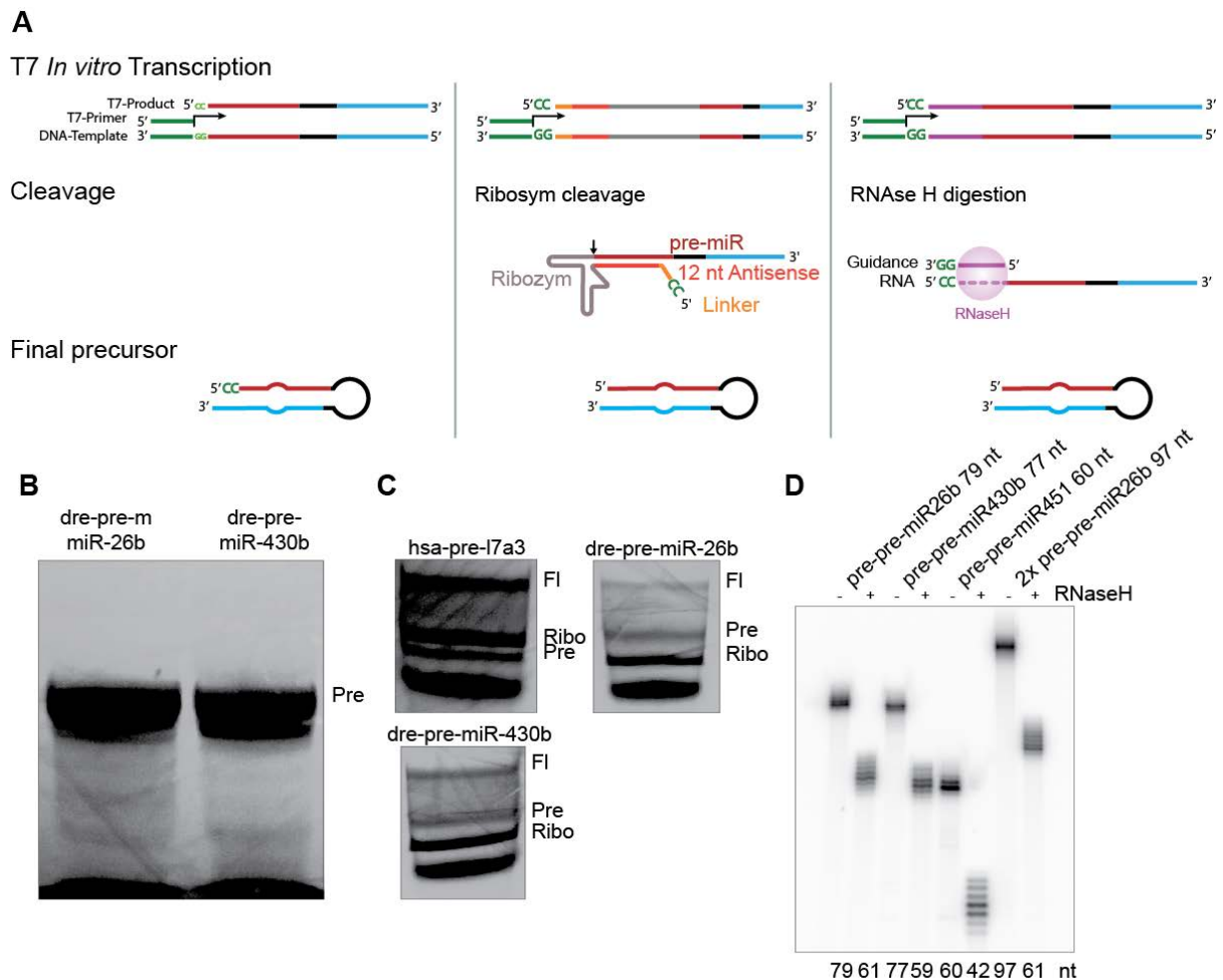


**Figure 28 pre-miR in vitro transcription**

**A** pre-miR *in vitro* transcription strategies: optimized pre-miR sequence for effective transcription (left); 5' hammerhead ribozyme pre-miR hybrid. Self-cleavage reaction will divide ribozyme and unchanged pre-miR (middle); 5' linker extended pre-miR. RNaseH digested with DNA template will trim the unchanged pre-miR (right) **B** UV shadowing image of transcripts from optimized precursor **C** UV shadowing image of hammerhead-pre-miR hybrid transcripts. Seen is the full length transcript, the pre-miR and the hammerhead ribozyme **D** Autoradiograph of linker-pre-miR and RNaseH digested pre-miR, length of RNA as indicated below the image

#### 6.2.6.14 Photometric analysis of DNA and RNA

The concentration of purified DNA and RNA was determined photometrically with an Eppendorf nanodrop biophotometer.

#### 6.2.6.15 Pull-down of miR hairpin-binding Proteins

RNA pull down experiments were performed in collaboration. The pull down using a 3' -biotinylated 2' -O-methyl-RNA adapter to immobilize the RNA on streptavidin beads was performed in collaboration with the laboratory of Prof. Dr. Gunter Meister (Department of Biochemistry, University of Regensburg). The pull down using a S1 aptamer intramolecular to immobilize the RNA was performed in collaboration with

the Falk Butter laboratory (IMB Mainz). Both methods are described in brief in the following chapter.

#### **6.2.6.15.1 RNA pull-down with biotinylated linker**

Pri-miR baits were synthesized by *in vitro* transcription similar to 6.2.6.12.1. The pri-miR were extended by a 5' sequence, which is complementary to the 3' -biotinylated 2' -O-methyl-RNA adaptor (5'-AGGCUAGGUCUCCC-Biotin-3').

For each pull down reaction 160 µl of M270 (Lifetech) were wash in Buffer (50 mM Tris-HCl pH 8, 150 mM NaCl, 5% Glycerol) and incubated with adapter oligo in 250 µl Buffer at 4°C for at least 1 h. After coupling the beads have been washed twice. Half of the coupled beads were used for pre-clear reaction and the other half was filled up again to 250 µl with buffer. Then 10 µg of purified RNA is added to the prepared beads and incubated at 4°C overnight rotating. After coupling the beads have been washed twice with buffer. Zebrafisch lysate (6.2.3.4) and cell lysate (6.2.4) was prepared and precleared by incubating the adapter conjugated beads for 6 h at 4°C rotating. After pre-clear incubation the beads were removed by centrifugation. 1 ml precleared Zebrafisch lysate in a concentration of 10 mg/ml was incubated with the RNA coupled beads over night at 4°C. The next day the lysate was removed and the beads have been washed with buffer containing the following supplements:

1<sup>st</sup> Wash Buffer plus protease inhibitors, 1 mM DTT and 150 mM NaCl

2<sup>nd</sup> Wash Buffer plus protease inhibitors, 1 mM DTT and 0,1% TritonX

3<sup>rd</sup> Wash Buffer plus protease inhibitors and 1 mM DTT

For elution the beads were boiled in SDS-Page buffer (Thermo Scientific) for 5' at 95°C. The samples were then briefly centrifuged and loaded on precast SDS gels and analyzed by mass spectroscopy.<sup>115</sup>

#### **6.2.6.15.2 S1 Aptamer pull downs**

The aptamer carrying RNA can be directly conjugated to magnetic streptavidin beads. For each reaction 55 µl Dynabeads MyOne Streptavidin C1 beads (Invitrogen) were washed twice in RNA binding Buffer (50 mM Hepes pH 7,6, 100 mM NaCl, 0,5% Igepal CA630, 10 mM MgCl<sub>2</sub>). Then 25 µg (aptamer containing) RNA was combined with the washed beads in a final volume of 200 µl and incubated at 4°C for 30' in RNA binding buffer. After incubation the beads were washed 3 time with RNA binding buffer. Zebrafisch lysate (6.2.3.4) and cell lysate (6.2.4) was prepared and the beads were incubated in RNA wash buffer (250 mM NaCl, 50 mM

Hepes pH 7,6, 0,5% Igepal CA630, 10 mM MgCl<sub>2</sub>) containing 400 µg lysate protein and 0,1 mg/ml tRNA for 30' at 4°C rotating. The supernatant was discarded and the beads were washed three times with wash buffer and eluted by heating 10' at 70°C in 25 µl NuPage LSD Buffer containing 100 mM DTT. The samples were then sent at room temperature to Mainz (IMB) for analysis by mass spectroscopy.

### **6.2.6.16 Filter binding assay**

*In vitro* interaction of pre-miR and recombinant protein was analyzed by filter binding assays. Therefore, 2 nmol of target RNA was incubated with gradually increasing concentration of protein for 30 min on ice. To separate free RNA from RNA protein complex the samples were applied to a dot blot apparatus (Biorad). Here two membranes are placed on top of 3 Whatman papers and the samples are sucked through by negative pressure. The upper membrane (first membrane that is passed) is Hybond ECL (GE healthcare) and prevents proteins from passing. The second membrane is a Hybond N<sup>+</sup> membrane (GE Healthcare), which stops RNA from passing. That means that unbound RNA goes through and RNA protein complexes stay at the first membrane. The membranes are measured via phosphorimaging and the dots are quantified by ImageQuant (GE Healthcare) and visualized using Prism software (GraphPad).

### **6.2.6.17 RNA Sequencing**

#### **6.2.6.17.1 Regular RNA Sequencing**

Total RNA from two different clones of the KO cell lines KO<sup>26b</sup>, dKO<sup>26a1/a2</sup> and tKO<sup>26b/26a1/a2</sup> in duplicates were isolated, using peqGold RNA pure (PeqLab) according to the manufacture's instruction. rRNA was removed using the Ribo-Zero rRNA Removal Kit (Illumina) followed by NEBNext Ultra Directional Library Prep kit (NEB). Sequenced reads were aligned to the murine genome version mm10 using TopHat<sup>131</sup>. Cufflinks and Cuffdiffs were used to determine differential gene expression<sup>131</sup>.

#### **6.2.6.17.2 Small RNA sequencing**

Total RNA containing 5' phosphorylated small RNAs was isolated from tissues (6.2.6.17.1) and a 3' barcoded adapter was ligated using truncated T4 RNA ligase (1-249; K227Q). Afterwards ligated RNAs were pooled and size selected by SDS PAGE, followed by the addition of a 5' adapter using T4 RNA ligase. RNA was



reverse transcribed using Superscript III (Invitrogen) and cDNA was PCR amplified by Taq Polymerase (Takara) and barcode specific primer. The adapter carrying PCR products are then size selected on 2,5% agarose gels and purified using Qia-Quick gel extraction kit according to the manufacturer's instructions. DNA was then sequenced by Illumina sequencing<sup>165</sup>. Reads were mapped against murine miR annotation database ([www.miRBase.org](http://www.miRBase.org)) using Burrow-Wheeler aligner and each miR profile was normalized to relative read frequencies<sup>166</sup>.

## **6.2.7 Bioinformatics' Methods**

### **6.2.7.1 Venn-Diagrams**

To visualize the relations between the sequencing dataset Venn diagrams have been prepared. The intersections were calculated using the online tool <http://bioinformatics.psb.ugent.be/webtools/Venn/>. Final visualization was performed using the open source eulerApe<sup>167</sup>.

### **6.2.7.2 Enriched gene ontology term analysis**

Analysis of enriched GO-terms was performed using the online interface of the gene ontology Consortium that is based on the PANTHER classification System (<http://geneontology.org/>)<sup>168</sup>.

### **6.2.7.3 RNA folding prediction**

For nucleic acid folding prediction the online software application 'mfold web server' (<http://unafold.rna.albany.edu/?q=mfold/RNA-Folding-Form>) was used<sup>169</sup>.

### **6.2.7.4 miR sequence information**

All miR sequence information used in thesis were obtained from the latest miRbase release (v20, June 2013) <http://www.mirbase.org/><sup>170</sup>.

### **6.2.7.5 miR target prediction**

For miR target analysis the online database targetscan with the release 7.1 (June 2016) was used<sup>139</sup>.

## **6.2.8 Cell Culture Work**

The following described methods were performed by Mark Sauer. For better understanding, they are described briefly. Methods will be described in more detail in the thesis of M. Sauer.

#### **6.2.8.1 Differentiation of ESC to NC**

ESCs (129/Sv x 129Sv) derived from inner cell mass of murine blastocysts were grown on gelantine-coded dishes. For further culturing, the cells were grown in suspension. After withdrawal of leukemia inhibitory factor, ESCs form embryoid bodies, which contain cells of all 3 germ layers. After 5 days in suspension culture, the cells were attached on tissue culture plates in a serum free media to isolate the ectodermal cells and to further differentiate them into NPCs. Retinoic acid is added at this time point to induce the neural fate. On day 9 the cells were transferred to poly-L-ornithine and laminin coated dishes where they spontaneously differentiate into neuronal cells.

#### **6.2.8.2 CRISPR/Cas9-mediated KO of miRs 26a1, 26a2 and 26b**

For gene deletion a CRISPR/Cas9-Nickase approach was used, which introduces sequence specific DNA single strand breaks guided by single guide RNA (sgRNA) and minimize Off-Target effects. Because a nickase was used 4 sgRNAs were needed per deletion. For target selection a 20-nt target sequences were selected to precede a 5'-NGG protospacer-adjacent motif (PAM). The MIT's CRISPR design tool (<http://crispr.mit.edu/>) was used for sgRNA design. sgRNAs for miR-26 deletions were designed so that the neighboring Ctdsp exons and splice signals remained untouched. DNA coding for sgRNA were cloned into the vector containing the Cas9-nickase. R1 ESCs were transfected with the vector expressing sgRNAs specific for miR-26b, 26a1 and 26a2 target sites. Two independent ESC clones for each homozygous miR deletion were thoroughly genotyped and used further.



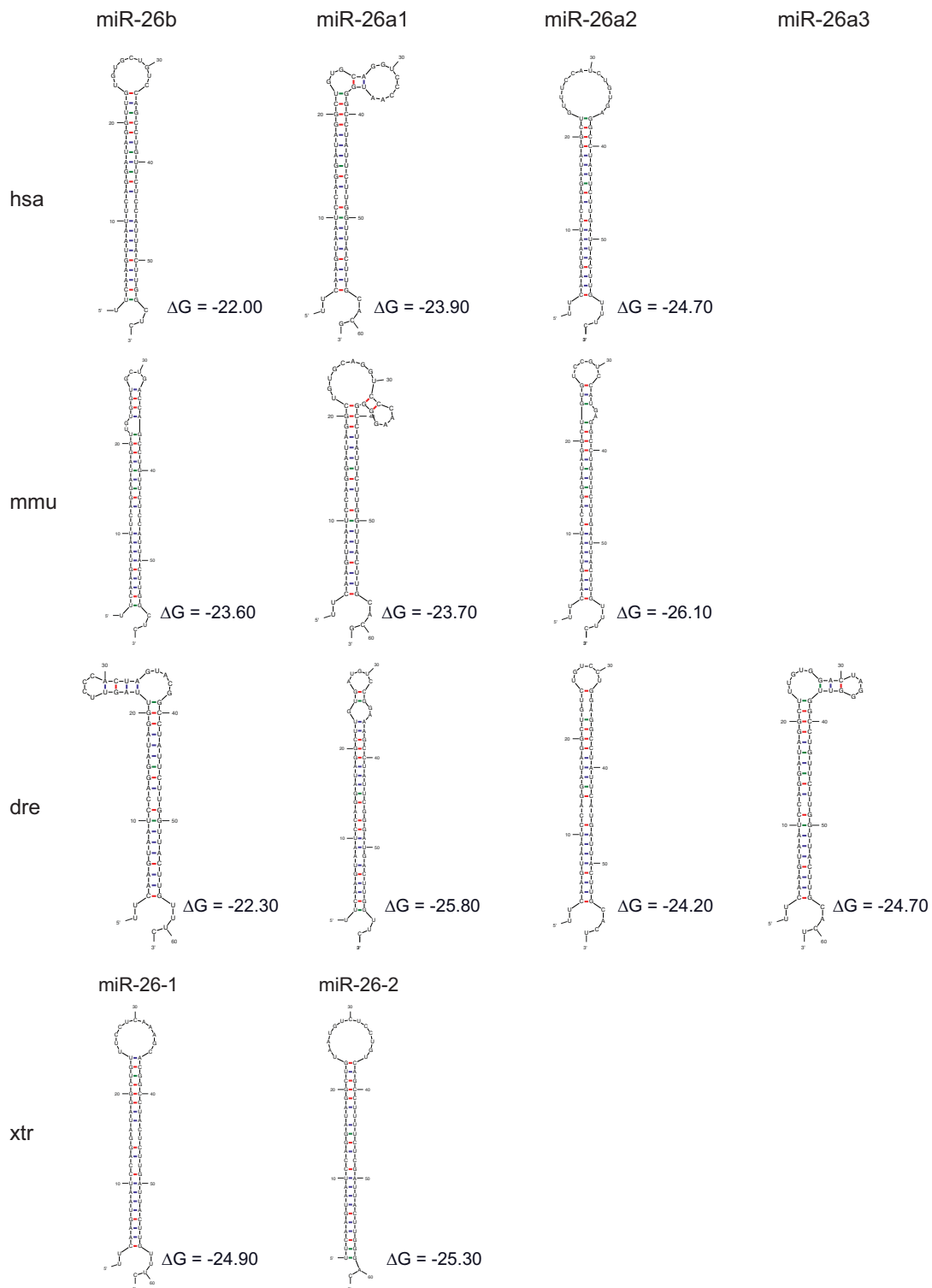


**Figure 30 miR-26 Stem loops in vertebrates**

Predicted stem loop (hairpin) with lowest possible free energy formation of the pre-miR in human (has, *Homo sapiens*), mouse (mmu, *Mus musculus*), zebrafish (dre, *Danio rerio*) and *Xenopus* (xtr, *Xenopus tropicalis*). Free energy of predicted stem loops as indicated.

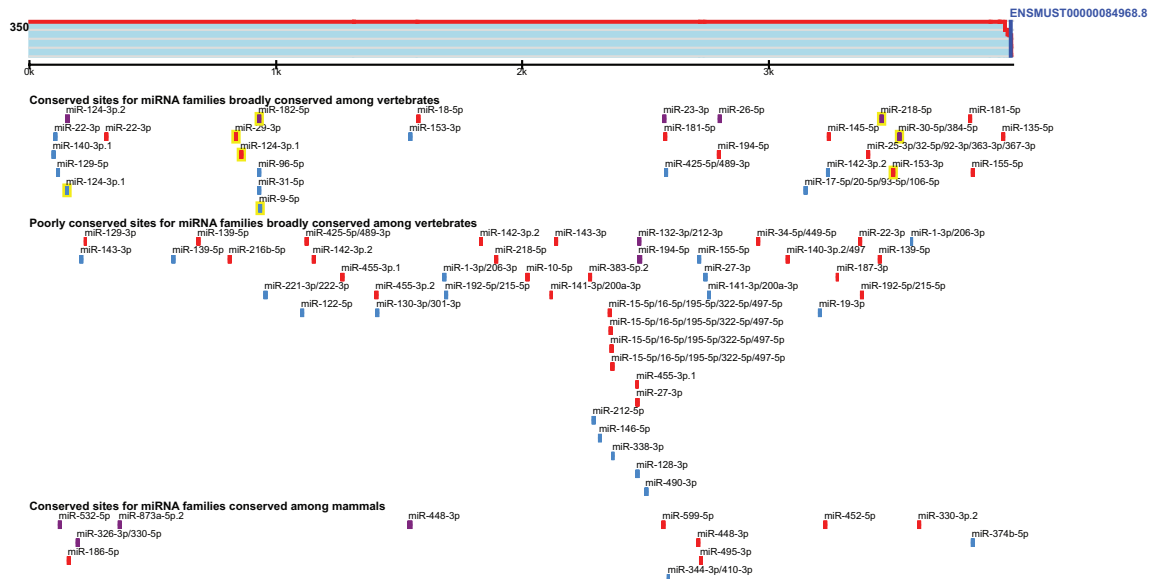
**A**

Human Rest ENSMUST0000080359.6 3' UTR length: 3448



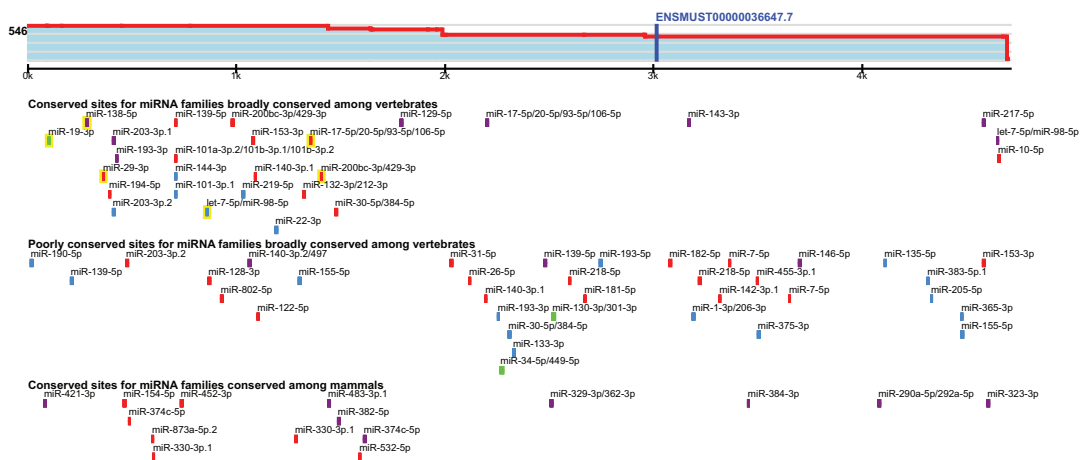
**B**

Human Rcor1 ENSMUST0000084968.8 3' UTR length: 3988



**C**

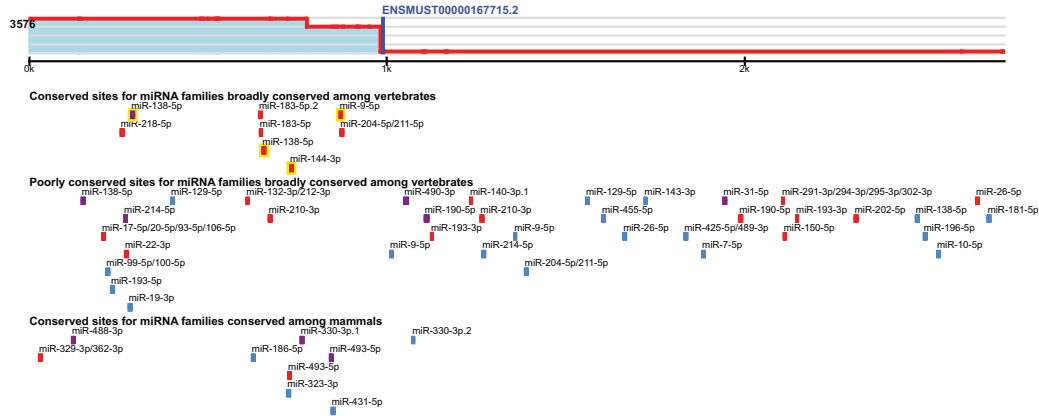
Human Ctsp2 ENSMUST0000036647.7 3' UTR length: 4711



# Appendix

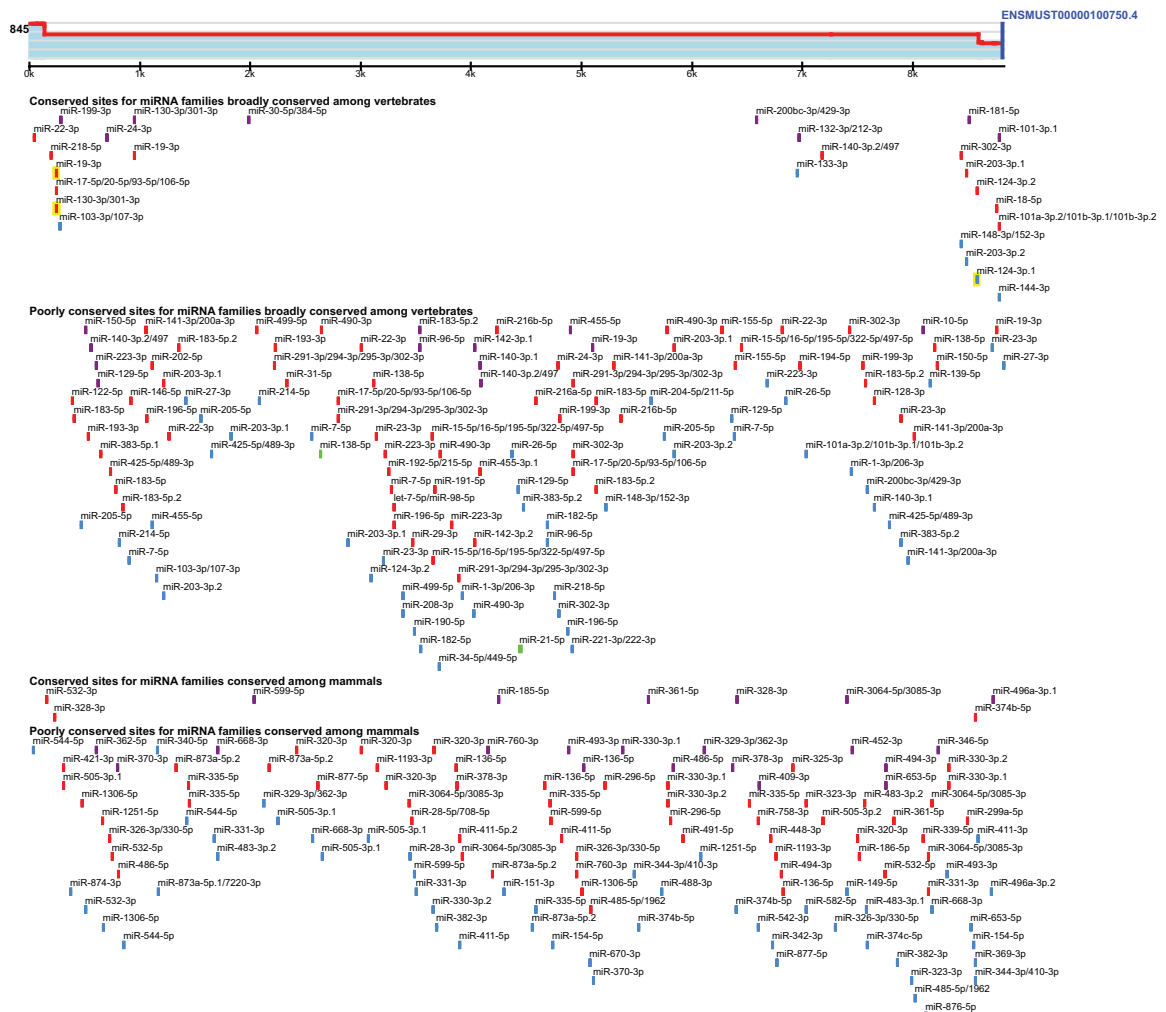
**D**

Human Sin3a ENSMUST00000167715.2 3' UTR length: 2725



**E**

Human Mecp2 ENSMUST00000100750.4 3' UTR length: 8825



■ 8mer ■ 7mer-m8 ■ 7mer-A1 ■ non-canonical

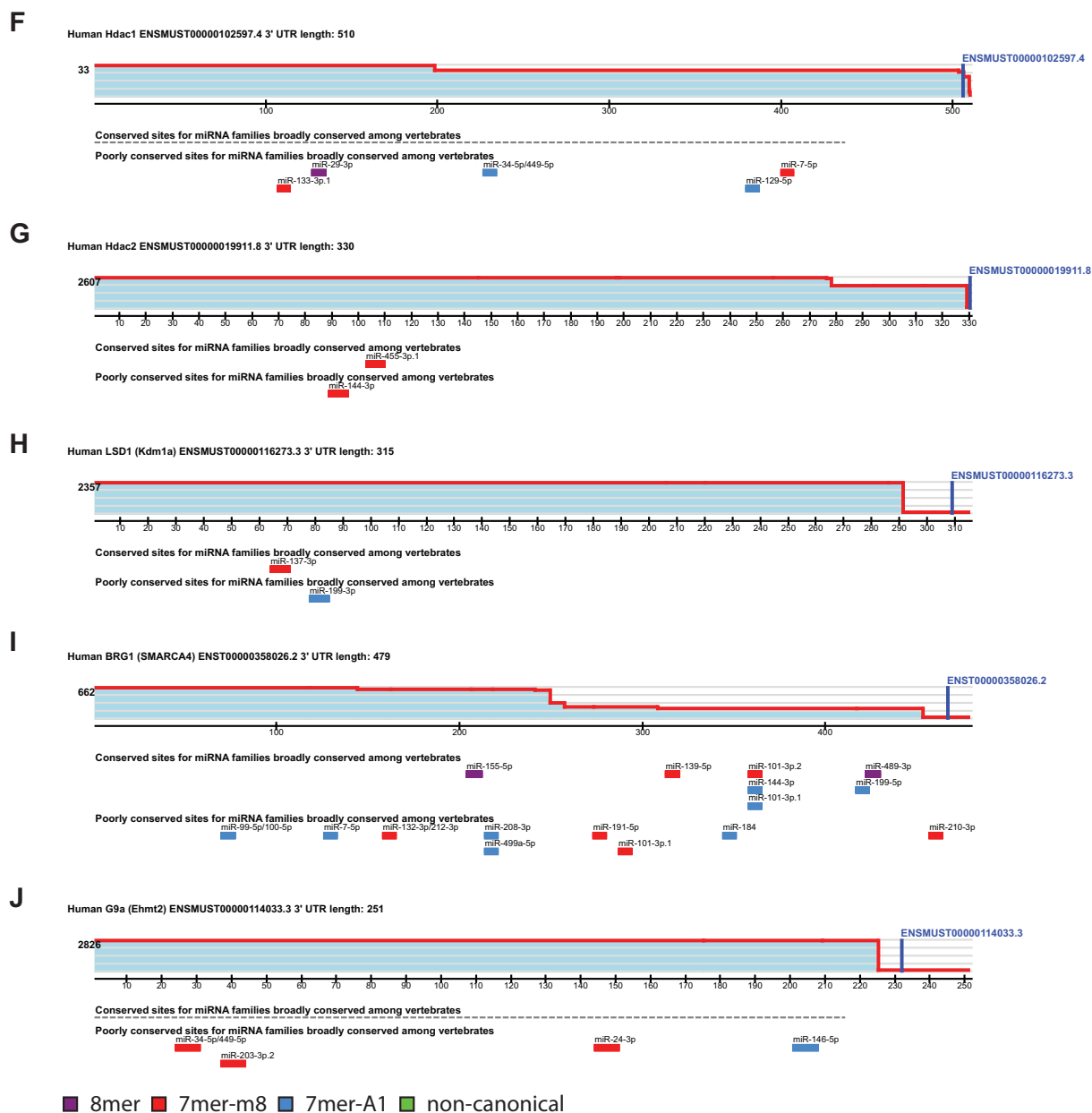


**Figure 31 miR target sites for members of the REST-Complex**

Predicted target site using target scan for the REST-complex members **A** REST, **B** CoREST (Rcor1), **C** CTDSP2, **D** Sin3a, **E** MECP2, **F** HDAC1, **G** HDAC2, **H** LSD1 (KDM1a), **I** BRG1, (SMARCA4) **J** G9a (EHMT2). Conserved/poorly conserved miR sites and conserved/poorly conserved miRs as indicated. Target site 8mer (purple), 7mer (red), 7mer-A1 (blue) non-canonical (green).

**Table 3 Individual contributions for the final figures represented in the thesis work. TZ Thomas Ziegenhals, MS Mark Sauer.**

Figure	TZ	MS
Figure 8 Possible processing regulation scenarios	100	
Figure 9 The miR-26 family is highly conserved in vertebrates	100	
Figure 10 Retained pre-miR export as pre-miR processing regulation	100	
Figure 11 pre-miR export assay	100	
Figure 12 pre-miR processing regulation by regulated pre-miR or DICER	100	
Figure 13 Zebrafisch <i>in vivo</i> and <i>in vitro</i> pre-miR cleavage assay	100	
Figure 14 Methods used for the identification of miR-26 regulatory proteins	100	
Figure 15 miR Hairpin binding proteins in 6 hpf Zebrafisch	100	
Figure 16 miR hairpin-binding proteins in undifferentiated murine P19 cells	100	
Figure 17 Analyzing the role of Znf-346 in miR 26 in miR maturation	80	20
Figure 18 Analyzing the role of FMRP/FXR1/2 in miR-26 maturation	100	
Figure 19 Proteom of pre-miRNPs using aptamer pre-miR	100	
Figure 20 Analyzing the role of Eral1 in miR 26 in miR maturation	100	
Figure 21 Effect of miR-26 KO on neuronal differentiation		100
Figure 22 Transcriptome analysis of miR-26 KO cells.	50	50
Figure 23 REST to miR/miR to REST regulation.	50	50
Figure 24 Impact of miR-26 on REST-miRs.	50	50
Figure 25 miR-26 induce REST-miRs.		100



## 8 References

- 1 Gotz, M. & Huttner, W. B. The cell biology of neurogenesis. *Nat Rev Mol Cell Biol* **6**, 777-788, doi:10.1038/nrm1739 (2005).
- 2 Paridaen, J. T. & Huttner, W. B. Neurogenesis during development of the vertebrate central nervous system. *EMBO Rep* **15**, 351-364, doi:10.1002/embr.201438447 (2014).
- 3 Thakurela, S. *et al.* Mapping gene regulatory circuitry of Pax6 during neurogenesis. *Cell Discov* **2**, 15045, doi:10.1038/celldisc.2015.45 (2016).
- 4 Nishihara, S., Tsuda, L. & Ogura, T. The canonical Wnt pathway directly regulates NRSF/REST expression in chick spinal cord. *Biochem Biophys Res Commun* **311**, 55-63 (2003).
- 5 Ooi, L. & Wood, I. C. Chromatin crosstalk in development and disease: lessons from REST. *Nat Rev Genet* **8**, 544-554, doi:10.1038/nrg2100 (2007).
- 6 Yeo, M. *et al.* Small CTD phosphatases function in silencing neuronal gene expression. *Science* **307**, 596-600, doi:10.1126/science.1100801 (2005).
- 7 Lunyak, V. V. *et al.* Corepressor-dependent silencing of chromosomal regions encoding neuronal genes. *Science* **298**, 1747-1752, doi:10.1126/science.1076469 (2002).
- 8 Battaglioli, E. *et al.* REST repression of neuronal genes requires components of the hSWI.SNF complex. *J Biol Chem* **277**, 41038-41045, doi:10.1074/jbc.M205691200 (2002).
- 9 Lee, M. G., Wynder, C., Cooch, N. & Shiekhatar, R. An essential role for CoREST in nucleosomal histone 3 lysine 4 demethylation. *Nature* **437**, 432-435, doi:10.1038/nature04021 (2005).
- 10 Ballas, N., Grunseich, C., Lu, D. D., Speh, J. C. & Mandel, G. REST and its corepressors mediate plasticity of neuronal gene chromatin throughout neurogenesis. *Cell* **121**, 645-657, doi:10.1016/j.cell.2005.03.013 (2005).
- 11 Zhang, Y. *et al.* SAP30, a novel protein conserved between human and yeast, is a component of a histone deacetylase complex. *Mol Cell* **1**, 1021-1031 (1998).
- 12 Egloff, S. & Murphy, S. Cracking the RNA polymerase II CTD code. *Trends Genet* **24**, 280-288, doi:10.1016/j.tig.2008.03.008 (2008).
- 13 Oelgeschlager, T. Regulation of RNA polymerase II activity by CTD phosphorylation and cell cycle control. *J Cell Physiol* **190**, 160-169, doi:10.1002/jcp.10058 (2002).
- 14 Shabalina, S. A. & Koonin, E. V. Origins and evolution of eukaryotic RNA interference. *Trends Ecol Evol* **23**, 578-587, doi:10.1016/j.tree.2008.06.005 (2008).
- 15 Landgraf, P. *et al.* A mammalian microRNA expression atlas based on small RNA library sequencing. *Cell* **129**, 1401-1414, doi:10.1016/j.cell.2007.04.040 (2007).
- 16 Lim, L. P. *et al.* Microarray analysis shows that some microRNAs downregulate large numbers of target mRNAs. *Nature* **433**, 769-773, doi:10.1038/nature03315 (2005).
- 17 Ramalingam, P. *et al.* Biogenesis of intronic miRNAs located in clusters by independent transcription and alternative splicing. *RNA* **20**, 76-87, doi:10.1261/rna.041814.113 (2014).
- 18 Kim, V. N., Han, J. & Siomi, M. C. Biogenesis of small RNAs in animals. *Nat Rev Mol Cell Biol* **10**, 126-139, doi:10.1038/nrm2632 (2009).

## References

---

- 19 Cai, X., Hagedorn, C. H. & Cullen, B. R. Human microRNAs are processed from capped, polyadenylated transcripts that can also function as mRNAs. *RNA* **10**, 1957-1966, doi:10.1261/rna.7135204 (2004).
- 20 Lee, Y. *et al.* MicroRNA genes are transcribed by RNA polymerase II. *EMBO J* **23**, 4051-4060, doi:10.1038/sj.emboj.7600385 (2004).
- 21 Borchert, G. M., Lanier, W. & Davidson, B. L. RNA polymerase III transcribes human microRNAs. *Nat Struct Mol Biol* **13**, 1097-1101, doi:10.1038/nsmb1167 (2006).
- 22 Pfeffer, S. *et al.* Identification of microRNAs of the herpesvirus family. *Nat Methods* **2**, 269-276, doi:10.1038/nmeth746 (2005).
- 23 Pfeffer, S. *et al.* Identification of virus-encoded microRNAs. *Science* **304**, 734-736, doi:10.1126/science.1096781 (2004).
- 24 Gregory, R. I. *et al.* The Microprocessor complex mediates the genesis of microRNAs. *Nature* **432**, 235-240, doi:10.1038/nature03120 (2004).
- 25 Nguyen, T. A. *et al.* Functional Anatomy of the Human Microprocessor. *Cell* **161**, 1374-1387, doi:10.1016/j.cell.2015.05.010 (2015).
- 26 Kwon, S. C. *et al.* Structure of Human DROSHA. *Cell* **164**, 81-90, doi:10.1016/j.cell.2015.12.019 (2016).
- 27 Lee, Y. *et al.* The nuclear RNase III Drosha initiates microRNA processing. *Nature* **425**, 415-419, doi:10.1038/nature01957 (2003).
- 28 Han, J. *et al.* Molecular basis for the recognition of primary microRNAs by the Drosha-DGCR8 complex. *Cell* **125**, 887-901, doi:10.1016/j.cell.2006.03.043 (2006).
- 29 Quick-Cleveland, J. *et al.* The DGCR8 RNA-binding heme domain recognizes primary microRNAs by clamping the hairpin. *Cell Rep* **7**, 1994-2005, doi:10.1016/j.celrep.2014.05.013 (2014).
- 30 Kim, Y. K. & Kim, V. N. Processing of intronic microRNAs. *EMBO J* **26**, 775-783, doi:10.1038/sj.emboj.7601512 (2007).
- 31 Okamura, K., Hagen, J. W., Duan, H., Tyler, D. M. & Lai, E. C. The mirtron pathway generates microRNA-class regulatory RNAs in *Drosophila*. *Cell* **130**, 89-100, doi:10.1016/j.cell.2007.06.028 (2007).
- 32 Ruby, J. G., Jan, C. H. & Bartel, D. P. Intronic microRNA precursors that bypass Drosha processing. *Nature* **448**, 83-86, doi:10.1038/nature05983 (2007).
- 33 Flynt, A. S., Greimann, J. C., Chung, W. J., Lima, C. D. & Lai, E. C. MicroRNA biogenesis via splicing and exosome-mediated trimming in *Drosophila*. *Mol Cell* **38**, 900-907, doi:10.1016/j.molcel.2010.06.014 (2010).
- 34 Okada, C. *et al.* A high-resolution structure of the pre-microRNA nuclear export machinery. *Science* **326**, 1275-1279, doi:10.1126/science.1178705 (2009).
- 35 Bohnsack, M. T., Czaplinski, K. & Gorlich, D. Exportin 5 is a RanGTP-dependent dsRNA-binding protein that mediates nuclear export of pre-miRNAs. *RNA* **10**, 185-191 (2004).
- 36 Lund, E., Guttinger, S., Calado, A., Dahlberg, J. E. & Kutay, U. Nuclear export of microRNA precursors. *Science* **303**, 95-98, doi:10.1126/science.1090599 (2004).
- 37 Yi, R., Qin, Y., Macara, I. G. & Cullen, B. R. Exportin-5 mediates the nuclear export of pre-microRNAs and short hairpin RNAs. *Genes Dev* **17**, 3011-3016, doi:10.1101/gad.1158803 (2003).
- 38 Macrae, I. J. *et al.* Structural basis for double-stranded RNA processing by Dicer. *Science* **311**, 195-198, doi:10.1126/science.1121638 (2006).

- 39 Zhang, H., Kolb, F. A., Jaskiewicz, L., Westhof, E. & Filipowicz, W. Single processing center models for human Dicer and bacterial RNase III. *Cell* **118**, 57-68, doi:10.1016/j.cell.2004.06.017 (2004).
- 40 Ha, M. & Kim, V. N. Regulation of microRNA biogenesis. *Nat Rev Mol Cell Biol* **15**, 509-524, doi:10.1038/nrm3838 (2014).
- 41 Park, J. E. *et al.* Dicer recognizes the 5' end of RNA for efficient and accurate processing. *Nature* **475**, 201-205, doi:10.1038/nature10198 (2011).
- 42 Tsutsumi, A., Kawamata, T., Izumi, N., Seitz, H. & Tomari, Y. Recognition of the pre-miRNA structure by Drosophila Dicer-1. *Nat Struct Mol Biol* **18**, 1153-1158, doi:10.1038/nsmb.2125 (2011).
- 43 Bernstein, E., Caudy, A. A., Hammond, S. M. & Hannon, G. J. Role for a bidentate ribonuclease in the initiation step of RNA interference. *Nature* **409**, 363-366, doi:10.1038/35053110 (2001).
- 44 Hutvagner, G. *et al.* A cellular function for the RNA-interference enzyme Dicer in the maturation of the let-7 small temporal RNA. *Science* **293**, 834-838, doi:10.1126/science.1062961 (2001).
- 45 Ketting, R. F. *et al.* Dicer functions in RNA interference and in synthesis of small RNA involved in developmental timing in *C. elegans*. *Genes Dev* **15**, 2654-2659, doi:10.1101/gad.927801 (2001).
- 46 Packer, A. N., Xing, Y., Harper, S. Q., Jones, L. & Davidson, B. L. The Bifunctional microRNA miR-9/miR-9\*Regulates REST and CoREST and Is Downregulated in Huntington's Disease. *J Neurosci* **28**, 14341-14346, doi:10.1523/Jneurosci.2390-08.2008 (2008).
- 47 Winter, J. *et al.* Loop-miRs: active microRNAs generated from single-stranded loop regions. *Nucleic Acids Res* **41**, 5503-5512, doi:10.1093/nar/gkt251 (2013).
- 48 Chendrimada, T. P. *et al.* TRBP recruits the Dicer complex to Ago2 for microRNA processing and gene silencing. *Nature* **436**, 740-744, doi:10.1038/nature03868 (2005).
- 49 Lee, Y. *et al.* The role of PACT in the RNA silencing pathway. *EMBO J* **25**, 522-532, doi:10.1038/sj.emboj.7600942 (2006).
- 50 Fukunaga, R. *et al.* Dicer partner proteins tune the length of mature miRNAs in flies and mammals. *Cell* **151**, 533-546, doi:10.1016/j.cell.2012.09.027 (2012).
- 51 Hammond, S. M., Boettcher, S., Caudy, A. A., Kobayashi, R. & Hannon, G. J. Argonaute2, a link between genetic and biochemical analyses of RNAi. *Science* **293**, 1146-1150, doi:10.1126/science.1064023 (2001).
- 52 Mourelatos, Z. *et al.* miRNPs: a novel class of ribonucleoproteins containing numerous microRNAs. *Genes Dev* **16**, 720-728, doi:10.1101/gad.974702 (2002).
- 53 Tabara, H. *et al.* The rde-1 gene, RNA interference, and transposon silencing in *C. elegans*. *Cell* **99**, 123-132 (1999).
- 54 Khvorova, A., Reynolds, A. & Jayasena, S. D. Functional siRNAs and miRNAs exhibit strand bias. *Cell* **115**, 209-216 (2003).
- 55 Schwarz, D. S. *et al.* Asymmetry in the assembly of the RNAi enzyme complex. *Cell* **115**, 199-208 (2003).
- 56 Jonas, S. & Izaurralde, E. Towards a molecular understanding of microRNA-mediated gene silencing. *Nat Rev Genet* **16**, 421-433, doi:10.1038/nrg3965 (2015).
- 57 Bartel, D. P. MicroRNAs: target recognition and regulatory functions. *Cell* **136**, 215-233, doi:10.1016/j.cell.2009.01.002 (2009).
- 58 Lewis, B. P., Shih, I. H., Jones-Rhoades, M. W., Bartel, D. P. & Burge, C. B. Prediction of mammalian microRNA targets. *Cell* **115**, 787-798 (2003).

## References

---

- 59 Chandradoss, S. D., Schirle, N. T., Szczepaniak, M., MacRae, I. J. & Joo, C. A Dynamic Search Process Underlies MicroRNA Targeting. *Cell* **162**, 96-107, doi:10.1016/j.cell.2015.06.032 (2015).
- 60 Herzog, V. A. & Ameres, S. L. Approaching the Golden Fleece a Molecule at a Time: Biophysical Insights into Argonaute-Instructed Nucleic Acid Interactions. *Mol Cell* **59**, 4-7, doi:10.1016/j.molcel.2015.06.021 (2015).
- 61 Salomon, W. E., Jolly, S. M., Moore, M. J., Zamore, P. D. & Serebrov, V. Single-Molecule Imaging Reveals that Argonaute Reshapes the Binding Properties of Its Nucleic Acid Guides. *Cell* **162**, 84-95, doi:10.1016/j.cell.2015.06.029 (2015).
- 62 Parker, J. S., Parizotto, E. A., Wang, M., Roe, S. M. & Barford, D. Enhancement of the seed-target recognition step in RNA silencing by a PIWI/MID domain protein. *Mol Cell* **33**, 204-214, doi:10.1016/j.molcel.2008.12.012 (2009).
- 63 Humphreys, D. T., Westman, B. J., Martin, D. I. & Preiss, T. MicroRNAs control translation initiation by inhibiting eukaryotic initiation factor 4E/cap and poly(A) tail function. *Proc Natl Acad Sci U S A* **102**, 16961-16966, doi:10.1073/pnas.0506482102 (2005).
- 64 Pillai, R. S. *et al.* Inhibition of translational initiation by Let-7 MicroRNA in human cells. *Science* **309**, 1573-1576, doi:10.1126/science.1115079 (2005).
- 65 Guo, H., Ingolia, N. T., Weissman, J. S. & Bartel, D. P. Mammalian microRNAs predominantly act to decrease target mRNA levels. *Nature* **466**, 835-840, doi:10.1038/nature09267 (2010).
- 66 Hutvagner, G. & Zamore, P. D. A microRNA in a multiple-turnover RNAi enzyme complex. *Science* **297**, 2056-2060, doi:10.1126/science.1073827 (2002).
- 67 Liu, J. *et al.* Argonaute2 is the catalytic engine of mammalian RNAi. *Science* **305**, 1437-1441, doi:10.1126/science.1102513 (2004).
- 68 Lazzaretti, D., Tournier, I. & Izaurralde, E. The C-terminal domains of human TNRC6A, TNRC6B, and TNRC6C silence bound transcripts independently of Argonaute proteins. *RNA* **15**, 1059-1066, doi:10.1261/rna.1606309 (2009).
- 69 Liu, J. *et al.* A role for the P-body component GW182 in microRNA function. *Nat Cell Biol* **7**, 1261-1266, doi:10.1038/ncb1333 (2005).
- 70 Braun, J. E., Huntzinger, E., Fauser, M. & Izaurralde, E. GW182 proteins directly recruit cytoplasmic deadenylase complexes to miRNA targets. *Mol Cell* **44**, 120-133, doi:10.1016/j.molcel.2011.09.007 (2011).
- 71 Chen, C. Y., Zheng, D., Xia, Z. & Shyu, A. B. Ago-TNRC6 triggers microRNA-mediated decay by promoting two deadenylation steps. *Nat Struct Mol Biol* **16**, 1160-1166, doi:10.1038/nsmb.1709 (2009).
- 72 Fabian, M. R. *et al.* Mammalian miRNA RISC recruits CAF1 and PABP to affect PABP-dependent deadenylation. *Mol Cell* **35**, 868-880, doi:10.1016/j.molcel.2009.08.004 (2009).
- 73 Valinezhad Orang, A., Safaralizadeh, R. & Kazemzadeh-Bavili, M. Mechanisms of miRNA-Mediated Gene Regulation from Common Downregulation to mRNA-Specific Upregulation. *Int J Genomics* **2014**, 970607, doi:10.1155/2014/970607 (2014).
- 74 Eichhorn, S. W. *et al.* mRNA destabilization is the dominant effect of mammalian microRNAs by the time substantial repression ensues. *Mol Cell* **56**, 104-115, doi:10.1016/j.molcel.2014.08.028 (2014).
- 75 Yao, B. *et al.* Epigenetic mechanisms in neurogenesis. *Nat Rev Neurosci* **17**, 537-549, doi:10.1038/nrn.2016.70 (2016).
- 76 Li, X. & Jin, P. Roles of small regulatory RNAs in determining neuronal identity. *Nat Rev Neurosci* **11**, 329-338, doi:10.1038/nrn2739 (2010).

- 77 Conaco, C., Otto, S., Han, J. J. & Mandel, G. Reciprocal actions of REST and a microRNA promote neuronal identity. *Proc Natl Acad Sci U S A* **103**, 2422-2427, doi:10.1073/pnas.0511041103 (2006).
- 78 Visvanathan, J., Lee, S., Lee, B., Lee, J. W. & Lee, S. K. The microRNA miR-124 antagonizes the anti-neural REST/SCP1 pathway during embryonic CNS development. *Genes Dev* **21**, 744-749, doi:10.1101/gad.1519107 (2007).
- 79 Klein, M. E. *et al.* Homeostatic regulation of MeCP2 expression by a CREB-induced microRNA. *Nat Neurosci* **10**, 1513-1514, doi:10.1038/nn2010 (2007).
- 80 Nielsen, J. A., Lau, P., Maric, D., Barker, J. L. & Hudson, L. D. Integrating microRNA and mRNA expression profiles of neuronal progenitors to identify regulatory networks underlying the onset of cortical neurogenesis. *BMC Neurosci* **10**, 98, doi:10.1186/1471-2202-10-98 (2009).
- 81 Dill, H., Linder, B., Fehr, A. & Fischer, U. Intronic miR-26b controls neuronal differentiation by repressing its host transcript, *ctdsp2*. *Genes Dev* **26**, 25-30, doi:10.1101/gad.177774.111 (2012).
- 82 Chen, Z., Zhao, L., Zhao, F., Yang, G. & Wang, J. MicroRNA-26b regulates cancer proliferation migration and cell cycle transition by suppressing TRAF5 in esophageal squamous cell carcinoma. *Am J Transl Res* **8**, 1957-1970 (2016).
- 83 Jiang, J. J. *et al.* MicroRNA-26a supports mammalian axon regeneration in vivo by suppressing GSK3beta expression. *Cell Death Dis* **6**, e1865, doi:10.1038/cddis.2015.239 (2015).
- 84 Liu, Y. *et al.* Overexpression of miR-26b-5p regulates the cell cycle by targeting CCND2 in GC-2 cells under exposure to extremely low frequency electromagnetic fields. *Cell Cycle* **15**, 357-367, doi:10.1080/15384101.2015.1120924 (2016).
- 85 Xu, G. *et al.* Obesity-associated microRNA-26b regulates the proliferation of human preadipocytes via arrest of the G1/S transition. *Mol Med Rep* **12**, 3648-3654, doi:10.3892/mmr.2015.3858 (2015).
- 86 Zhu, Y. *et al.* MicroRNA-26a/b and their host genes cooperate to inhibit the G1/S transition by activating the pRb protein. *Nucleic Acids Res* **40**, 4615-4625, doi:10.1093/nar/gkr1278 (2012).
- 87 Cui, C., Xu, G., Qiu, J. & Fan, X. Up-regulation of miR-26a promotes neurite outgrowth and ameliorates apoptosis by inhibiting PTEN in bupivacaine injured mouse dorsal root ganglia. *Cell Biol Int* **39**, 933-942, doi:10.1002/cbin.10461 (2015).
- 88 Gu, Q. H. *et al.* miR-26a and miR-384-5p are required for LTP maintenance and spine enlargement. *Nat Commun* **6**, 6789, doi:10.1038/ncomms7789 (2015).
- 89 Gao, J. & Liu, Q. G. The role of miR-26 in tumors and normal tissues (Review). *Oncol Lett* **2**, 1019-1023, doi:10.3892/ol.2011.413 (2011).
- 90 Absalon, S., Kochanek, D. M., Raghavan, V. & Krichevsky, A. M. MiR-26b, upregulated in Alzheimer's disease, activates cell cycle entry, tau-phosphorylation, and apoptosis in postmitotic neurons. *J Neurosci* **33**, 14645-14659, doi:10.1523/JNEUROSCI.1327-13.2013 (2013).
- 91 Liu, H., Chu, W., Gong, L., Gao, X. & Wang, W. MicroRNA-26b is upregulated in a double transgenic mouse model of Alzheimer's disease and promotes the expression of amyloid-beta by targeting insulin-like growth factor 1. *Mol Med Rep* **13**, 2809-2814, doi:10.3892/mmr.2016.4860 (2016).
- 92 Bak, M. *et al.* MicroRNA expression in the adult mouse central nervous system. *RNA* **14**, 432-444, doi:10.1261/rna.783108 (2008).
- 93 Lagos-Quintana, M. *et al.* Identification of tissue-specific microRNAs from mouse. *Curr Biol* **12**, 735-739 (2002).

- 94 Ludwig, N. *et al.* Distribution of miRNA expression across human tissues. *Nucleic Acids Res* **44**, 3865-3877, doi:10.1093/nar/gkw116 (2016).
- 95 Wienholds, E. *et al.* MicroRNA expression in zebrafish embryonic development. *Science* **309**, 310-311, doi:10.1126/science.1114519 (2005).
- 96 Chen, P. Y. *et al.* The developmental miRNA profiles of zebrafish as determined by small RNA cloning. *Genes Dev* **19**, 1288-1293, doi:10.1101/gad.1310605 (2005).
- 97 Watanabe, T. *et al.* Stage-specific expression of microRNAs during *Xenopus* development. *FEBS Lett* **579**, 318-324, doi:10.1016/j.febslet.2004.11.067 (2005).
- 98 Heo, I. *et al.* Lin28 mediates the terminal uridylation of let-7 precursor MicroRNA. *Mol Cell* **32**, 276-284, doi:10.1016/j.molcel.2008.09.014 (2008).
- 99 Rybak, A. *et al.* A feedback loop comprising lin-28 and let-7 controls pre-let-7 maturation during neural stem-cell commitment. *Nat Cell Biol* **10**, 987-993, doi:10.1038/ncb1759 (2008).
- 100 Newman, M. A., Thomson, J. M. & Hammond, S. M. Lin-28 interaction with the Let-7 precursor loop mediates regulated microRNA processing. *RNA* **14**, 1539-1549, doi:10.1261/rna.1155108 (2008).
- 101 Viswanathan, S. R., Daley, G. Q. & Gregory, R. I. Selective blockade of microRNA processing by Lin28. *Science* **320**, 97-100, doi:10.1126/science.1154040 (2008).
- 102 Heo, I. *et al.* TUT4 in concert with Lin28 suppresses microRNA biogenesis through pre-microRNA uridylation. *Cell* **138**, 696-708, doi:10.1016/j.cell.2009.08.002 (2009).
- 103 Chang, H. M., Triboulet, R., Thornton, J. E. & Gregory, R. I. A role for the Perlman syndrome exonuclease Dis3l2 in the Lin28-let-7 pathway. *Nature* **497**, 244-248, doi:10.1038/nature12119 (2013).
- 104 Ustianenko, D. *et al.* Mammalian DIS3L2 exoribonuclease targets the uridylated precursors of let-7 miRNAs. *RNA* **19**, 1632-1638, doi:10.1261/rna.040055.113 (2013).
- 105 Smirnova, L. *et al.* Regulation of miRNA expression during neural cell specification. *Eur J Neurosci* **21**, 1469-1477, doi:10.1111/j.1460-9568.2005.03978.x (2005).
- 106 Liu, J. *et al.* Conserved miR-26b enhances ovarian granulosa cell apoptosis through HAS2-HA-CD44-Caspase-3 pathway by targeting HAS2. *Sci Rep* **6**, 21197, doi:10.1038/srep21197 (2016).
- 107 Lewis, B. P., Burge, C. B. & Bartel, D. P. Conserved seed pairing, often flanked by adenosines, indicates that thousands of human genes are microRNA targets. *Cell* **120**, 15-20, doi:10.1016/j.cell.2004.12.035 (2005).
- 108 Monteys, A. M. *et al.* Structure and activity of putative intronic miRNA promoters. *RNA* **16**, 495-505, doi:10.1261/rna.1731910 (2010).
- 109 Bartel, D. P. MicroRNAs: genomics, biogenesis, mechanism, and function. *Cell* **116**, 281-297 (2004).
- 110 Pante, N. Use of intact *Xenopus* oocytes in nucleocytoplasmic transport studies. *Methods Mol Biol* **322**, 301-314, doi:10.1007/978-1-59745-000-3\_21 (2006).
- 111 Izaurralde, E. *et al.* A role for the M9 transport signal of hnRNP A1 in mRNA nuclear export. *J Cell Biol* **137**, 27-35 (1997).
- 112 Andres, M. E. *et al.* CoREST: a functional corepressor required for regulation of neural-specific gene expression. *Proc Natl Acad Sci U S A* **96**, 9873-9878 (1999).
- 113 Giraldez, A. J. *et al.* Zebrafish MiR-430 promotes deadenylation and clearance of maternal mRNAs. *Science* **312**, 75-79, doi:10.1126/science.1122689 (2006).

- 114 Lund, E., Sheets, M. D., Imboden, S. B. & Dahlberg, J. E. Limiting Ago protein restricts RNAi and microRNA biogenesis during early development in *Xenopus laevis*. *Genes Dev* **25**, 1121-1131, doi:10.1101/gad.2038811 (2011).
- 115 Treiber, T. *et al.* A Compendium of RNA-Binding Proteins that Regulate MicroRNA Biogenesis. *Mol Cell* **66**, 270-284 e213, doi:10.1016/j.molcel.2017.03.014 (2017).
- 116 Srisawat, C. & Engelke, D. R. Streptavidin aptamers: affinity tags for the study of RNAs and ribonucleoproteins. *RNA* **7**, 632-641 (2001).
- 117 Leppek, K. & Stoecklin, G. An optimized streptavidin-binding RNA aptamer for purification of ribonucleoprotein complexes identifies novel ARE-binding proteins. *Nucleic Acids Res* **42**, e13, doi:10.1093/nar/gkt956 (2014).
- 118 Stottrup, B. L., Heussler, A. M. & Bibelnieks, T. A. Determination of line tension in lipid monolayers by Fourier analysis of capillary waves. *J Phys Chem B* **111**, 11091-11094, doi:10.1021/jp074898r (2007).
- 119 Ascano, M., Hafner, M., Cekan, P., Gerstberger, S. & Tuschl, T. Identification of RNA-protein interaction networks using PAR-CLIP. *Wiley Interdiscip Rev RNA* **3**, 159-177, doi:10.1002/wrna.1103 (2012).
- 120 Xu, X. L. *et al.* FXR1P but not FMRP regulates the levels of mammalian brain-specific microRNA-9 and microRNA-124. *J Neurosci* **31**, 13705-13709, doi:10.1523/JNEUROSCI.2827-11.2011 (2011).
- 121 Burge, R. G., Martinez-Yamout, M. A., Dyson, H. J. & Wright, P. E. Structural characterization of interactions between the double-stranded RNA-binding zinc finger protein JAZ and nucleic acids. *Biochemistry* **53**, 1495-1510, doi:10.1021/bi401675h (2014).
- 122 Gessert, S., Bugner, V., Tecza, A., Pinker, M. & Kuhl, M. FMR1/FXR1 and the miRNA pathway are required for eye and neural crest development. *Dev Biol* **341**, 222-235, doi:10.1016/j.ydbio.2010.02.031 (2010).
- 123 Fernandez, E., Rajan, N. & Bagni, C. The FMRP regulon: from targets to disease convergence. *Front Neurosci* **7**, 191, doi:10.3389/fnins.2013.00191 (2013).
- 124 Guo, W. *et al.* Fragile X Proteins FMRP and FXR2P Control Synaptic GluA1 Expression and Neuronal Maturation via Distinct Mechanisms. *Cell Rep* **11**, 1651-1666, doi:10.1016/j.celrep.2015.05.013 (2015).
- 125 Cox, J. & Mann, M. MaxQuant enables high peptide identification rates, individualized p.p.b.-range mass accuracies and proteome-wide protein quantification. *Nat Biotechnol* **26**, 1367-1372, doi:10.1038/nbt.1511 (2008).
- 126 Nagarajan, V. K., Jones, C. I., Newbury, S. F. & Green, P. J. XRN 5'-->3' exoribonucleases: structure, mechanisms and functions. *Biochim Biophys Acta* **1829**, 590-603, doi:10.1016/j.bbagr.2013.03.005 (2013).
- 127 Kappei, D. *et al.* Phylointeractomics reconstructs functional evolution of protein binding. *Nat Commun* **8**, 14334, doi:10.1038/ncomms14334 (2017).
- 128 Dennerlein, S., Rozanska, A., Wydro, M., Chrzanowska-Lightowlers, Z. M. & Lightowlers, R. N. Human Ernl1 is a mitochondrial RNA chaperone involved in the assembly of the 28S small mitochondrial ribosomal subunit. *Biochem J* **430**, 551-558, doi:10.1042/BJ20100757 (2010).
- 129 Dinger, T. C. *et al.* Androgenetic embryonic stem cells form neural progenitor cells in vivo and in vitro. *Stem Cells* **26**, 1474-1483, doi:10.1634/stemcells.2007-0877 (2008).
- 130 Wolber, W. *et al.* Phenotype and Stability of Neural Differentiation of Androgenetic Murine ES Cell-Derived Neural Progenitor Cells. *Cell Med* **5**, 29-42, doi:10.3727/215517913X666468 (2013).

## References

---

- 131 Trapnell, C. *et al.* Differential gene and transcript expression analysis of RNA-seq experiments with TopHat and Cufflinks. *Nat Protoc* **7**, 562-578, doi:10.1038/nprot.2012.016 (2012).
- 132 Sims, D., Sudbery, I., Ilott, N. E., Heger, A. & Ponting, C. P. Sequencing depth and coverage: key considerations in genomic analyses. *Nat Rev Genet* **15**, 121-132, doi:10.1038/nrg3642 (2014).
- 133 Johnson, R. *et al.* Regulation of neural macroRNAs by the transcriptional repressor REST. *RNA* **15**, 85-96, doi:10.1261/rna.1127009 (2009).
- 134 Wu, J. & Xie, X. Comparative sequence analysis reveals an intricate network among REST, CREB and miRNA in mediating neuronal gene expression. *Genome Biol* **7**, R85, doi:10.1186/gb-2006-7-9-r85 (2006).
- 135 Johnson, R. & Buckley, N. J. Gene dysregulation in Huntington's disease: REST, microRNAs and beyond. *Neuromolecular Med* **11**, 183-199, doi:10.1007/s12017-009-8063-4 (2009).
- 136 Johnson, R. *et al.* A microRNA-based gene dysregulation pathway in Huntington's disease. *Neurobiol Dis* **29**, 438-445, doi:10.1016/j.nbd.2007.11.001 (2008).
- 137 Yoo, A. S., Staahl, B. T., Chen, L. & Crabtree, G. R. MicroRNA-mediated switching of chromatin-remodelling complexes in neural development. *Nature* **460**, 642-646, doi:10.1038/nature08139 (2009).
- 138 Yoo, A. S. *et al.* MicroRNA-mediated conversion of human fibroblasts to neurons. *Nature* **476**, 228-231, doi:10.1038/nature10323 (2011).
- 139 Agarwal, V., Bell, G. W., Nam, J. W. & Bartel, D. P. Predicting effective microRNA target sites in mammalian mRNAs. *Elife* **4**, doi:10.7554/eLife.05005 (2015).
- 140 Janzer, A. *et al.* Lysine-specific demethylase 1 (LSD1) and histone deacetylase 1 (HDAC1) synergistically repress proinflammatory cytokines and classical complement pathway components. *Biochem Biophys Res Commun* **421**, 665-670, doi:10.1016/j.bbrc.2012.04.057 (2012).
- 141 Metzger, E. *et al.* LSD1 demethylates repressive histone marks to promote androgen-receptor-dependent transcription. *Nature* **437**, 436-439, doi:10.1038/nature04020 (2005).
- 142 Wang, Y. *et al.* LSD1 is a subunit of the NuRD complex and targets the metastasis programs in breast cancer. *Cell* **138**, 660-672, doi:10.1016/j.cell.2009.05.050 (2009).
- 143 Mosammamarast, N. & Shi, Y. Reversal of histone methylation: biochemical and molecular mechanisms of histone demethylases. *Annu Rev Biochem* **79**, 155-179, doi:10.1146/annurev.biochem.78.070907.103946 (2010).
- 144 Kawahara, Y., Zinshteyn, B., Chendrimada, T. P., Shiekhattar, R. & Nishikura, K. RNA editing of the microRNA-151 precursor blocks cleavage by the Dicer-TRBP complex. *EMBO Rep* **8**, 763-769, doi:10.1038/sj.embor.7401011 (2007).
- 145 Bicker, S. *et al.* The DEAH-box helicase DHX36 mediates dendritic localization of the neuronal precursor-microRNA-134. *Genes Dev* **27**, 991-996, doi:10.1101/gad.211243.112 (2013).
- 146 Ascano, M., Jr. *et al.* FMRP targets distinct mRNA sequence elements to regulate protein expression. *Nature* **492**, 382-386, doi:10.1038/nature11737 (2012).
- 147 Shamay-Ramot, A. *et al.* Fmrp Interacts with Adar and Regulates RNA Editing, Synaptic Density and Locomotor Activity in Zebrafish. *PLoS Genet* **11**, e1005702, doi:10.1371/journal.pgen.1005702 (2015).
- 148 Caudy, A. A., Myers, M., Hannon, G. J. & Hammond, S. M. Fragile X-related protein and VIG associate with the RNA interference machinery. *Genes Dev* **16**, 2491-2496, doi:10.1101/gad.1025202 (2002).



- 149 Ishizuka, A., Siomi, M. C. & Siomi, H. A Drosophila fragile X protein interacts with components of RNAi and ribosomal proteins. *Genes Dev* **16**, 2497-2508, doi:10.1101/gad.1022002 (2002).
- 150 Jin, P. *et al.* Biochemical and genetic interaction between the fragile X mental retardation protein and the microRNA pathway. *Nat Neurosci* **7**, 113-117, doi:10.1038/nn1174 (2004).
- 151 Meza-Sosa, K. F., Pedraza-Alva, G. & Perez-Martinez, L. microRNAs: key triggers of neuronal cell fate. *Front Cell Neurosci* **8**, 175, doi:10.3389/fncel.2014.00175 (2014).
- 152 Akiyama, T. *et al.* Mammalian homologue of E. coli Ras-like GTPase (ERA) is a possible apoptosis regulator with RNA binding activity. *Genes Cells* **6**, 987-1001 (2001).
- 153 Jeske, M. *et al.* The Crystal Structure of the Drosophila Germline Inducer Oskar Identifies Two Domains with Distinct Vasa Helicase- and RNA-Binding Activities. *Cell Rep* **12**, 587-598, doi:10.1016/j.celrep.2015.06.055 (2015).
- 154 Shi, Y. *et al.* Expression and function of orphan nuclear receptor TLX in adult neural stem cells. *Nature* **427**, 78-83, doi:10.1038/nature02211 (2004).
- 155 Zhao, C., Sun, G., Li, S. & Shi, Y. A feedback regulatory loop involving microRNA-9 and nuclear receptor TLX in neural stem cell fate determination. *Nat Struct Mol Biol* **16**, 365-371, doi:10.1038/nsmb.1576 (2009).
- 156 Lessard, J. *et al.* An essential switch in subunit composition of a chromatin remodeling complex during neural development. *Neuron* **55**, 201-215, doi:10.1016/j.neuron.2007.06.019 (2007).
- 157 Makeyev, E. V., Zhang, J., Carrasco, M. A. & Maniatis, T. The MicroRNA miR-124 promotes neuronal differentiation by triggering brain-specific alternative pre-mRNA splicing. *Mol Cell* **27**, 435-448, doi:10.1016/j.molcel.2007.07.015 (2007).
- 158 Linder, B. *et al.* Tdrd3 is a novel stress granule-associated protein interacting with the Fragile-X syndrome protein FMRP. *Hum Mol Genet* **17**, 3236-3246, doi:10.1093/hmg/ddn219 (2008).
- 159 Neuenkirchen, N. *et al.* Reconstitution of the human U snRNP assembly machinery reveals stepwise Sm protein organization. *EMBO J* **34**, 1925-1941, doi:10.15252/embj.201490350 (2015).
- 160 Kibbe, W. A. OligoCalc: an online oligonucleotide properties calculator. *Nucleic Acids Res* **35**, W43-46, doi:10.1093/nar/gkm234 (2007).
- 161 Grudzien-Nogalska, E. *et al.* Synthesis of anti-reverse cap analogs (ARCAs) and their applications in mRNA translation and stability. *Methods Enzymol* **431**, 203-227, doi:10.1016/S0076-6879(07)31011-2 (2007).
- 162 Pasquinelli, A. E., Dahlberg, J. E. & Lund, E. Reverse 5' caps in RNAs made in vitro by phage RNA polymerases. *RNA* **1**, 957-967 (1995).
- 163 Kolb, F. A. *et al.* Human dicer: purification, properties, and interaction with PAZ PIWI domain proteins. *Methods Enzymol* **392**, 316-336, doi:10.1016/S0076-6879(04)92019-8 (2005).
- 164 Price, S. R., Ito, N., Oubridge, C., Avis, J. M. & Nagai, K. Crystallization of RNA-protein complexes. I. Methods for the large-scale preparation of RNA suitable for crystallographic studies. *J Mol Biol* **249**, 398-408 (1995).
- 165 Hafner, M. *et al.* Barcoded cDNA library preparation for small RNA profiling by next-generation sequencing. *Methods* **58**, 164-170, doi:10.1016/j.ymeth.2012.07.030 (2012).

## References

---

- 166 Farazi, T. A. *et al.* Bioinformatic analysis of barcoded cDNA libraries for small RNA profiling by next-generation sequencing. *Methods* **58**, 171-187, doi:10.1016/j.ymeth.2012.07.020 (2012).
- 167 Micallef, L. & Rodgers, P. eulerAPE: drawing area-proportional 3-Venn diagrams using ellipses. *PLoS One* **9**, e101717, doi:10.1371/journal.pone.0101717 (2014).
- 168 The Gene Ontology, C. Expansion of the Gene Ontology knowledgebase and resources. *Nucleic Acids Res* **45**, D331-D338, doi:10.1093/nar/gkw1108 (2017).
- 169 Zuker, M. Mfold web server for nucleic acid folding and hybridization prediction. *Nucleic Acids Res* **31**, 3406-3415 (2003).
- 170 Kozomara, A. & Griffiths-Jones, S. miRBase: annotating high confidence microRNAs using deep sequencing data. *Nucleic Acids Res* **42**, D68-73, doi:10.1093/nar/gkt1181 (2014).

## 9 Table of figures

Figure 1 Cellular differentiation during neurogenesis .....	14
Figure 2 The REST-complex in action .....	16
Figure 3 Genomic organisation of miR genes.....	17
Figure 4 miR processing.....	18
Figure 5 Vertebrate miR Biogenesis.....	20
Figure 6 functionality of the RNA induced silencing complex .....	22
Figure 7 miR-26 and CTDSP regulatory feedback loop.....	24
Figure 8 Possible processing regulation scenarios.....	27
Figure 9 The miR-26 family is highly conserved in vertebrates .....	29
Figure 10 Retained pre-miR export as pre-miR processing regulation.....	30
Figure 11 pre-miR export assay.....	31
Figure 12 pre-miR processing regulation by regulated pre-miR or DICER.....	32
Figure 13 Zebrafisch <i>in vivo</i> and <i>in vitro</i> pre-miR cleavage assay.....	33
Figure 14 Methods used for the identification of miR-26 regulatory proteins.....	34
Figure 15 miR Hairpin binding proteins in 6 hpf Zebrafisch .....	36
Figure 16 miR hairpin-binding proteins in undifferentiated murine P19 cells.....	37
Figure 17 Analyzing the role of Znf-346 in miR 26 in miR maturation .....	40
Figure 18 Analyzing the role of FMRP/FXR1/2 in miR-26 maturation .....	43
Figure 19 Proteom of pre-miRNPs using aptamer pre-miR .....	46
Figure 20 Analyzing the role of Eral1 in miR 26 in miR maturation .....	48
Figure 21 Effect of miR-26 KO on neuronal differentiation .....	52
Figure 22 Transcriptome analysis of miR-26 KO cells.....	55
Figure 23 REST to miR/miR to REST regulation. ....	57
Figure 24 Impact of miR-26 on REST-miRs. ....	59
Figure 25 miR-26 induce REST-miRs.....	61
Figure 26 REST to miR; miR to REST regulation. ....	72
Figure 27 Model: role of miR-26 in neurogenesis .....	74
Figure 28 pre-miR in vitro transcription.....	102
Figure 29 human miR-26 expression.....	107
Figure 30 miR-26 Stem loops in vertebrates .....	108
Figure 31 miR target sites for members of the REST-Complex.....	111

## **10 Publication**

Part of this Work will be published in the following Paper:

Sauer M.\*, Ziegenhals T.\*, Juranek SA., Wang X, Hafner M, Fischer U, Müller A miR-26 initiates neurogenesis through stepwise inactivation of the REST complex The miR-26 family is a key factor for neurogenesis initiation (to be submitted)

## 11 Acknowledgment

I would like to express my thanks to everyone helped me in this project and in preparing this PhD-thesis and thus contributed to successfully finishing it:

First and foremost, I would like to thank Prof. Utz Fischer for giving me an opportunity to work under his supervision and funding throughout the course of this work.

I would like to thank Prof. Albrecht Müller, for collaboration, scientific discussions, being the second examiner of this dissertation and supervision.

Dr. Stefan Juranek for introducing me to biochemistry, supervision and being third member of the oral defense commission.

Prof. Alexander Buchberger for being Chairperson of my defense. Also for the scientific and non-scientific discussions.

My sincere thanks to Mark Sauer for collaboration, scientific and non scientific discussion, helpfulness and boulder intelligence.

Markus Hafner, for providing bioinformatics expertise, sequencing platforms and scientific input.

I would like to thank the labs of Prof. Gunter Meister (especially Dr. Thomas & Dr. Nora Treiber, Johannes Danner, Dr. Astrid Bruckmann) and the lab of Dr. Falk Butter (especially Dr. Marion Scheibe) for help, giving expertise and the platform to perform the RNA pull downs.

I would like to thank the heads of our used Fish rooms Dr. Peter Fischer and Dr. Daniel Liedtke for taking amazing care and for their scientific input.

Prof. Marie-Christine Dabouvalle und Daniela Feicht for providing me with countless *Xenopus* oocytes.

## Acknowledgment

---

I would like Dr. Michael Grimm for scientific discussion and especially the chemical and biochemical input.

Of course, I would like to thank the current and former lab members for the good times. Especially the kitchen table members. Jürgen “The duke/orange ist meine Lieblingsfarbe” Ohmer, Schorschiene: Dr. Georg “Schorsch” Stoll & Nadine “Naddin” Stoll, Markus “der liebste Feind” Sauer, Conny “the sport oracle” Brosi, Sanjay “Guppy” Gupta, and of course Dr. Clemens “Mr. Tricky” Englbrecht, Christopher “the hammer” Stapf, Eike Schwindt, Maritta Küspert, Anja Hirmer and Dr. Bastian Linder.

Also every member of the Department for scientific support and Help.

A big Thank you to Lizzy, Sonja, Andrea, and Farah for support.

I would also like to thank Magnus, Philipp, Niklas, Julia und Thomas for the help.

Ein sehr großes Dankeschön geht an meine Familie die mich, immer großartig unterstützend, auf allen Wegen begleitet hat und ohne diese das alles nicht möglich gewesen wäre. Ganz besonders Romy und Lea.

## 12 Curriculum vitae

### Education

---

- Since Mai 12      **PhD thesis:** “The role of the miR-26 family in neurogenesis“  
Department of Biochemistry, University of Würzburg  
Supervisors: Prof. Dr. Utz Fischer (University of Würzburg)  
Prof. Dr. Albrecht Müller (University of Würzburg)  
Dr. Stefan Juranek (ERIBA, Groningen)
- Oct 10 – Aug 11      **Diploma thesis** “Studying microglial response to open brain injury“, Developmental Biology, Peri Group, EMBL Heidelberg  
Supervisor: Dr. Francesca Peri  
Dr. Dirk Sieger
- Oct 06 – Sep 10      **Studies of Biology** (Diploma)  
Julius-Maximilians-Universität Würzburg, DE  
Degree: Diplom-Biologe (Dipl.-Biol.)  
Major: Neurobiology,  
Minor: Biotechnology,  
Minor: Microbiology
- Sep 97 – May 05      **Abitur**  
Gymnasium Markneukirchen

### Professional Experiences / Internships

---

- Sep 11 – Dec 11      **Visiting Scientist**  
Developmental Biology, Peri Group, EMBL Heidelberg
- Oct 09 – Feb 10      **Semester abroad Université Joseph Fourier Grenoble I, FR**
- Nov 09 – Jan 10      **Internship**, Grenoble Institute des Neuroscience, Grenoble, FR  
Depaulis Group “Synchrotron-generated microbeam radiation as a possible tool to eliminate seizure generators in the GAERS”
- Jan. 10 – Feb. 10      **Internship**, Institute de Biologie Structurale Jean-Pierre Ebel,  
Grenoble FR, Petosa Group “The Epstein-Barr virus ZEBRA protein and its nuclear import factors”
- Oct 05 – Jul 06      **Military Service**  
Laupheim, Nürnberg DE

## Teaching Experiences

---

- 2014 - 2015      **Supervision of Bachelor Theses**  
2014 Magnus Charsten Hupperts "Functional analysis of the microRNA 26b structure"  
2015 Niklas Hauptstein „Untersuchung potentiell regulativer Proteine während der miRNA Prozessierung in *Danio rerio*“  
2015 Phillip Schreiner "Etablierung einer Verletzungsmethodik in *Danio rerio* mit anschließendem Knock-Down des Integrins  $\beta 6$ "
- WS 16 / WS 17      **Lecture** biological/chemical basics  
BSc Lecture, food safety  
University of Cooperative Education, BA Plauen
- WS 16 / WS 17      **Lecture** "ncRNA", in lecture series "RNA World"  
MSc Lecture, Biochemistry, University of Würzburg

## Scientific Initiatives

---

- Oct 13 – Oct 14      Member of the organizing committee of the 9<sup>th</sup> International Symposium organized by the Doctoral Researchers of the Graduate School of Life Sciences "Eureka!"  
Würzburg, Germany

## Conferences

---

- Oct 12                7<sup>th</sup> International Symposium organized by the Doctoral Researchers of the Graduate School of Life Sciences "EPOS"  
Würzburg, Germany  
Poster: "miR-26 Biogenesis during neurogenesis"
- Oct 13                8<sup>th</sup> International Symposium organized by the Doctoral Researchers of the Graduate School of Life Sciences "Scientific Crosstalk"  
Würzburg, Germany  
Poster: "miR-26 Biogenesis during neurogenesis"
- Oct 14                9<sup>th</sup> International Symposium organized by the Doctoral Researchers of the Graduate School of Life Sciences "Eureka!"  
Würzburg, Germany  
Poster: "miR-26 Biogenesis during neurogenesis"
- Jun 17                Non-coding RNAs in Nervous System Development, Plasticity and Disease"  
Marburg, Germany  
Talk: "The role of the miR-26 family in neurogenesis"



**Publications**

---

Sieger D, Moritz C, Ziegenhals T, Prykhozij S, Peri F. Long-range Ca<sup>2+</sup> waves transmit brain-damage signals to microglia. *Dev Cell*. 2012 Jun 12;22(6):1138-48. doi: 10.1016/j.devcel.2012.04.012

Neuenkirchen N, Englbrecht C, Ohmer J, Ziegenhals T, Chari A, Fischer U. Reconstitution of the human U snRNP assembly machinery reveals stepwise Sm protein organization. *EMBO J*. 2015 Jul 14;34(14):1925-41. doi: 10.15252/embj.201490350

Tao Chen\*, Bin Zhang\*, Thomas Ziegenhals\*, Sebastian Fröhler, Archana Prusty, Bianca Hartmann, Nadine Kraemer, Angela M. Kaindl, Utz Fischer, Wei Chen *SNRPE* mutation that disturbs spliceosome availability links aberrant mRNA splicing to Non-syndromal Microcephaly. (to be submitted)

Sauer M.\*, Ziegenhals T.\*, Juranek SA., Wang X, Hafner M, Fischer U, Müller A miR-26 initiates neurogenesis through stepwise inactivation of the REST complex/ The miR-26 family is a key factor for neurogenesis initiation (to be submitted)

**Languages**

---

German	Native speaker
English	Fluent
French	Basic

## 13 Affidavit

I hereby confirm that my thesis entitled “The role of the miR-26 family in neurogenesis” is the result of my own work. I did not receive any help or support from commercial consultants. All sources and / or materials applied are listed and specified in the thesis.

Furthermore, I confirm that this thesis has not yet been submitted as part of another examination process neither in identical nor in similar form.

Place, Date

Signature

## Eidesstattliche Erklärung

Hiermit erkläre ich an Eides statt, die Dissertation “Die Rolle der miR-26 Familie in der Neurogenese“ eigenständig, d.h. insbesondere selbständig und ohne Hilfe eines kommerziellen Promotionsberaters, angefertigt und keine anderen als die von mir angegebenen Quellen und Hilfsmittel verwendet zu haben.

Ich erkläre außerdem, dass die Dissertation weder in gleicher noch in ähnlicher Form bereits in einem anderen Prüfungsverfahren vorgelegen hat.

Ort, Datum

Unterschrift